MULTIUSER MIMO WIRELESS COMMUNICATIONS: OPTIMAL AND EFFICIENT SCHEMES FOR RATE MAXIMIZATION AND POWER MINIMIZATION

WINSTON W. L. HO

B.Eng.(Hons.), NUS

A THESIS SUBMITTED

FOR THE DEGREE OF DOCTOR OF PHILOSOPHY

NUS Graduate School for
Integrative Sciences and Engineering

NATIONAL UNIVERSITY OF SINGAPORE

2008

Acknowledgements

I have been exceedingly fortunate to have interacted with numerous people who have inspired me during the course of my doctoral degree. I would like to deeply thank my supervisors Assoc. Prof. Ying-Chang Liang and Prof. Kin-Mun Lye for their insight and guidance. Assoc. Prof. Ying-Chang Liang's thorough understanding of modern communications and his creativity has never failed to amaze me. His foresight and keen perception have helped to chart the course of my research. Prof. Kin-Mun Lye has provided substantial support and inspiration over the years. He has also offered much constructive advice. Moreover, I am grateful to Assoc. Prof. Samir Attallah who has also been on my thesis advisory committee. His ideas and suggestions have been very helpful.

I am thankful for the scholarship provided by A*STAR, which allowed me to interact with experts in various fields, who have motivated me in my research. My gratitude extends to my friends and my fellow A*STAR scholars who have been in the Institute for Infocomm Research (I^2R), including Shaowei Lin, Sze-Ling Yeo, Derek Leong, Trina Kok, Meng-Wah Chia, Siew-Eng Nai, Edward Peh, Yiyang Pei, Choong-Hock Mar, Fiona Chua, Desmond Kow, Kelly Lee, The-Hanh Pham, Lijuan Geng, Terry Lam, Suriyani Lukman, Helmi Kurniawan, Joonsang Baek, Martin Zimmermann, Vijay Chandrasekhar, Ruben de Francisco, and Lokesh Thiagarajan. They have made my post-graduate course enjoyable and enriching. Furthermore, I appreciate the efforts of Sze-Ling, Timothy, and most importantly, Dr. Liang, for meticulously reading my thesis and offering judicious advice. I also wish

to thank the countless other people inside and outside of the National University of Singapore (NUS) for their support and intellectually stimulating discussions.

Above all, I sincerely appreciate the dedication of my parents and sisters who have encouraged me to pursue my dreams.

Contents

Abstract

A few years after the turn of the century, there have been significant and remarkable breakthroughs in the area of multiuser space-time wireless communications, with the discovery of the multiple-input multiple-output (MIMO) broadcast channel (BC) capacity region [74–77] and the augmenting use of convex optimization theory [99, 100] in MIMO wireless systems.

In this thesis, a new matrix decomposition, called the block diagonal geometric mean decomposition (BD-GMD), is proposed for the MIMO BC. Based on the BD-GMD, novel transceiver schemes are proposed, that maximize the sum rate via dirty paper coding (DPC), and decompose each user's MIMO channel into parallel subchannels with *identical* SNRs. Thus the equal-rate coding can be applied across the subchannels. Next, the BD-GMD is extended to the block diagonal uniform channel decomposition (BD-UCD), which creates subchannels with *identical* SINRs. By combining BD-UCD and DPC, an optimal scheme that achieves the MIMO BC sum capacity is proposed. The proposed BD-GMD-based designs are the low-complexity zero-forcing (ZF) counterparts to the BD-UCD-based designs. Simulations show that the proposed schemes demonstrate better BER performances over conventional schemes.

Following that, we investigate the corresponding problem of minimizing the sum power given user rate requirements for the MIMO BC. The optimal interference-balancing (IB) methods [87–89] require iterative algorithms of high complexity, and may involve time-sharing between different user encoding orders. With a view to

create efficient algorithms for real-time implementation, the problem of power minimization using ZF-DPC is considered, thereby facilitating a closed-form solution. With limited computations, the optimum user encoding order can be found. Later, subchannel selection is incorporated into the solution. Subchannel selection offers an improved performance, especially when there is channel correlation. Efficient solutions are provided to find the encoding order and subchannel selection for each user. These methods have low complexity due to their non-iterative nature. Simulations show that a transmit power close to the optimal IB solution [87–89] can be achieved.

Next, broadband communications is considered. Future wireless systems such as MIMO orthogonal frequency division multiplexing (MIMO-OFDM) need to handle a larger user population as well as higher throughput demands per user. To achieve the best overall system performance, resource allocation for multiuser MIMO-OFDM systems is crucial in optimizing the subcarrier and power allocations. An efficient solution to minimize the total transmit power subject to each user's data rate requirement is proposed, with the help of convex optimization techniques [99, 100]. The complexity is reduced from one that is exponential in the number of subcarriers M to one that is only linear in M, through the use of a Lagrangian dual decomposition. Although frequency-flat fading may have an adverse effect on decomposition-based techniques, a concept termed *dual proportional fairness* handles all fading scenarios seamlessly. Simulation results show superior performance of the proposed efficient algorithm over conventional schemes. Due to the non-convexity of the optimization problem, the proposed solution is not guaranteed to be optimal. However, for a realistic number of subcarriers, the duality gap is practically zero, and the optimal resource allocation can be evaluated efficiently.

List of Figures

List of Abbreviations

BC	Broadcast Channel
BD-GMD	Block Diagonal Geometric Mean Decomposition
BD-UCD	Block Diagonal Uniform Channel Decomposition
bps/Hz	bits per second per hertz
BS	Base Station
CDMA	Code Division Multiple Access
CSCG	Circularly Symmetric Complex Gaussian
CSI	Channel State Information
DPC	Dirty Paper Coding
DFE	Decision Feedback Equalization
ER	Equal-Rate
FDMA	Frequency Division Multiple Access
GMD	Geometric Mean Decomposition
i.i.d.	Independent and Identically Distributed
IB	Interference-Balancing
ISI	Intersymbol Interference
IUI	Inter-User Interference
LBD	Linear Block Diagonalization

MAC	Multiple Access Channel
MCS	Modulation and Coding Scheme
MIMO	Multiple-Input Multiple-Output
MMSE	Minimum Mean Squared Error
MSE	Mean Squared Error
OFDM	Orthogonal Frequency Division Multiplexing
SCM	Successive Closest Match
SIC	Successive Interference Cancellation
SINR	Signal-to-Interference-plus-Noise-Ratio
SISO	Single-Input Single-Output
SNR	Signal-to-Noise-Ratio
SS	Subchannel Selection
SVD	Singular Value Decomposition
TDMA	Time Division Multiple Access
THP	Tomlinson-Harashima Precoding
UCD	Uniform Channel Decomposition
ZF	Zero-Forcing

Notation

In this thesis, the following conventions hold.

- Boldface letters denote matrices and vectors.
- Scalars are denoted by non-boldface italics.
- $\mathbb{E}[\cdot]$ represents the expectation operator.
- $|x|$ is the absolute value of a complex scalar x.
- $\lfloor x \rfloor$ denotes the floor of a real number x, while $\lceil x \rceil$ denotes the ceiling of a real number x.
- $\|\mathbf{x}\|_2$ is the Euclidean norm of a complex vector $\mathbf{x}$.
- $\mathbf{I}_N$ is the $N \times N$ identity matrix.
- $\mathbb{C}^{M \times N}$ is the set of complex $M \times N$ matrices.
- $\mathbb{R}^{M \times N}$ is the set of real $M \times N$ matrices.
- $\mathrm{Tr}(\mathbf{X})$ stands for the trace of a complex matrix $\mathbf{X}$.
- $\det(\mathbf{X})$ represents the determinant of $\mathbf{X}$.
- $\mathbf{X}^T$ is the transpose of $\mathbf{X}$.
- $\mathbf{X}^H$ is the conjugate transpose of $\mathbf{X}$.

- $\mathbf{X}^{-1}$ is the inverse of $\mathbf{X}$.
- $\mathbf{X} = \text{blkdiag}(\mathbf{X}_1, \mathbf{X}_2, \ldots, \mathbf{X}_K)$ represents the block-diagonal matrix of the form

$$\mathbf{X} = \begin{bmatrix} \mathbf{X}_1 & 0 & \ldots & 0 \\ 0 & \mathbf{X}_2 & \ldots & 0 \\ \vdots & \vdots & \ddots & \vdots \\ 0 & 0 & \ldots & \mathbf{X}_K \end{bmatrix}. \tag{1}$$

- $\text{diag}(x_1, \ldots, x_n)$ denotes the diagonal matrix with elements $x_1, \ldots, x_n$
- $\text{diag}(\mathbf{X})$ represents the diagonal matrix with the same diagonal as the matrix $\mathbf{X}$.
- $\mathbf{X}(i, :)$ stands for the i-th row of the matrix $\mathbf{X}$.
- $[\mathbf{X}]_{i,j}$ denotes the matrix element at the i-th row and j-th column.

Chapter 1

Introduction

Wireless communications has advanced tremendously since the success of the first long range transatlantic radio link by Marconi in 1901. Evolving from analogue cellular phones and radio paging, global connectivity is now made possible by new wireless technologies. We can communicate with another person at the other end of the world within seconds, with just our mobile phones or personal communications devices, while the satellite and cellular systems work seamlessly in the background.

Currently, the ever-increasing population of wireless technology consumers demand faster and more convenient communications, progressively saturating the radio frequency (RF) bands. However, there is limit to the data throughput of the wireless channel. This is termed the channel capacity, the maximum data rate for reliable (error-free) data communication, assuming an involved coding scheme. In 1948, Shannon defined this capacity in terms of the available bandwidth and signal power [1]. In a digital system, the capacity for a channel of bandwidth W perturbed by white thermal noise of power N, with an average transmit power of P, is given by

$$C = W \log_2 \left(1 + \frac{P}{N}\right) \quad \text{bits/second} . \tag{1.1}$$

Bandwidth and signal power are precious and limited resources. Wireless consumers share these resources through frequency division multiple access (FDMA), time division multiple access (TDMA), code division multiple access (CDMA) or a combination of these. To meet the demand for higher data rates, new technologies need to be developed, while still maintaining robustness to intersymbol interference (ISI), co-channel interference and fading.

1.1 Motivation

Just about a decade ago, Telatar [2], and Foschini and Gans [3] have revealed that another dimension, space, can be exploited to increase the data throughput of a wireless system, *without* requiring an increase in transmission power or expansion of bandwidth. Multiple-input multiple-output (MIMO) or space-time communications describe the methods that make use of this spatial dimension.

Digital wireless communications using MIMO has since emerged as one of the most remarkable scientific revolutions in modern communications. Among the recent developments to relieve the bottleneck of wireless data transmission, MIMO techniques show tremendous potential. MIMO offers an increase in traffic capacity for future cellular systems, to face the challenge of internet-intensive applications. The future 4G wireless networks will combine the powerful technologies of MIMO, adaptive and reconfigurable systems (software radio) and wireless access technologies such as orthogonal frequency division multiple access (OFDMA) [4] and multiple-carrier code division multiple access (MC-CDMA).

MIMO communications can be described simply. There are multiple antennas

at both the transmitter and the receiver, in contrast to single-input single-output (SISO) communications that only has a single antenna at each of the transmitter and receiver. MIMO wireless communications creates virtual spatial subchannels, over which multiple data streams can be transmitted. Each subchannel uses the same frequency, and the transmissions occur simultaneously.

For a point-to-point MIMO link under frequency non-selective fading (or flat fading) with N_T transmit antennas and N_R receive antennas, the input-output relation can be expressed as

$$\mathbf{y}(n) = \mathbf{H}\mathbf{x}(n) + \mathbf{u}(n) \ , \tag{1.2}$$

where $\mathbf{x}(n)$ is the $N_T \times 1$ transmitted signal vector at time instance n, $\mathbf{y}(n)$ is the $N_R \times 1$ received signal vector, $\mathbf{H}$ is the $N_R \times N_T$ channel matrix subject to block fading, and $\mathbf{u}(n)$ is the $N_R \times 1$ received noise vector with spatial covariance matrix $N_0\mathbf{I}_{N_R}$. The noise received at each antenna element is a vector of zero-mean circularly symmetric complex Gaussian (CSCG) random variables.

The equations for flat-fading MIMO immediately apply to MIMO orthogonal frequency division multiplexing (MIMO-OFDM), due to the existence of decoupled narrow frequency bands. Flat fading results can also be generalized to frequency-selective fading results by considering an augmented matrix with sub-matrices corresponding to the channel response at each time delay [69].

The idea behind MIMO is that these spatial subchannels can be combined in such a way as to improve the quality (bit error rate or BER) or data rate (bits/sec/Hz) of communication. As the radio waves are transmitted over the air, these virtual spatial subchannels suffer from interference or leakage between themselves. Therefore, space-time processing is required to decouple these spatial subchannels. MIMO systems can be viewed as an extension of *smart antenna systems*, a popular technique, dating back several decades, for improving link

reliability through the use of antenna array beamforming.

Multipath propagation has long been a pitfall for wireless communications. The goal of wireless design has been to combat the multipath fading, by dynamic modulation and channel coding schemes, using Rayleigh fading as a worst-case scenario for design purposes. MIMO wireless systems, on the other hand, exploit this multipath to *enhance* the transmission over wireless links. MIMO systems provide a large increase in capacity at no cost of additional frequency bands (just requiring more complexity and hardware).

The enormous capacity gain of MIMO is based on the premise of a rich scattering environment. The MIMO link has effectively $\min(N_T, N_R)$ spatial subchannels, and the capacity of a MIMO link scales linearly with $\min(N_T, N_R)$ relative to a SISO link. Therefore, multiple independent data streams can be transmitted simultaneously to increase throughput and increase spectral efficiency, to obtain *multiplexing gain*. On the other hand, link reliability and a better BER performance can be achieved by beamforming or space-time coding techniques like space-time block codes (STBC) [9, 10] or space-time trellis codes (STTC) [11], hence providing *diversity gain*. A trade-off exists between these two types of gains [12], depending on the coding scheme.

The many-fold increase in performance afforded by MIMO techniques show the great potential of MIMO communications as a research topic. This includes diverse fields such as channel modelling [40–43], channel estimation [13], information theory [14–16], space-time coding [17–19], signal processing [20–22], adaptive modulation and coding [23–25], equalization [26, 27], antennas and propagation [28], space-time OFDM [4–6], space-time CDMA [7, 8], cognitive radio [30–35], relay network design [36, 37], and development of smaller, faster and cheaper hardware.

1.2 Objectives

It has been known that the capacity of the MIMO multiple access channel (MAC) is achievable via the minimum mean squared error (MMSE) decision feedback equalizer (DFE) [45]. Recently, it has been shown that the capacity of the MIMO BC is likewise achievable via dirty paper coding (DPC) [74–77]. An uplink-downlink duality facilitates the transformation between the solutions of the MIMO MAC and the MIMO BC. This has great implication for multiuser MIMO wireless communications because optimal transceiver schemes can be designed to attain the channel capacity, given the channel state and the transmit power constraint. Moreover, efficient schemes can be designed while the performance of the optimal scheme serves as a point of reference. Although suboptimal, efficient schemes are essential for practical hardware implementation due to their low complexity. There are three practical challenges that must be overcome for successful MIMO implementation [38]:

1. There may be insufficient space on the device to support the use of multiple antennas. This could be true for cellular phones.

2. MIMO works best in a rich scattering environment, where uncorrelated fading occurs between the different pairs of antennas. However, the physical channel may not provide enough multipath propagation for a reasonable performance gain.

3. MIMO requires additional processing power at both the transmitter and the receiver. Generally, increased power consumption is not encouraged, especially for mobile devices.

Nevertheless, it may be possible to surmount the first two challenges if advances in circuit design technology permit an increase in the frequency of the radio waves.

The shorter wavelength that results would mean that antennas can be placed closer together, while maintaining sufficient decorrelation.

Granted, the sizes of electronic components have been steadily decreasing, conforming to the notable Moore's Law. However, power consumption and battery life remain a major concern. There is widespread use of wireless devices such as mobile phones, laptops, and personal digital assistants (PDAs). Consumers would not only desire high data rate, but also a long battery life per charge as well. Battery life is influenced by both the hardware complexity and transmit power. The higher the complexity, the shorter the battery life. Also, it is clear that a higher transmit power reduces the battery life.

When future devices exploit the powerful MIMO technology, they would be able to achieve higher data rates without requiring an increase in transmit power. However, if the hardware complexity is too high, this drains the source of energy. Effectively, for the same amount of energy provided by the battery, the benefits of MIMO will be severely eroded. Therefore, the overarching theme in this thesis is in the design of efficient schemes for multiuser MIMO wireless communications.

1.3 Contributions

In this thesis, a new matrix decomposition, called the block diagonal geometric mean decomposition (BD-GMD), is proposed and transceiver designs that combine DPC with BD-GMD for MIMO broadcast channels are developed. Next, the BD-GMD is extended to the block diagonal uniform channel decomposition (BD-UCD) with which the MIMO broadcast channel capacity can be achieved. Sum rate maximizing transceiver schemes are proposed, which decompose each user's MIMO channel into parallel subchannels with *identical* subchannel gains, thus the same modulation and coding scheme (MCS) can be applied across the subchannels of each user.

Singular value decomposition (SVD) generates subchannels which usually have widely ranging SNRs. Diverse MCSs have to be used, and the best subchannel may be assigned a very high order constellation. In contrast, the proposed BD-GMD spreads out the data rate evenly over the subchannels. As a result, smaller signal constellations can be employed, which is useful if there are hardware limitations such as phase noise and synchronization errors. Smaller signal constellations are not only less affected by propagation conditions, but they also result in lower complexity receivers. Although the constellation size for each subchannel is smaller than what the best subchannel in SVD-based schemes would require, it is possible to distribute the data rate among the subchannels without any loss of capacity. Numerical simulations show that the proposed schemes demonstrate superior BER performance over conventional schemes.

Following that, the problem of power minimization given user rate requirements for the MIMO broadcast channel is investigated. The optimal interference-balancing (IB) methods [87–89] result in a high computational complexity due to their iterative nature. In this thesis, the power minimization problem using zero-forcing (ZF)-DPC is considered, thereby facilitating a closed-form solution which results in a simple implementation. Furthermore, subchannels with identical SNRs are also created. The optimum user encoding order can be found with limited computations. Later, subchannel selection is incorporated to further reduce the transmit power. Optimal and efficient solutions for the ZF-DPC problems are provided to find the encoding order and subchannel selection for each user. The advantages of the methods proposed are their non-iterative nature and much reduced computational complexity. Simulations run on both uncorrelated and correlated channels show that a transmit power close to the optimal solution [87–89] can be reached.

Future wireless systems such as MIMO-OFDM need to cater to not only a

burgeoning subscriber pool, but also to a higher throughput per user. Therefore, resource allocation for multiuser MIMO-OFDM systems is vital in optimizing the subcarrier and power allocations to improve the overall system performance. Using convex optimization techniques [99, 100], an efficient solution to minimize the total transmit power subject to each user's data rate requirement is proposed. Through the use of a Lagrangian dual decomposition, the complexity is reduced from one that is exponential in the number of subcarriers M to one that is only linear in M. To keep the complexity low, linear beamforming is applied at both the transmitter and the receiver. Although frequency-flat fading has been known to plague OFDM resource allocation systems, a modification termed *dual proportional fairness* handles flat or partially frequency-selective fading seamlessly. The proposed solution is not guaranteed to be optimal due to the non-convexity of the optimization problem. However, for practical number of subcarriers, the duality gap is effectively zero, and the optimal resource allocation can be evaluated efficiently. Simulation results also show significant performance gains over conventional subcarrier allocations.

1.3.1 Publications

The contributions in this thesis have been published or accepted for publication as listed below:

Journals

[$J1$] S. Lin, W. W. L. Ho, and Y.-C. Liang, "Block Diagonal Geometric Mean Decomposition (BD-GMD) for MIMO Broadcast Channels," *IEEE Trans. Wireless Commun.*, vol. 7, no. 7, pp. 2778–2789, Jul. 2008.

[$J2$] W. W. L. Ho and Y.-C. Liang, "Optimal Resource Allocation for Multiuser MIMO-OFDM Systems with User Rate Constraints," *IEEE Trans.*

Vehicular Technology, accepted for publication.

Conferences

[*C*1] W. W. L. Ho and Y.-C. Liang, "Precoder Design for MIMO Systems with Transmit Antenna Correlations," *Proc. IEEE Vehicular Technology Conf.*, pp. 1382–1386, May 2006.

[*C*2] S. Lin, W. W. L. Ho, and Y.-C. Liang, "Block-diagonal Geometric Mean Decomposition (BD-GMD) for Multiuser MIMO Broadcast Channels," *Int. Symp. Personal, Indoor and Mobile Radio Commun.*, pp. 1–5, Helsinki, 11–14 Sep. 2006.

[*C*3] S. Lin, W. W. L. Ho, and Y.-C. Liang, "MIMO Broadcast Communications using Block-Diagonal Uniform Channel Decomposition (BD-UCD)," *Int. Symp. Personal, Indoor and Mobile Radio Commun.*, pp. 1–5, Helsinki, 11–14 Sep. 2006.

[*C*4] W. W. L. Ho and Y.-C. Liang, "Efficient Power Minimization for MIMO Broadcast Channels with BD-GMD," *Proc. Int. Conf. Commun.*, pp. 2791–2796, Glasgow, Jun. 2007.

[*C*5] W. W. L. Ho and Y.-C. Liang, "User Ordering and Subchannel Selection for Power Minimization in MIMO Broadcast Channels using BD-GMD," *Proc. IEEE Vehicular Technology Conf.*, accepted for publication, Sep. 2008.

[*C*6] W. W. L. Ho and Y.-C. Liang, "Efficient Resource Allocation for Power Minimization in MIMO-OFDM Downlink," *Proc. IEEE Vehicular Technology Conf.*, accepted for publication, Sep. 2008.

[*C*7] W. W. L. Ho and Y.-C. Liang, "Two-Way Relaying with Multiple Antennas using Covariance Feedback," *Proc. IEEE Vehicular Technology Conf.*,

accepted for publication, Sep. 2008.

1.4 Outline

Chapter 2 presents an overview of MIMO communications, including linear vs nonlinear transmission strategies, and single-user vs multiuser MIMO communications. In the following chapters, multiuser communications is studied. The BD-GMD is proposed, in Chapter 3, for the MIMO broadcast channel. The BD-GMD is applied in designing both ZF-based and MMSE-based schemes on which equal-rate coding can be applied. Chapter 4 then addresses the issue of minimizing the transmit power subject to user rate requirements for the MIMO broadcast channel. Low-complexity ZF solutions are proposed, with and without incorporating subchannel selection.

Moving on to broadband communications, Chapter 5 considers multiuser MIMO-OFDM. Sum power is minimized subject to user rate requirements. A low-complexity and near-optimal scheme is proposed. Finally, the last chapter concludes the thesis, with a summary and some discussion on future work.

Chapter 2

MIMO Transmission: An Overview

In this chapter, an overview of MIMO communications is provided. Section 2.1 describes the general categories of MIMO techniques. Following that, Section 2.2 reviews some basic transceiver designs that will be useful in the following chapters. Lastly, Section 2.3 covers multiuser communications, particularly the channel capacity and uplink-downlink duality.

2.1 General Types of MIMO Communications

2.1.1 ZF vs IB Techniques

Transmission strategies (precoding and receiver equalization) can be classified according whether they are based on zero-forcing (ZF) or interference-balancing (IB) [56] considerations. ZF strategies ignore the effect of noise and seek to completely eliminate the ISI. Therefore, they are usually easier to implement than IB-based ones. However, they lead to noise enhancement at low SNR. IB schemes, on the other hand, consider the effect of noise and allow some ISI, in order to achieve

a better performance. For example, the minimum mean squared error (MMSE) receiver minimizes the mean squared error (MSE) between the transmitted and received symbols. At high SNR, the performance of a ZF-based scheme approaches that of the corresponding IB-based scheme.

2.1.2 Linear vs Nonlinear Techniques

Here, a brief comparison is made between linear and nonlinear techniques. Linear transmission techniques often have lower computational complexity than nonlinear ones. However nonlinear techniques often come with the advantage of improved performance.

Linear transmission techniques can be represented by linear matrix operations alone. In ZF linear equalization, the pseudoinverse of the channel matrix is used. For transmitter pre-equalization using the right pseudoinverse, a problem that arises is the increase in transmit power. Alternatively, receive equalization, using the left pseudoinverse can be applied. However, this may result in noise enhancement. To reduce the noise enhancement, MMSE equalization using the regularized inverse [29] of the channel matrix can be applied.

In contrast, nonlinear techniques involve nonlinear operations. For example, successive cancellation and/or modulo. Nonlinear transmission strategies include decision feedback equalization (DFE) at the receiver or dirty-paper coding at the transmitter.

Role of Matrix Decompositions

It has generally been noted that matrix decompositions play an important role in the capacity analysis and transceiver design for MIMO channels. In single user MIMO, the QR-decomposition [52, 53] can be used to perform DFE [71] or Tomlinson-Harashima precoding [50, 51]. For a matrix $\mathbf{H} \in \mathbb{C}^{M \times N}$, $M \geq N$, the

QR-decomposition of $\mathbf{H}$ is $\mathbf{H} = \mathbf{QR}$, where $\mathbf{Q} \in \mathbb{C}^{M\times M}$ is unitary and $\mathbf{R} \in \mathbb{C}^{M\times N}$ is upper triangular. Alternatively, a thin QR-decomposition has $\mathbf{Q} \in \mathbb{C}^{M\times N}$ where $\mathbf{Q}^H\mathbf{Q} = \mathbf{I}_N$ and $\mathbf{R} \in \mathbb{C}^{N\times N}$ upper triangular.

If channel state information (CSI) is available at the transmitter, the singular value decomposition (SVD) and water-filling can be employed to maximize the channel throughput [2, 69]. For a matrix $\mathbf{H} \in \mathbb{C}^{M\times N}$, the SVD of $\mathbf{H}$ is $\mathbf{H} = \mathbf{USV}^H$, where $\mathbf{U} \in \mathbb{C}^{M\times M}$ is unitary, $\mathbf{S} \in \mathbb{R}^{M\times N}$ is diagonal, and $\mathbf{V} \in \mathbb{C}^{N\times N}$ is unitary. This generates decoupled SISO subchannels, usually with different signal-to-noise ratios (SNRs). A different matrix decomposition can also create subchannels with identical SNRs.

2.1.3 Single-user vs Multiuser Communications

MIMO communications can be broadly classified into single-user and multiuser communications. While most communication systems are multiuser in nature, single-user MIMO communication remains of great importance due to the understanding they provide and their relevance to channelized systems, where users are assigned orthogonal resources like time, frequency, and code, i.e. in TDMA, FDMA, and CDMA respectively. Single-user communications involve a point-to-point MIMO link as in (1.2).

In multiuser communications, multiple users can simultaneously share the same time and frequency interval. This is known as space division multiple access (SDMA), and can be implemented in a cellular system or a wireless local area network (WLAN). Multiuser communication is of significant value as it provides huge capacity gains over single-user communication. There are two main types of multiuser MIMO channels — the multiple access channel (MAC) and the broadcast channel (BC). In the MAC or uplink, decentralized mobile users transmit to a base station (BS), while in the BC or downlink, the BS transmits to decentralized

mobile users.

Some Single-user Techniques

In the DFE, successive interference cancellation (SIC) is applied to cancel the interference caused by previously detected data streams. A common problem encountered is error propagation. To reduce the deleterious effect of error propagation, the Vertical Bell Labs Layered Space Time (V-BLAST) [98] scheme optimally orders the sequence of detection of the data streams. The receiver operations of the V-BLAST are fundamentally equivalent to either a ZF or MMSE generalized DFE (GDFE) [44]. In particular, the MMSE-DFE with successive decoding has been shown to be capable of achieving the channel capacity of the MAC [45].

If this nonlinear equalization is moved to the transmitter, the problem of error propagation is avoided. Dirty-paper coding (DPC) [46, 47] is a unique theory that states that the capacity of a system in which the interference is known to the transmitter is as high as that where the interference is not present at all. If we assume that the transmitter has perfect CSI, the interference between these spatial subchannels will be known at the transmitter. Accordingly, DPC can then be applied to pre-subtract the interference even before transmission. ZF techniques involve complete interference pre-subtraction, while IB techniques involve partial interference pre-subtraction.

Tomlinson [48] and Harashima [49] independently introduced a precoding technique for intersymbol interference mitigation, now known as Tomlinson-Harashima precoding (THP). THP is a low-complexity, suboptimal implementation of DPC. THP for the MIMO channel is described in [50]. Simply pre-subtracting away the interference does not immediately achieve capacity — an intricate coding scheme is still required. Vector quantization and lattice precoding [54, 55] is a more involved implementation of DPC that approaches the channel capacity.

In [72], the authors proposed another matrix decomposition called the geometric mean decomposition (GMD). For a matrix $\mathbf{H} \in \mathbb{C}^{M\times N}$, $M \leq N$, the GMD of $\mathbf{H}$ is $\mathbf{H} = \mathbf{PLQ}^H$, where $\mathbf{P} \in \mathbb{C}^{M\times M}$ is unitary, $\mathbf{L} \in \mathbb{C}^{M\times N}$ is lower triangular with each diagonal element equal to the geometric mean of the singular values of $\mathbf{H}$, and $\mathbf{Q} \in \mathbb{C}^{N\times N}$ is unitary. Using the GMD on the channel matrix of point-to-point MIMO, a ZF scheme combining linear precoding and nonlinear DFE receivers that achieves identical SNRs for all subchannels was designed. Instead of DFE at the receiver, interference can also be cancelled via DPC at the transmitter. For both the DFE and DPC schemes, equal-rate codes can be applied on all the subchannels. In [73], the GMD was further used to design a capacity-achieving MMSE-based scheme called the uniform channel decomposition (UCD). This scheme also depends on DPC or DFE for interference cancellation, and achieves identical SINRs for all subchannels so that equal-rate codes can be applied.

Some Multiuser Techniques

For transmission strategies concerning the multiuser MIMO MAC and BC, there has been much more research done on the MAC than on the BC, due to the simpler nature of the problems. It has been found that the MAC capacity can be achieved without requiring any coordination between the mobile users, using the MMSE-DFE. Most of the results from the MIMO MAC can be translated to the MIMO BC via an interesting duality, which will be described in section 2.3.1. For the BC, linear ZF strategies [82, 83] are known as ZF beamforming, block diagonalization or orthogonal space division multiplexing (OSDM). They ensure zero inter-user interference (IUI), by forcing the precoder for each user to lie in the null space of all the other users' channels. This makes the combined channel matrix block diagonal. However, this comes at the price of an increased transmit power, especially when the angle between the different users' channels' eigenvectors

is small. Therefore, user scheduling may have to be employed to select users whose channels are closer to being orthogonal to one another.

MMSE or other IB strategies allow some IUI, in exchange for lower transmit power. For example, [57] presents a pragmatic, suboptimal approach for spatial multiplexing with equal rate on the spatial subchannels. Another linear IB method is found in [58], which maximizes the minimum signal-to-interference-plus-noise-ratio (SINR) over all receivers. [59] uses linear beamforming to maximize the jointly achievable SINR margin under a total power constraint.

Nonlinear transmission strategies can also be ZF or IB based. ZF-DPC methods are found in [60, 61]. Additionally, [62, 63] consider per-antenna power constraints. In [67], linear block diagonalization (LBD) is applied for users with multiple antennas, while users with single antennas are grouped together so that nonlinear THP can be performed.

Coming to IB-DPC methods, [64] minimizes the MSE between the transmit and receive data vectors, where each user has multiple data streams. [65] uses DPC with beamforming to minimize the transmit power given SINR requirements for the MISO BC. MMSE precoding with a sphere encoder is used in [66] which asymptotically achieves the BC sum capacity at high SNR.

2.2 Review of Basic Transceiver Techniques

In the following subsections, a review of some basic transceiver techniques is given. The concepts behind them will be crucial to the construction of proposed schemes for MIMO broadcast channels in Chapter 3. Section 2.2.1 presents a MMSE-based DFE scheme for MIMO point-to-point channels. Section 2.2.2 develops a general view of MMSE-based DPC. Section 2.2.3 highlights two conventional ZF-based THP schemes for MIMO broadcast channels.

2.2.1 MMSE-DFE

Consider the $N_T \times N_R$ point-to-point channel $\mathbf{y} = \mathbf{H}\mathbf{x} + \mathbf{u}$ where $\mathbb{E}[\mathbf{x}\mathbf{x}^H] = (E_s/N_T)\mathbf{I}$ and $\mathbb{E}[\mathbf{u}\mathbf{u}^H] = N_0\mathbf{I}$. The MMSE-based DFE can be represented by the block diagram in Figure 2.1. The columns $\mathbf{w}_i$ of its nulling matrix $\mathbf{W}$ are given by

$$\mathbf{w}_i = \left(\sum_{j=1}^{i} \mathbf{h}_j\mathbf{h}_j^H + \eta\mathbf{I}\right)^{-1} \mathbf{h}_i \ , \quad 1 \le i \le N_T \tag{2.1}$$

where $\eta = N_0(N_T/E_s)$ and $\mathbf{H} = [\mathbf{h}_1, \ldots, \mathbf{h}_{N_T}]$.

For a square matrix $\mathbf{X}$, define $\mathcal{U}(\mathbf{X})$ as follows.

$$[\mathcal{U}(\mathbf{X})]_{i,j} = \begin{cases} [\mathbf{X}]_{i,j} & \text{if } i < j \ , \\ [\mathbf{I}]_{i,j} & \text{otherwise.} \end{cases} \tag{2.2}$$

For convenience, also define $\mathcal{L}(\mathbf{X}) = \mathcal{U}(\mathbf{X}^H)^H$ for a square matrix $\mathbf{X}$. In other words, $\mathcal{U}(\mathbf{X})$ and $\mathcal{L}(\mathbf{X})$ denote the upper and lower triangular matrices, respectively, formed using the matrix $\mathbf{X}$.

The MMSE-DFE applies successive interference cancellation (SIC) via the feedback matrix $\mathbf{B} - \mathbf{I}$, where $\mathbf{B}$ is a monic upper triangular matrix given by $\mathbf{B} = \mathcal{U}(\mathbf{W}^H\mathbf{H})$. $\mathbf{B}$ is referred to as the interference matrix. Now, alternatively, the nulling and interference matrices can be found via the QR-decomposition [71]

$$\begin{bmatrix} \mathbf{H} \\ \sqrt{\eta}\mathbf{I} \end{bmatrix} = \mathbf{Q}_1\mathbf{R}_1 \ , \quad \mathbf{Q}_1 = \begin{bmatrix} \mathbf{Q}_{1u} \\ \mathbf{Q}_{1d} \end{bmatrix} \ , \quad \mathbf{R}_1 = \mathbf{\Lambda}_1\mathbf{B}_1 \ , \tag{2.3}$$

where $\mathbf{Q}_1$ has orthonormal columns, $\mathbf{Q}_{1u}$ is $N_R \times N_T$, and $\mathbf{Q}_{1d}$ is $N_T \times N_T$. $\mathbf{R}_1$ is $N_T \times N_T$ and upper triangular with positive diagonal elements. $\mathbf{\Lambda}_1 = \text{diag}(\mathbf{R}_1)$, and $\mathbf{B}_1$ is a monic upper triangular matrix. (Note that $\mathbf{Q}_{1u}$ and $\mathbf{Q}_{1d}$ are not

unitary.) Then, the nulling and interference matrices satisfy

$$\mathbf{W}^H = \mathbf{\Lambda}_1^{-1}\mathbf{Q}_{1u}^H \quad \text{and} \quad \mathbf{B} = \mathbf{B}_1 \ . \tag{2.4}$$

The symbols are detected from $\hat{x}_{N_T}$ to $\hat{x}_1$ as follows:

`for` $i = N_T : -1 : 1$

$\quad \hat{x}_i = \mathcal{C}\left[[\mathbf{W}^H\mathbf{y}]_i - \sum_{j=i+1}^{N_T}[\mathbf{B}]_{i,j}\hat{x}_j\right]$

`end`

where $\mathcal{C}$ denotes the mapping to the nearest signal point in the constellation. Ignoring the effect of error propagation, the MMSE-DFE scheme produces decoupled subchannels of the form $y_i = r_i x_i + u_i$ where r_i is the i-th diagonal element of $\mathbf{\Lambda}_1$. In [73], it was shown that

$$\eta(1+\rho_i) = r_i^2 \ , \tag{2.5}$$

where ρ_i is the SINR of the i-th subchannel. Thus, the capacity of the scheme can be written as

$$\sum_{i=1}^{N_T}\log(1+\rho_i) = \sum_{i=1}^{N_T}\log\left(\frac{r_i^2}{\eta}\right) = \log\det\left(\mathbf{I} + \frac{1}{\eta}\mathbf{H}^H\mathbf{H}\right) \ . \tag{2.6}$$

This gives another proof that the MMSE-DFE receiver is information lossless [45], [73].

2.2.2 MMSE-based DPC

One major problem with DFEs is error propagation. If CSI is known at the transmitter, interference between subchannels can be cancelled completely before transmission via DPC. Here, a general view of MMSE-based DPC via successive interference pre-subtraction is developed. Consider once again the $N_T \times N_R$ point-

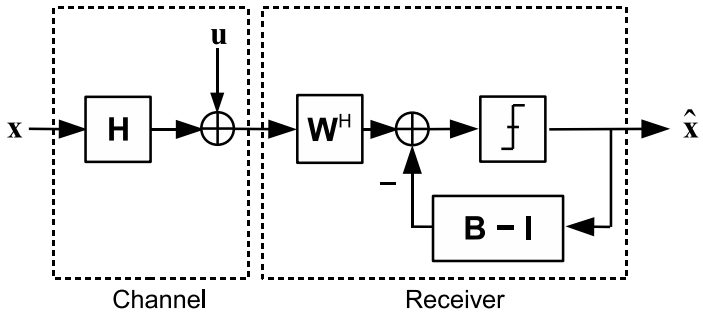

Figure 2.1: Block diagram of the MMSE-DFE scheme.

to-point channel $\mathbf{y} = \mathbf{Hx} + \mathbf{u}$ from Section 2.2.1. However, it will not be required that $\mathbb{E}[\mathbf{uu}^H] = N_0\mathbf{I}$ but only that $\mathbb{E}[|u_i|^2] = N_0$ for each i. Assume that there is no collaboration between the receive antennas. Writing $h_{ij} = [\mathbf{H}]_{i,j}$, the i-th subchannel is

$$y_i = (\sum_{j<i} h_{ij}x_j) + h_{ii}x_i + (\sum_{j>i} h_{ij}x_j) + u_i \ . \tag{2.7}$$

The hope is to treat $(\sum_{j<i} h_{ij}x_j)$ as interference terms to be cancelled at the transmitter. If these interference terms are cancelled perfectly, then a single input single output (SISO) MMSE receiver that sees $(\sum_{j>i} h_{ij}x_j) + u_i$ as noise terms can be used on each subchannel. The corresponding MMSE coefficient for the i-th subchannel is

$$d_i = \frac{h_{ii}^*}{\eta + \sum_{j\geq i} |h_{ij}|^2} \ , \tag{2.8}$$

where x^* is the conjugate of a complex number x. Denoting $\mathbf{D}_d = \mathrm{diag}(d_1, \ldots, d_{N_R})$, the equivalent channel is now $\mathbf{D}_d\mathbf{H}$. Thus, the interference terms can be represented by the lower triangular unit-diagonal matrix $\mathbf{B} = \mathcal{L}(\mathbf{D}_d\mathbf{H})$, called the interference matrix. Meanwhile, the SINR of the i-th subchannel is given by

$$\rho_i = \frac{|h_{ii}|^2}{\eta + \sum_{j>i} |h_{ij}|^2} \ . \tag{2.9}$$

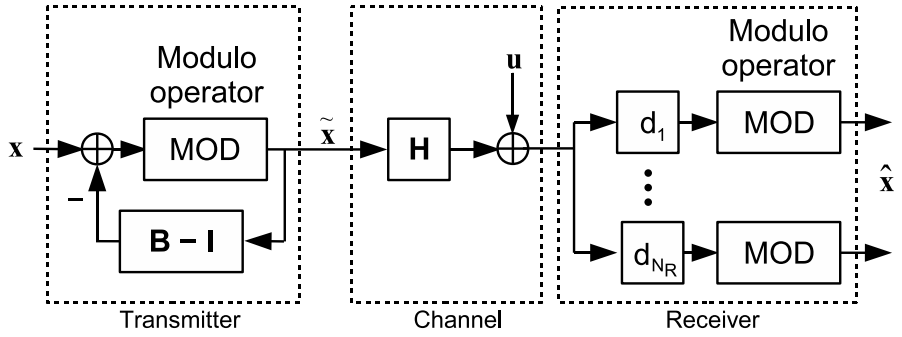

Figure 2.2: Block diagram of the MMSE-DPC scheme using THP.

A simple and useful relation between (2.8) and (2.9) can be noted at this point. Let $\Sigma_0 = \eta + \sum_{j>i} |h_{ij}|^2$. Then, $\rho_i = |h_{ii}|^2/\Sigma_0$ and $d_i = h_{ii}^*/(\Sigma_0 + |h_{ii}|^2)$. Eliminating Σ_0 gives

$$d_i = \frac{\rho_i}{h_{ii}(1+\rho_i)} \ . \tag{2.10}$$

One low-complexity suboptimal implementation of DPC is Tomlinson-Harashima precoding (THP) [92]. The block diagram of a MMSE-based DPC scheme using THP is shown in Figure 2.2. The vector $\tilde{\mathbf{x}}$ to be transmitted can be evaluated from $\tilde{x}_1$ to $\tilde{x}_{N_T}$ using

$\tilde{x}_1 = x_1$

`for` $i = 2:1:N_T$

$\quad \tilde{x}_i = \mathrm{mod}\left[x_i - \sum_{j=1}^{i-1} [\mathbf{B}]_{i,j} \tilde{x}_j\right]$

`end`

A downside of THP is the slight increase in the average transmit power by a factor of $M/(M-1)$ for M-QAM symbols, called the *precoding loss*. For large constellations, this loss is negligible.

2.2.3 ZF-DPC

Consider the MIMO broadcast channel described in Section 2.1.3. If CSI is available at the transmitter, interference cancellation via dirty paper precoding or THP can be performed. Conventional precoding schemes often treat multiple antennas of different users as different virtual users. One example is the zero-forcing THP (ZF-THP) scheme [92]. It is based on the QR decomposition $\mathbf{H}^H = \mathbf{QR}$, or $\mathbf{H} = \mathbf{R}^H\mathbf{Q}^H$. The linear precoder $\mathbf{Q}$ is applied before transmission so that $\mathbf{x} = \mathbf{Qs}$, where $\mathbf{s}$ is the vector of information symbols to be sent. This transforms the channel to $\mathbf{y} = \mathbf{R}^H\mathbf{s} + \mathbf{u}$, on which THP is applied to pre-subtract the interference represented by the lower triangular matrix $\mathbf{R}^H$. Thus, N_R decoupled subchannels $y_i = r_i s_i + u_i$, where r_i is the ith diagonal element of $\mathbf{R}$, are obtained. Note that the QR decomposition is applied on the transpose of $\mathbf{H}$ because the receive antennas may not be co-located, thereby precluding joint receive processing.

Another example comes from [93]. The authors considered pre-equalization matrices $\mathbf{F}$ such that the resulting channel matrix $\mathbf{HF}$ is lower triangular and has diagonal elements all equal to a certain value, say r. Here, $\mathbf{F}$ need not be unitary but only has to satisfy the power constraint $\mathrm{Tr}(\mathbf{FF}^H) \leq E_s$. The precoder $\mathbf{F}$ that maximizes r in $\mathbf{HF}$ can be found algorithmically. The scheme now only needs to perform THP to cancel the interference represented by the lower triangular matrix $\mathbf{HF}$ before pre-equalizing with $\mathbf{F}$ and transmitting the signal. This scheme generates N_R decoupled subchannels $y_i = rs_i + u_i$ on which equal-rate coding can be applied. Hence, their scheme will be referred to as the Equal-Rate ZF-THP scheme.

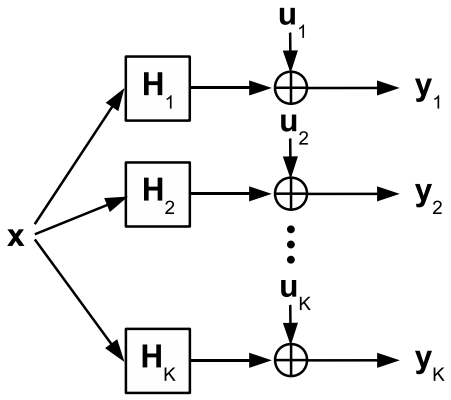

Figure 2.3: System model of the MIMO BC channel.

2.3 Multiuser Communications

In the following section, the capacity results for the multiuser MIMO wireless channel are reviewed. The capacity region of the MIMO BC is related to that of the MIMO MAC via an uplink-downlink duality. This duality will be useful in the construction of the transceiver designs in Chapter 3.

2.3.1 MIMO BC Capacity and Uplink-Downlink Duality

Consider the broadcast channel from a BS to K mobile users. The BS is equipped with N_T antennas, and the k-th mobile user has n_k antennas. Let $N_R = \sum_{k=1}^{K} n_k$ be the total number of receive antennas. Denote this setup by $N_T \times \{n_1, \ldots, n_K\}$. The input-output relation can be represented as

$$\mathbf{y} = \mathbf{H}\mathbf{x} + \mathbf{u} \ , \tag{2.11}$$

where $\mathbf{x}$ is the $N_T \times 1$ transmit signal vector at the BS, $\mathbf{y}$ the $N_R \times 1$ receive signal vector with $\mathbf{y} = [\mathbf{y}_1^T, \cdots, \mathbf{y}_K^T]^T$, and each $\mathbf{y}_k$ the $n_k \times 1$ receive signal vector of user k. The MIMO BC model is shown in Figure 2.3.

Assume that the noise vector $\mathbf{u}$ is a zero-mean, CSCG vector with $\mathbb{E}[\mathbf{u}\mathbf{u}^H] = N_0\mathbf{I}$, and $\mathbf{u}$ is independent of $\mathbf{x}$. Assume also that $\mathbb{E}[\|\mathbf{x}\|_2^2] = E_s$, and let $\rho = E_s/N_0$

be the SNR. It will also be useful to write $\mathbf{H} = [\mathbf{H}_1^T, \mathbf{H}_2^T, \ldots, \mathbf{H}_K^T]^T$, where $\mathbf{H}_k$ is the $n_k \times N_T$ channel matrix of user k.

If $\mathbf{x}$ is a Gaussian random vector, the sum-capacity of this broadcast channel is given by [74–77]

$$\sup_{\mathrm{Tr}(\mathbf{F}\mathbf{F}^H) \leq E_s} \log\det\left(\mathbf{I} + \frac{1}{N_0}\mathbf{H}^H\mathbf{F}\mathbf{F}^H\mathbf{H}\right) , \tag{2.12}$$

where $\mathbf{F}$ is of the block diagonal form

$$\mathbf{F} = \begin{bmatrix} \mathbf{F}_1 & 0 & \ldots & 0 \\ 0 & \mathbf{F}_2 & \ldots & 0 \\ \vdots & \vdots & \ddots & \vdots \\ 0 & 0 & \ldots & \mathbf{F}_K \end{bmatrix} \tag{2.13}$$

and each block $\mathbf{F}_k$ is a $n_k \times n_k$ matrix. This sum-capacity can be achieved by a scheme that combines DPC with linear precoding. A fundamental step in proving this theorem is showing that there is a dual relationship between uplink DFE and downlink DPC schemes. In [78], the authors extended the capacity theorem by verifying that the capacity *region* of the Gaussian MIMO broadcast channel is precisely the DPC rate region. At the boundary of this region, $\mathrm{Tr}(\mathbf{F}\mathbf{F}^H) = E_s$.

For the $N_T \times \{n_1, \ldots, n_K\}$ MIMO broadcast channel described earlier, the uplink-downlink duality results [74, 75] will now be used to construct a DPC scheme that consumes the same power E_s and achieves the same rate-tuple as a given MMSE-DFE scheme. This DPC scheme is *dual* to the MMSE-DFE scheme.

First, suppose the following MMSE-DFE scheme is given. Consider the $\{n_1, \ldots, n_K\} \times N_T$ dual uplink channel

$$\mathbf{y} = \mathbf{H}^H\mathbf{x} + \mathbf{u} = \sum_{k=1}^{K} \mathbf{H}_k^H\mathbf{x}_k + \mathbf{u} , \tag{2.14}$$

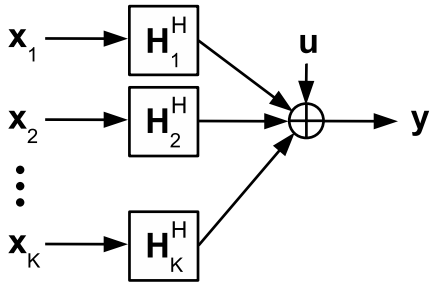

Figure 2.4: System model of the dual MIMO MAC channel.

which has K mobile users with $n_1, \ldots, n_K$ transmit antennas respectively, and a BS with N_T receive antennas. Here, $\mathbf{H}^H = [\mathbf{H}_1^H, \mathbf{H}_2^H, \ldots, \mathbf{H}_K^H]$ is the uplink channel matrix, $\mathbf{x} = [\mathbf{x}_1^T, \mathbf{x}_2^T, \ldots, \mathbf{x}_K^T]^T$ is the transmitted signal vector, $\mathbf{y}$ is the received signal vector and $\mathbf{u}$ is the received noise vector. This MAC model is shown in Figure 2.4.

Let $\mathbb{E}[\mathbf{u}\mathbf{u}^H] = N_0\mathbf{I}$, and $\mathbb{E}[\|\mathbf{x}\|_2^2] = E_s$. This channel is dual to the broadcast channel mentioned earlier. Meanwhile, let each user k be equipped with a predetermined linear precoder $\mathbf{F}_k$. Combine all the precoders in a block diagonal matrix $\mathbf{F}$ of the form (2.13), and consider a MMSE-DFE receiver at the BS. Using (2.3), the QR decomposition for the equivalent channel $\mathbf{H}^H\mathbf{F}$ is as follows:

$$\begin{bmatrix} \mathbf{H}^H\mathbf{F} \\ \sqrt{N_0}\mathbf{I} \end{bmatrix} = \begin{bmatrix} \mathbf{Q}_u \\ \mathbf{Q}_d \end{bmatrix} \mathbf{\Lambda}\mathbf{B} \ . \tag{2.15}$$

It implies that the nulling matrix is $\mathbf{W}^H = \mathbf{\Lambda}^{-1}\mathbf{Q}_u^H$, and that the interference matrix is $\mathbf{B}$. Normalize the columns of $\mathbf{F}$ by writing its i-th column as $\sqrt{p_i}\mathbf{f}_i$ where $\sqrt{p_i}$ is the norm and $\mathbf{f}_i$ a unit column vector. Since

$$\mathbf{x} = \mathbf{F}\mathbf{s} = \sum_{i=1}^{N_R} \sqrt{p_i}\mathbf{f}_i s_i \ , \tag{2.16}$$

p_i represents the power allocated to the i-th information symbol s_i. Thus, the total power is $\sum_{i=1}^{N_R} p_i = \mathrm{Tr}[\mathbf{F}\mathbf{F}^H] = E_s$. Also, normalize the columns of $\mathbf{W}$, writing the

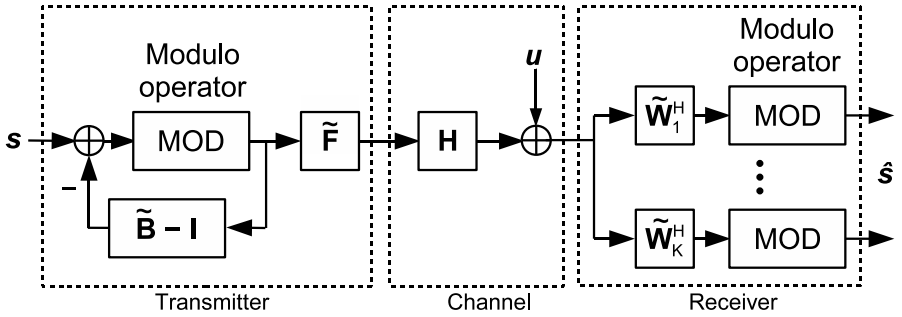

Figure 2.5: Block diagram of dual DPC scheme.

i-th column as $c_i\mathbf{w}_i$ where c_i is the norm. Here, c_i can be thought of as an MMSE weight similar to that in (2.8), since it scales the signal in the i-th subchannel. Assuming that the symbols are cancelled perfectly in the SIC, the SINR of the i-th subchannel is given by

$$\rho_i = \frac{p_i|\mathbf{w}_i^H\mathbf{H}^H\mathbf{f}_i|^2}{N_0 + \sum_{j<i} p_j|\mathbf{w}_i^H\mathbf{H}^H\mathbf{f}_j|^2} \ . \tag{2.17}$$

Now, construct the dual DPC scheme for the broadcast channel as follows. Let $\widetilde{\mathbf{F}}$ be the linear precoder at the BS, $\widetilde{\mathbf{B}}$ the interference matrix, and $\widetilde{\mathbf{W}}^H$ the combined nulling matrix of the mobile users. The block diagram for this scheme is shown in Figure 2.5, where $\widetilde{\mathbf{W}}_k^H$ is the k-th sub-block of the block diagonal matrix $\widetilde{\mathbf{W}}^H$. First, define the i-th column of $\widetilde{\mathbf{F}}$ to be $\sqrt{q_i}\mathbf{w}_i$. Here, q_i is an unknown representing the power allocated to the i-th information symbol. Next, define the i-th column of $\widetilde{\mathbf{W}}$ to be $d_i\mathbf{f}_i$ where d_i is an unknown MMSE weight. Since the goal is to achieve the same SINRs, by (2.9), the power coefficients q_i need to satisfy

$$\rho_i = \frac{q_i|\mathbf{f}_i^H\mathbf{H}\mathbf{w}_i|^2}{N_0 + \sum_{j>i} q_j|\mathbf{f}_i^H\mathbf{H}\mathbf{w}_j|^2} \quad \text{for } 1 \le i \le N_R \ . \tag{2.18}$$

Using the notation $\mathbf{q} = [q_1, \ldots, q_{N_R}]^T$, $\boldsymbol{\rho} = [\rho_1, \ldots, \rho_{N_R}]^T$ and $\alpha_{ij} = |\mathbf{f}_i^H\mathbf{H}\mathbf{w}_j|^2$,

rewrite (2.18) in matrix form [73]:

$$\begin{bmatrix} \alpha_{11} & -\rho_1\alpha_{12} & \dots & -\rho_1\alpha_{1N_R} \\ 0 & \alpha_{22} & \dots & -\rho_2\alpha_{2N_R} \\ \vdots & \vdots & \ddots & \vdots \\ 0 & 0 & \dots & \alpha_{N_RN_R} \end{bmatrix} \mathbf{q} = N_0\boldsymbol{\rho} \ . \tag{2.19}$$

Thus, $\mathbf{q}$ can be derived. In [74], the authors showed that $\sum_{i=1}^{N_R} q_i = \sum_{i=1}^{N_R} p_i$, so both the MMSE-DFE scheme and the dual DPC scheme consume the same total power E_s.

To compute the MMSE weights d_i, the relation in (2.10) is exploited:

$$d_i = \frac{\rho_i}{(1+\rho_i)\sqrt{q_i}\mathbf{f}_i^H\mathbf{H}\mathbf{w}_i} \ . \tag{2.20}$$

By the same reasoning on c_i, the MMSE weights for the uplink channel, it follows that

$$c_i = \frac{\rho_i}{(1+\rho_i)\sqrt{p_i}\mathbf{w}_i^H\mathbf{H}^H\mathbf{f}_i} \ . \tag{2.21}$$

Since c_i is defined to be a vector norm, c_i is real so $\mathbf{w}_i^H\mathbf{H}^H\mathbf{f}_i$ is real. Consequently, $\mathbf{w}_i^H\mathbf{H}^H\mathbf{f}_i = \mathbf{f}_i^H\mathbf{H}\mathbf{w}_i$ and thus $d_i\sqrt{q_i} = c_i\sqrt{p_i}$. Denote $\mathbf{D}_q = \mathrm{diag}(\sqrt{q_1}, \dots, \sqrt{q_{N_R}})$ and similarly define diagonal matrices $\mathbf{D}_p$, $\mathbf{D}_c$ and $\mathbf{D}_d$ for $\{\sqrt{p_i}\}$, $\{c_i\}$ and $\{d_i\}$. Thus, $\mathbf{D}_d\mathbf{D}_q = \mathbf{D}_c\mathbf{D}_p$. Finally, to complete the dual DPC scheme, the interference

matrix $\widetilde{\mathbf{B}}$ is computed. Using the relations

$$\begin{aligned}
\mathbf{B} &= \mathcal{U}(\mathbf{W}^H\mathbf{H}^H\mathbf{F}) \\
\widetilde{\mathbf{W}} &= \mathbf{F}\mathbf{D}_p^{-1}\mathbf{D}_d = \mathbf{F}\mathbf{D}_q^{-1}\mathbf{D}_c \\
\widetilde{\mathbf{F}} &= \mathbf{W}\mathbf{D}_c^{-1}\mathbf{D}_q \\
\mathcal{L}(\mathbf{X})^H &= \mathcal{U}(\mathbf{X}^H) \ ,
\end{aligned} \tag{2.22}$$

the following result is derived:

$$\widetilde{\mathbf{B}} = \mathcal{L}(\widetilde{\mathbf{W}}^H\mathbf{H}\widetilde{\mathbf{F}}) = \mathbf{D}_c\mathbf{D}_q^{-1}\mathbf{B}^H\mathbf{D}_c^{-1}\mathbf{D}_q \ . \tag{2.23}$$

Note that $\mathcal{U}(\cdot)$ and $\mathcal{L}(\cdot)$ are defined at (2.2). Using (2.5), the achievable sum rate for both the MMSE-DFE and dual DPC scheme can be written as

$$\sum_{i=1}^{N_R}\log(1+\rho_i) = \sum_{i=1}^{N_R}\log\left(\frac{\lambda_i^2}{N_0}\right) = \log\det(\mathbf{I}+\frac{1}{N_0}\mathbf{H}^H\mathbf{F}\mathbf{F}^H\mathbf{H}) \ . \tag{2.24}$$

Chapter 3

Block Diagonal Geometric Mean Decomposition for MIMO Broadcast Channels

For single-user MIMO communications, the SVD can be used to generate multiple subchannels if channel state information (CSI) is available at the transmitter. However, the usually large condition number of the channel matrix results in subchannels with vastly different signal-to-noise-ratios (SNRs). From the information theoretical viewpoint, in order to achieve the channel capacity, variable-rate coding can be used across these decoupled subchannels. However, this may require special code design due to the variation of the supported rate of the subchannels. In practice, bit loading is designed to match the supported rates of each subchannel, i.e., each subchannel is allocated with one modulation/coding scheme (MCS). By doing so, however, the good subchannels may require very high order QAMs, which may be difficult to implement for wireless systems due to the existence of phase noises and synchronization errors. On the other hand, if the same MCS is used on all the subchannels, the BER performance will be dominated by the weakest subchannel. Recently, geometric mean decomposition (GMD) [72] has been proposed to resolve

this problem by decomposing the MIMO channel into multiple subchannels with identical SNRs, with the help of dirty paper coding (DPC) [46] or interference cancellation. With that, the same MCS can be applied across all the subchannels, thus the order of the required QAM can be relatively small due to the sharing among all subchannels. Therefore, the GMD-based scheme is useful when there is a limitation on the order of QAM being used in practical system design.

Multiuser communications is an area of intense research, especially since the recent discovery of the MIMO broadcast channel capacity [74–77]. It has been shown that when CSI is available at the transmitter, the capacity region of the MIMO broadcast channel is exactly equal to the capacity region of its dual uplink multiple access channel. While the uplink capacity is achievable by the minimum mean squared error (MMSE) decision feedback equalizer (DFE) [45], the broadcast channel capacity is likewise achievable via DPC. In multiuser broadcast channels, unlike the single-user MIMO, joint processing is not permitted between different users as they are not co-located. However, receive equalization is possible for each user. There have been several schemes proposed for low complexity MIMO broadcast communications. These include schemes based on TDMA [80], linear block diagonalization [81–83], and random / opportunistic beamforming [84, 85]. However, these schemes would normally fail to achieve the DPC broadcast channel capacity.

In this chapter, the single-user GMD is extended to the multiuser MIMO broadcast scenario. Our design criteria is that for each user, subchannels with identical SNRs are to be created. To achieve this, a new matrix decomposition, called the block diagonal geometric mean decomposition (BD-GMD), is first proposed. Four applications of the BD-GMD are then designed. The first two applications are low-complexity zero-forcing (ZF)-based schemes, while the later two are MMSE-based schemes of higher complexity. All four of them use DPC at the transmitter.

Tomlinson-Harashima precoding (THP) [50, 51], a simple suboptimal implementation of DPC, can also be used in conjunction with these new schemes. In the first application, a BD-GMD-based DPC scheme is designed, that generates subchannels with identical SNRs for each user, while different rates may be experienced between different users. Such a scheme is said to be *block-equal-rate*. In the second application, a scheme that allows equal-rate coding among the subchannels of *all* users is constructed. Such a scheme is said to be *equal-rate*. Power control via channel inversion is shown to optimize the achievable sum rate. The resulting scheme is called the Equal-Rate BD-GMD. User ordering is proposed to improve the fairness of the BD-GMD-based DPC scheme or to increase the achievable sum rate for the Equal-Rate BD-GMD scheme.

ZF-based schemes are inherently capacity lossy. In the third application, using the uplink-downlink duality [74, 75], the BD-GMD is extended to the block diagonal uniform channel decomposition (BD-UCD) which achieves the sum capacity for the MIMO broadcast channel. Specifically, Jindal *et al.*'s sum power iterative water-filling algorithm [79] is used to obtain the optimal transmit power allocation and precoder for the scheme. In the fourth application, an equal-rate scheme called the Equal-Rate BD-UCD is proposed. This is done by first considering the problem of uplink beamforming under signal-to-interference-plus-noise-ratio (SINR) constraints [91] for mobile users with multiple antennas. An efficient algorithm which finds a near-optimal solution is then given, and duality is applied to produce the desired scheme.

The first two applications are ZF extensions to the GMD scheme, while the later two applications can be considered as MMSE extensions to the uniform channel decomposition (UCD) scheme [73]. For each of the ZF and MMSE cases, the first scheme proposed is a block-equal-rate scheme, while the second is an equal-rate scheme. For the equal-rate schemes, besides the fairness achieved among the

different users, by providing each user with the same rate and if THP is used, the same modulus operator can be used for *all* subchannels across *all* the users. This obviates the need to implement multiple modulus operators to match the different modulation schemes used by the various users. Simulation results show that our proposed schemes exhibit superior performance over existing schemes.

The chapter is organized as follows. In Section 3.1, the block diagonal geometric mean decomposition is proposed. In Sections 3.2.1 and 3.2.2, the ZF-based schemes, BD-GMD and Equal-Rate BD-GMD, are designed. Sections 3.3.1 and 3.3.2 lay out the design of the MMSE-based schemes, BD-UCD and Equal-Rate BD-UCD. Simulation results are presented and discussed in Section 3.4, and a summary is given in Section 3.5.

3.1 Block Diagonal Geometric Mean Decomposition

In this section, the block diagonal geometric mean decomposition (BD-GMD) is developed. We begin by describing the motivation for developing such a decomposition. In the case where some of the mobile users have multiple antennas, performance gain can be expected from doing equalization on the receiver side. This equalization can only be done for the data streams of the same user, and not between users. It can be represented as a pre-multiplication of the receive signal $\mathbf{y}(n)$ by a block diagonal matrix $\mathbf{A}$: $\mathbf{A} = \text{blkdiag}(\mathbf{A}_1, \cdots, \mathbf{A}_K)$, where each block $\mathbf{A}_k$ is the $n_k \times n_k$ equalization matrix of user k. Each row of $\mathbf{A}_k$ is assumed to be of unit norm so that the noise vector $\mathbf{u}$ is not amplified by $\mathbf{A}$. Note that the situation where the mobile users have single antennas is represented by the case $\mathbf{A} = \mathbf{I}$. Equalization by $\mathbf{A}$ gives the equivalent channel matrix $\mathbf{AH}$ which can then be cancelled by transmitter techniques such as ZF-THP or MMSE-THP.

Suppose ZF-THP is used at the transmitter, and the QR-decomposition $\mathbf{AH} = \mathbf{R}^H\mathbf{Q}^H$ is considered. Since the aim is to construct a block-equal-rate scheme, it is natural to ask if it can be accomplished by choosing an appropriate equalization matrix $\mathbf{A}$. To simplify the problem, assume further that $\mathbf{A}$ is unitary. Our problem can now be stated as follows. Let $\mathbf{H}$ be an $N_R \times N_T$ matrix, and $n_1, ..., n_K$ a sequence of integers such that $N_R = \sum_{k=1}^{K} n_k$. Consider matrix decompositions of the following form [72]: $\mathbf{H} = \mathbf{PLQ}^H$, where $\mathbf{Q}$ is a $N_T \times N_R$ matrix with orthonormal columns, $\mathbf{L}$ is a $N_R \times N_R$ lower triangular matrix, and $\mathbf{P}$ is a $N_R \times N_R$ block diagonal matrix of the form $\text{blkdiag}(\mathbf{P}_1, \mathbf{P}_2, \ldots, \mathbf{P}_K)$ where each block $\mathbf{P}_k$ is a unitary $n_k \times n_k$ matrix. The task is to find a matrix decomposition such that the diagonal elements of $\mathbf{L}$ are positive and equal in blocks of $n_1, \ldots, n_K$ elements respectively.

3.1.1 Proposed Algorithm

The algorithm to solve the above problem is as follows. Write the product $\mathbf{H} = \mathbf{PLQ}^H$ as

$$\begin{bmatrix} \mathbf{H}_1 \\ \boldsymbol{\mathcal{H}} \end{bmatrix} = \begin{bmatrix} \mathbf{P}_1 & \mathbf{0} \\ \mathbf{0} & \boldsymbol{\mathcal{P}} \end{bmatrix} \begin{bmatrix} \mathbf{L}_1 & \mathbf{0} \\ \boldsymbol{\Xi} & \boldsymbol{\mathcal{L}} \end{bmatrix} \begin{bmatrix} \mathbf{Q}_1^H \\ \boldsymbol{\mathcal{Q}}^H \end{bmatrix} , \tag{3.1}$$

where $\mathbf{H}_1$ and $\mathbf{Q}_1^H$ are $n_1 \times N_T$ sub-matrices, and $\mathbf{L}_1$ and $\mathbf{P}_1$ are $n_1 \times n_1$ square matrices. $\boldsymbol{\mathcal{H}}$ denotes the combined channel matrix of all the remaining users. $\boldsymbol{\mathcal{P}}$, $\boldsymbol{\Xi}$, $\boldsymbol{\mathcal{L}}$, and $\boldsymbol{\mathcal{Q}}^H$ are the remaining sub-matrices of the decomposition. Expanding (3.1) gives the following two equations

$$\mathbf{H}_1 = \mathbf{P}_1\mathbf{L}_1\mathbf{Q}_1^H , \tag{3.2}$$

$$\boldsymbol{\mathcal{H}} = \boldsymbol{\mathcal{P}}\boldsymbol{\Xi}\mathbf{Q}_1^H + \boldsymbol{\mathcal{P}}\boldsymbol{\mathcal{L}}\boldsymbol{\mathcal{Q}}^H . \tag{3.3}$$

From equation (3.2), it can be seen that by using the GMD, the diagonal elements of $\mathbf{L}_1$ can be made equal. Now, since $\mathbf{Q}$ has orthonormal columns, the sub-matrices $\mathbf{Q}_1$ and $\boldsymbol{\mathcal{Q}}$ are orthonormal to each other. Thus, from equation (3.3), multiplication by the projection matrix $\mathbf{I} - \mathbf{Q}_1\mathbf{Q}_1^H$ gives

$$\boldsymbol{\mathcal{H}}(\mathbf{I} - \mathbf{Q}_1\mathbf{Q}_1^H) = \boldsymbol{\mathcal{P}}\boldsymbol{\mathcal{L}}\boldsymbol{\mathcal{Q}}^H \ . \tag{3.4}$$

Here, the right side of (3.4) has the same form as (3.1), so the algorithm proceeds recursively. Finally, to solve for $\boldsymbol{\Xi}$, equation (3.3) is pre-multiplied by $\boldsymbol{\mathcal{P}}^H$ and post-multiplied by $\mathbf{Q}_1$, giving

$$\boldsymbol{\Xi} = \boldsymbol{\mathcal{P}}^H\boldsymbol{\mathcal{H}}\mathbf{Q}_1 \ . \tag{3.5}$$

The decomposition that achieves equal diagonal elements in each block of $\mathbf{L}$ will be referred to as the block diagonal geometric mean decomposition (BD-GMD).

3.1.2 Diagonal Elements

Consider a BD-GMD decomposition $\mathbf{H} = \mathbf{PLQ}^H$. Let the diagonal element of the k-th block of $\mathbf{L}$ be r_k. To calculate each r_k, equations (3.1) and (3.2) are generalized to get

$$\begin{bmatrix} \widehat{\mathbf{H}}_k \\ \boldsymbol{\mathcal{H}} \end{bmatrix} = \begin{bmatrix} \widehat{\mathbf{P}}_k & \mathbf{0} \\ \mathbf{0} & \boldsymbol{\mathcal{P}} \end{bmatrix} \begin{bmatrix} \widehat{\mathbf{L}}_k & \mathbf{0} \\ \boldsymbol{\Xi} & \boldsymbol{\mathcal{L}} \end{bmatrix} \begin{bmatrix} \widehat{\mathbf{Q}}_k^H \\ \boldsymbol{\mathcal{Q}}^H \end{bmatrix} \tag{3.6}$$

$$\widehat{\mathbf{H}}_k = \widehat{\mathbf{P}}_k\widehat{\mathbf{L}}_k\widehat{\mathbf{Q}}_k^H \ , \tag{3.7}$$

where $\widehat{\mathbf{H}}_k$ represents the combined channel matrix of users 1 to k. The sub-matrices $\widehat{\mathbf{H}}_k$, $\widehat{\mathbf{P}}_k$, $\widehat{\mathbf{L}}_k$ and $\widehat{\mathbf{Q}}_k^H$ each have $\sum_{l=1}^{k} n_l$ rows. Because $\widehat{\mathbf{P}}_k$ and $\widehat{\mathbf{Q}}_k$ have orthonormal columns, equation (3.7) shows that the singular values of $\widehat{\mathbf{H}}_k$ and $\widehat{\mathbf{L}}_k$ must be the

same. Thus,

$$\det(\widehat{\mathbf{H}}_k\widehat{\mathbf{H}}_k^H) = \det(\widehat{\mathbf{L}}_k\widehat{\mathbf{L}}_k^H) = \prod_{l=1}^{k} r_l^{2n_l} \ . \tag{3.8}$$

Therefore, the k-th diagonal element is given by

$$r_k = \sqrt[2n_k]{\frac{\det(\widehat{\mathbf{H}}_k\widehat{\mathbf{H}}_k^H)}{\det(\widehat{\mathbf{H}}_{k-1}\widehat{\mathbf{H}}_{k-1}^H)}} \ . \tag{3.9}$$

3.2 ZF-based Schemes

The previous section introduced the new decomposition for multiuser communications. In this section, transceiver designs based on this decomposition would be described. The following two schemes are ZF-based schemes. This means that they are of a relatively low complexity, and offer a reasonable trade-off between performance and efficiency.

3.2.1 BD-GMD-based DPC Scheme

Having more than one user means that different decompositions can be obtained by changing the encoding order of the users. As a result, different sets of values for the diagonal elements of $\mathbf{L}$ can be obtained. Let $\{\pi_1, \pi_2, \ldots, \pi_K\}$ be the ordering of the users where the previous π_1-th user is now the first user, and so on. Since the ordering of the users results in the ordering of the rows of $\mathbf{H}$, this ordering may also be represented by a permutation matrix $\mathbf{D}$ such that $\mathbf{DH} = \mathbf{PLQ}^H$. Here, the k-th block $\mathbf{P}_k$ of $\mathbf{P}$ has dimensions $n_{\pi_k} \times n_{\pi_k}$. Suppose $\mathbf{s} = [\mathbf{s}_1^T, \cdots, \mathbf{s}_K^T]^T$ is the vector of information symbols to be sent, where $\mathbf{s}_k$ is the corresponding $n_k \times 1$ vector of user k. Write $\mathbf{L} = \mathbf{\Lambda B}$ with $\mathbf{\Lambda} = \mathrm{diag}(\mathbf{L})$, and $\mathbf{B}$ a monic lower triangular

matrix. Multiplying the relation $\mathbf{y} = \mathbf{H}\mathbf{x} + \mathbf{u}$ by $\mathbf{D}$ gives

$$\widetilde{\mathbf{y}} = \mathbf{P}\mathbf{L}\mathbf{Q}^H\mathbf{x} + \widetilde{\mathbf{u}} \,, \tag{3.10}$$

where $\widetilde{\mathbf{y}}$ is the reordered received signal vector. Let $\widetilde{\mathbf{s}} = \mathbf{D}\mathbf{s}$ be the reordered information symbol vector. Using $\mathbf{x} = \mathbf{Q}\widetilde{\mathbf{s}}$ and $\widetilde{\mathbf{z}} = \mathbf{P}^H\widetilde{\mathbf{y}}$ for the transmit and receive equalization respectively transforms the channel to

$$\widetilde{\mathbf{z}} = \mathbf{L}\widetilde{\mathbf{s}} + \widetilde{\mathbf{u}}' \,. \tag{3.11}$$

Now, DPC is performed at the transmitter to pre-subtract the interference represented by $\mathbf{L}$. As a result, user π_k enjoys n_{π_k} independent and equivalent subchannels of the form: $z_i = r_k s_i + u_i$, where r_k is the diagonal element of the k-th block of $\mathbf{L}$. The available transmit power E_s is distributed equally among the N_R subchannels. Then, the achievable sum rate for the scheme is given by

$$C = \sum_{k=1}^{K} n_{\pi_k} \log_2 \left(1 + \frac{E_s}{N_0 N_R} r_k^2\right). \tag{3.12}$$

Figure 3.1 shows the block diagram of the BD-GMD-based scheme that performs user ordering and uses THP instead of DPC. Here, $\mathbf{P}_k^H$ is the k-th sub-block of the block diagonal unitary matrix $\mathbf{P}^H$. To improve the performance of the scheme, different constellations can be applied to the users. The base station and mobile users decide *a priori* on a fixed set of constellations to use. Before data transmission over a block period of time, the BS informs each user which constellation to apply, depending on the performance of their channels. The user then uses the same constellation for all his subchannels since the subchannels have identical SNRs. In certain scenarios, it may be better to use a modified form of the BD-GMD that involves subchannel selection. The reason is similar to that of the

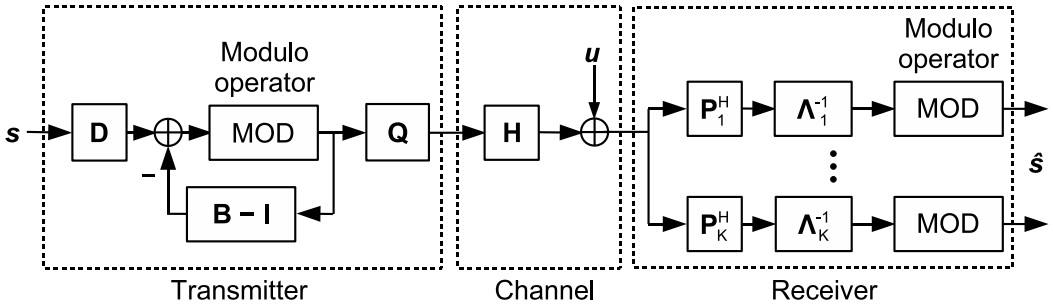

Figure 3.1: Block diagram of BD-GMD-based scheme with user ordering and THP.

subchannel selection principle for the single-user GMD [72]. Additionally, in the case of multiuser communications, subchannel selection for one user may actually provide a better performance for later encoded users, due to the provision of more spatial degrees of freedom. For conciseness and clarity, subchannel selection will not be further developed in this chapter. However, this is an interesting concept that could be considered in future works.

Ordering for the BD-GMD-based Scheme

From Section 2.2.3, it is seen that the i-th diagonal element corresponds to the channel gain of the i-th subchannel. Here, assume that $\mathbf{H}$ contains i.i.d. Gaussian entries. Now, the diagonal elements of $\mathbf{L}$ will usually be in decreasing order, because $\mathbf{L}\mathbf{Q}^H$ is the QR-decomposition of $\mathbf{P}^H\mathbf{H}$. The first diagonal element can often be many times that of the last one. Thus, the first subchannel usually enjoys much better performance than the last subchannel. Equation (3.9) tells us that the diagonal elements r_k depend on the ordering of the rows of $\mathbf{H}$ or, in other words, the ordering of the users. The hope is to improve the fairness of the scheme by ordering the users to increase the size of the last few diagonal elements.

A method inspired by the BLAST [98] ordering is used. First, note that $\det(\widehat{\mathbf{H}}_{k-1}\widehat{\mathbf{H}}_{k-1}^H)$ does not change with the order of the rows of $\widehat{\mathbf{H}}_{k-1}$. Thus, from (3.9), it is seen that the value of r_K depends only on the choice of $\mathbf{H}_K$ and not the order of the first $K-1$ users. Therefore, to maximize r_K, $\mathbf{H}_K$ is chosen to

maximize (3.9). Following that, $\mathbf{H}_{K-1}$ is chosen to maximize (3.9), and so on. The decomposition that optimizes the diagonal elements in such a way is called the *ordered* BD-GMD. For the BD-GMD-based scheme, this ordering tends to increase the user fairness.

3.2.2 Equal-Rate BD-GMD Scheme

While BD-GMD achieves equal rates for the sub-channels of each user, the achievable rates between different users vary greatly. In this section, equal rates for all subchannels across all the users is achieved by relying on optimal transmit power control. This is the Equal-Rate BD-GMD scheme. It maximizes the sum rate while ensuring overall equal rates.

Following the example of Section 3.2.1, we will now construct a ZF-based scheme which maximizes the achievable sum rate given overall equal rates. Let $\mathbf{F}$, $\mathbf{J}$ and $\mathbf{A}$ be the pre-equalization, interference and receive equalization matrices respectively of a general equal-rate ZF-based scheme. Let α be the subchannel gain which is identical for all the subchannels. To optimize the achievable sum rate, we only need to maximize the channel gain:

$$\begin{aligned} \text{maximize} \quad & \alpha \\ \text{subject to} \quad & \mathbf{J} \in \mathbb{L} \ , \ \mathbf{A} \in \mathbb{B} \ , \\ & \mathbf{AHF} = \alpha \mathbf{J} \ , \\ & \mathrm{Tr}(\mathbf{F}^H \mathbf{F}) \leq E_s \ , \\ & \|\mathbf{A}(i,:)\|_2 = 1 \qquad \text{for } 1 \leq i \leq N_R \ . \end{aligned} \tag{3.13}$$

where $\mathbb{L}$ is the set of all monic lower triangular matrices and $\mathbb{B}$ is the set of all block diagonal matrices in which the k-th block is a $n_k \times n_k$ sub-matrix. The solution of this problem is by channel inversion, as the following theorem shows.

Theorem 1. *Suppose* $\det(\mathbf{H}\mathbf{H}^H) \neq 0$. *Let* $\mathbf{H} = \mathbf{P}\mathbf{L}\mathbf{Q}^H$ *be the BD-GMD of* $\mathbf{H}$, *and let* $\mathbf{\Lambda} = \mathrm{diag}(\mathbf{L})$. *Then, the optimization problem (3.13) is solved by*

$$\begin{aligned} \mathbf{F} = \alpha\mathbf{Q}\mathbf{\Lambda}^{-1}, \quad \mathbf{J} = \mathbf{L}\mathbf{\Lambda}^{-1}, \\ \mathbf{A} = \mathbf{P}^H, \quad \alpha = \sqrt{\frac{E_s}{\mathrm{Tr}(\mathbf{\Lambda}^{-2})}} \ . \end{aligned} \tag{3.14}$$

Proof. See Appendix A. □

Using the pre-equalization and receive equalization matrices given in Theorem 1, the channel becomes $\mathbf{z} = \alpha\mathbf{J}\mathbf{s} + \mathbf{u}'$. DPC is then done at the transmitter to cancel the interference. As a result, every user enjoys independent and equivalent subchannels of the form $z = \alpha s + u$. The achievable sum rate for the scheme is given by

$$C = N_R \log_2(1 + {N_0}^{-1}\alpha^2) \ . \tag{3.15}$$

Given a fixed order of users, Theorem 1 tells us that the above Equal-Rate BD-GMD scheme optimizes the zero-forcing linear beamforming vectors and power allocation required to achieve maximum throughput and equal rates for every subchannel of every user.

Ordering for the Equal-Rate BD-GMD Scheme

Some improvement in performance can be expected by ordering the users appropriately. From (3.14), we have

$$\alpha^2 = \frac{E_s}{\mathrm{Tr}(\mathbf{\Lambda}^{-2})} = \frac{E_s}{\sum_{k=1}^{K} n_k r_k^{-2}} \ , \tag{3.16}$$

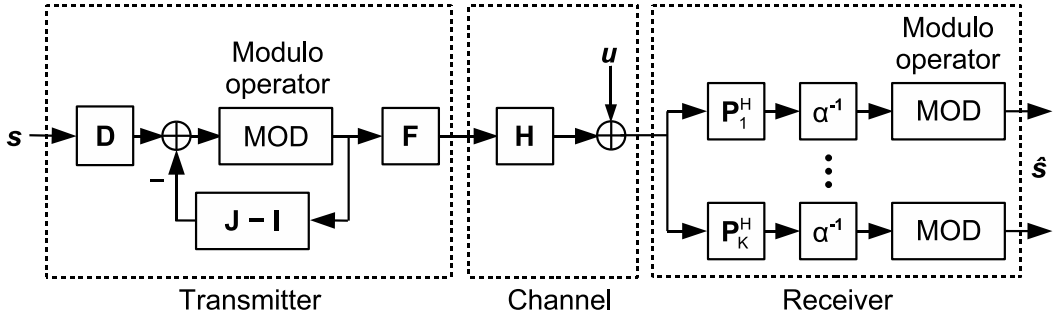

Figure 3.2: Block diagram of equal-rate BD-GMD scheme with user ordering and THP.

where r_k is the diagonal element of the k-th block of $\mathbf{\Lambda}$. Hence, given the constraint that $\prod_{k=1}^{K} r_k^{2n_k} = \det(\mathbf{H}\mathbf{H}^H)$ is constant, (3.16) is maximized when the r_k's are equal. In general, the channel gain α increases when the spread among $\{r_k\}_{k=1}^{K}$ decreases. This can be accomplished by using the *ordered* BD-GMD which reduces the gap between the largest and smallest diagonal elements of $\mathbf{\Lambda}$. The ordering described in Section 3.2.1 is near-optimal for maximizing the sum rate, for the case where $\mathbf{H}$ contains i.i.d. Gaussian entries. The best ordering may be found by an exhaustive search. Figure 3.2 shows the block diagram of an Equal-Rate BD-GMD scheme that applies the ordered BD-GMD. As before, THP is used in this scheme.

3.3 MMSE-based Schemes

The previous section described ZF-based schemes. In this section, two MMSE-based schemes are introduced. These schemes would have improved performance over the ZF-based schemes, but at the cost of a moderately higher complexity. At high SNRs, the sum rates of the ZF-based schemes approach that of the MMSE-based schemes.

3.3.1 BD-UCD Scheme

In this section, a DPC scheme that is block-equal-rate and achieves the broadcast channel capacity is constructed. The idea is to first design a capacity-achieving MMSE-DFE scheme that generates subchannels with identical SINRs for each user by choosing an appropriate precoder $\mathbf{F}$. Then, the results from Section 2.3.1 gives us the dual DPC scheme. This BD-UCD scheme is capacity-achieving and ensures equal rates per block.

We begin with the dual uplink channel from Section 2.3.1. Let $\bar{\mathbf{F}}$ be a linear precoder for this uplink channel that achieves its sum-capacity, i.e. $\bar{\mathbf{F}}$ solves the optimization problem in (2.12). Different methods of solving this problem are described in [79], including Jindal et al.'s sum power iterative water-filling algorithm which will be used in this chapter. Note that for any block diagonal unitary $\bar{\mathbf{P}}$, the precoder $\bar{\mathbf{F}}\bar{\mathbf{P}}$ gives the same sum-capacity as $\bar{\mathbf{F}}$. It remains for us to choose $\bar{\mathbf{P}}$ such that the MMSE-DFE scheme using the precoder $\mathbf{F} = \bar{\mathbf{F}}\bar{\mathbf{P}}$ is block-equal-rate. From (2.3), this is equivalent to finding $\bar{\mathbf{P}}$ such that the QR decomposition

$$\begin{bmatrix} \mathbf{H}^H\bar{\mathbf{F}}\bar{\mathbf{P}} \\ \sqrt{N_0}\mathbf{I} \end{bmatrix} = \begin{bmatrix} \mathbf{Q}_u \\ \mathbf{Q}_d \end{bmatrix} \mathbf{\Lambda}\mathbf{B} \tag{3.17}$$

gives a $\mathbf{\Lambda}$ whose diagonal elements are equal in blocks of $n_1, \ldots, n_K$ elements respectively. Following [73], rewrite the left hand side of (3.17) as

$$\begin{bmatrix} \mathbf{I} & \mathbf{0} \\ \mathbf{0} & \bar{\mathbf{P}}^H \end{bmatrix} \begin{bmatrix} \mathbf{H}^H\bar{\mathbf{F}} \\ \sqrt{N_0}\mathbf{I} \end{bmatrix} \bar{\mathbf{P}} \ . \tag{3.18}$$

Consider the BD-GMD of the middle term

$$\begin{bmatrix} \mathbf{H}^H\bar{\mathbf{F}} \\ \sqrt{N_0}\mathbf{I} \end{bmatrix}^H = \mathbf{PLQ}^H \ , \tag{3.19}$$

where $\mathbf{P}$ is block diagonal, $\mathbf{L}$ is lower triangular, and both $\mathbf{P}$ and $\mathbf{Q}$ have orthonormal columns. Consequently, (3.17) becomes

$$\begin{bmatrix} \mathbf{I} & \mathbf{0} \\ \mathbf{0} & \bar{\mathbf{P}}^H \end{bmatrix} \mathbf{QL}^H\mathbf{P}^H\bar{\mathbf{P}} = \begin{bmatrix} \mathbf{Q}_u \\ \mathbf{Q}_d \end{bmatrix} \mathbf{\Lambda B} \ . \tag{3.20}$$

Hence, we can choose $\bar{\mathbf{P}} = \mathbf{P}$, $\mathbf{\Lambda B} = \mathbf{L}^H$ and $\mathbf{Q}_u$ to be the top N_T rows of $\mathbf{Q}$. This gives us our desired capacity-achieving block-equal-rate MMSE-DFE scheme.

The dual DPC scheme that is block-equal-rate and capacity-achieving can now be constructed. Figure 2.5 shows the block diagram of this scheme using THP. Using the duality technique in Section 2.3.1, the pre-equalization, interference and nulling matrices are

$$\begin{aligned} \widetilde{\mathbf{F}} &= \mathbf{Q}_u\mathbf{\Lambda}^{-1}\mathbf{D}_c^{-1}\mathbf{D}_q \ , \\ \widetilde{\mathbf{B}} &= \mathbf{D}_c\mathbf{D}_q^{-1}\mathbf{L}\mathbf{\Lambda}^{-1}\mathbf{D}_c^{-1}\mathbf{D}_q \ , \\ \widetilde{\mathbf{W}} &= \bar{\mathbf{F}}\mathbf{P}\mathbf{D}_q^{-1}\mathbf{D}_c \ , \end{aligned} \tag{3.21}$$

where $\mathbf{D}_q$ is calculated from the matrix equation (2.19) and $\mathbf{D}_c$ contains the column norms of $\mathbf{Q}_u\mathbf{\Lambda}^{-1}$. To speed up the calculation of $\mathbf{D}_q$, (2.5) can be used instead of (2.17) to compute ρ_i, as both give identical results. This dual DPC scheme is called the block diagonal UCD (BD-UCD), since the special single-user case of $K = 1$ is the UCD scheme in [73]. Its sum-capacity, as shown by (2.24), is precisely the broadcast channel sum-capacity.

For the BD-UCD scheme, the bulk of the complexity lies in the initial sum

power iterative water-filling algorithm [79]. Following that, the BD-GMD processing and the conversion from uplink to downlink are straightforward and non-iterative.

3.3.2 Equal-Rate BD-UCD Scheme

In this section, a near-optimal DPC scheme for the broadcast channel that generates decoupled subchannels all with identical SINRs will be constructed. This Equal-Rate BD-UCD scheme maximizes the sum rate given overall equal rates. This construction can be generalized to other rate constraints for the users. The crux lies in choosing the right uplink precoder $\bar{\mathbf{F}}$ so that the method in Section 3.3.1 produces the desired equal-rate scheme. The resulting scheme is called the *Equal-Rate* BD-UCD. The rest of this section will focus on finding this precoder. Let $\mathbf{H}^H = [\mathbf{H}_1^H, \mathbf{H}_2^H, \ldots, \mathbf{H}_K^H]$ be the uplink channel, where each $\mathbf{H}_k^H$ has n_k columns. Let $\bar{\mathbf{F}}_k$ be the k-th block of the block diagonal $\bar{\mathbf{F}}$. Then, the rate of user k, where user K is decoded first, is [75]

$$R_k = \log \frac{\det(\mathbf{I} + \frac{1}{N_0} \sum_{l \leq k} \mathbf{H}_l^H \bar{\mathbf{F}}_l \bar{\mathbf{F}}_l^H \mathbf{H}_l)}{\det(\mathbf{I} + \frac{1}{N_0} \sum_{l < k} \mathbf{H}_l^H \bar{\mathbf{F}}_l \bar{\mathbf{F}}_l^H \mathbf{H}_l)} \ . \tag{3.22}$$

Ideally, for each k, $R_k = n_k \bar{R}$ for some $\bar{R}$, and $\mathrm{Tr}(\bar{\mathbf{F}}\bar{\mathbf{F}}^H) \leq E_s$. The goal is to find $\bar{\mathbf{F}}$ such that $\bar{R}$ is maximized. While [87] has solved the symmetric capacity maximization, the scheme proposed here adds a further constraint that for any particular user, its subchannels have equal SINRs. The symmetric capacity maximizing solution would require time-sharing between schemes with different encoding orders. However, in order to minimize the complexity for our scheme, only a single decoding order is chosen, which may be suboptimal. In this section, the general equal-rate problem is solved with a fixed user ordering. A near-optimal algorithm of low complexity inspired by [91] and [79] is proposed below.

The basic building block of the algorithm is as follows: given a target rate $\bar{R}$,

find a precoder $\bar{\mathbf{F}}$ that achieves the rate $\bar{R}$ for every subchannel with minimum power. Using a trick from [79], rewrite (3.22) as

$$n_k \bar{R} = \log\det(\mathbf{I} + \frac{1}{N_0}\mathbf{G}_k \bar{\mathbf{F}}_k \bar{\mathbf{F}}_k^H \mathbf{G}_k^H) \ , \tag{3.23}$$

where $\mathbf{G}_k = (\mathbf{I} + \frac{1}{N_0}\sum_{l<k} \mathbf{H}_l^H \bar{\mathbf{F}}_l \bar{\mathbf{F}}_l^H \mathbf{H}_l)^{-1/2}\mathbf{H}_k$ is the equivalent channel with the interference of all the other users. Thus, if $\mathbf{G}_k$ is given, then the minimum power $\bar{\mathbf{F}}_k$ satisfying (3.23) can be found by water-filling over it. Since $\mathbf{G}_k$ only depends on $\bar{\mathbf{F}}_l$ for $l < k$, equation (3.23) can be solved successively from $k = 1$ to $k = K$. Of course, to find the $\bar{\mathbf{F}}$ with minimum power satisfying the equations in (3.23) for all k, the $\bar{\mathbf{F}}_k$'s may need to be optimized jointly using iterative methods. However, to avoid incurring a high complexity cost, the above non-iterative algorithm will suffice for now. Let $\mathrm{P}(\bar{R})$ be the power $\mathrm{Tr}(\bar{\mathbf{F}}\bar{\mathbf{F}}^H)$ of the precoder $\bar{\mathbf{F}}$ computed by the above algorithm for a target rate ($\bar{R}$). The algorithm can now be completed by iteratively finding $\bar{R}$ such that $\mathrm{P}(\bar{R}) = E_s$. Since there is a near-linear relation between $\bar{R}$ and $\log \mathrm{P}(\bar{R})$, a simple numerical method like the secant method can be used. Simulations show that convergence is typically achieved in less than six iterations.

Compared to the Equal-Rate BD-GMD scheme, the Equal-Rate BD-UCD scheme has a higher complexity due to the initial step of successive water-filling.

3.4 Simulation Results

In this section, computer simulation results are presented to evaluate the performance of the four schemes proposed in this chapter. In the simulations, the $12 \times \{4, 4, 4\}$ setup for the broadcast channel is considered. The elements of the channel matrix $\mathbf{H}$ are assumed to be independent and CSCG with zero mean and unit variance. The SNR (dB) is defined as $10\log_{10}\frac{E_s}{N_0}$. The results are based on

3000 Monte Carlo realizations of $\mathbf{H}$. To compute the BER curves illustrated in Figures 3.3, 3.4 and 3.7, THP is applied for interference pre-subtraction at the transmitter. The transmit power is scaled down by a factor of $(M-1)/M$ for M-QAM to account for the THP precoding loss. All the schemes shown use 16-QAM unless otherwise indicated. The table below gives a summary of the schemes discussed in this chapter, with italics to indicate the new proposed schemes. Existing schemes are the ZF-DPC [92], the Equal-Rate ZF-DPC [93], and the MMSE-DPC [77] schemes.

	ZF-based		**MMSE-based**	
	Block-equal-rate	Equal-rate	Block-equal-rate	Equal-rate
Single User	GMD-DPC		UCD-DPC	
Multiple Users				
- Single Antenna	ZF-DPC	ER-ZF-DPC	MMSE-DPC	-
- Multiple Antennas	*BD-GMD-DPC*	*ER-BD-GMD-DPC*	*BD-UCD-DPC*	*ER-BD-UCD-DPC*

3.4.1 ZF-based Schemes

The ZF schemes are the BD-GMD-based scheme and the Equal-Rate BD-GMD scheme. In the figures, the solid lines represent the new schemes while the dotted ones represent conventional schemes. Also, the squares and triangles indicate block-equal-rate schemes, while the circles indicate equal-rate ones. In Figures 3.4 and 3.5, all the schemes implement user ordering.

Figure 3.3 shows the gains in BER performance due to ordering users in the scheme. The unordered schemes are represented by shapes with crosses. Both the ordered BD-GMD and ordered Equal-Rate BD-GMD showed an improvement of about 1 dB at BER of 10^{-4} over their unordered counterparts respectively. The improvement is more appreciable for the Equal-Rate ZF-THP [93], with a gain of 6 dB even at BER of 10^{-3}. This gain in BER performance is due primarily to the improvement that user ordering has on the channel gain of the worst subchannel

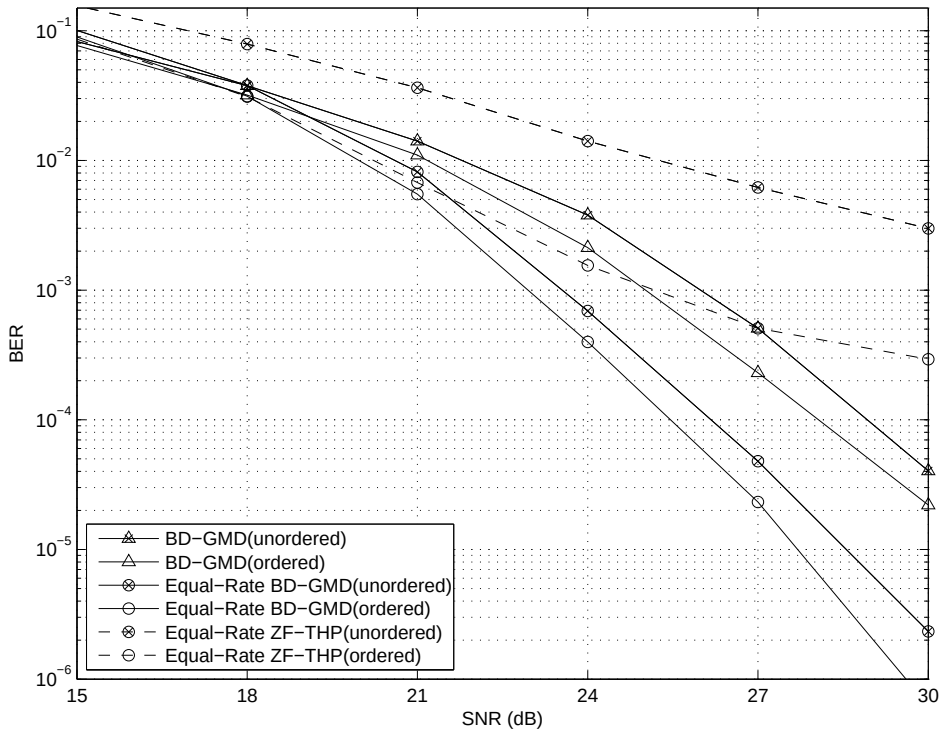

Figure 3.3: BER performance comparison for ordered and unordered ZF-based schemes using THP and 16-QAM.

whose BER constitutes a major part of the average BER. Figure 3.4 demonstrates the effect of using different constellations on BER performance. 16-QAM is used for every user, unless "64,16,4-QAM" is stated, where the user with the largest channel gain is assigned 64-QAM, the next user 16-QAM, and the last user 4-QAM. (For simplicity, this assignment is fixed.) As expected, the BD-GMD(64,16,4-QAM) experiences a gain of 3 dB at BER of 10^{-5} over the BD-GMD, because in the latter scheme, the BER performance is dominated by the weakest user. The ZF-THP(64,16,4-QAM) sees an improvement of more than 4 dB at BER of 10^{-3} over the ZF-THP. These gains are achieved without significant increase in receiver complexity. Although the chosen combination of 64,16,4-QAM may not be optimal, by fitting the users with appropriate constellations to suit their channel gains, higher data rates can be achieved.

Figure 3.4 also highlights the significant improvement in BER performance of

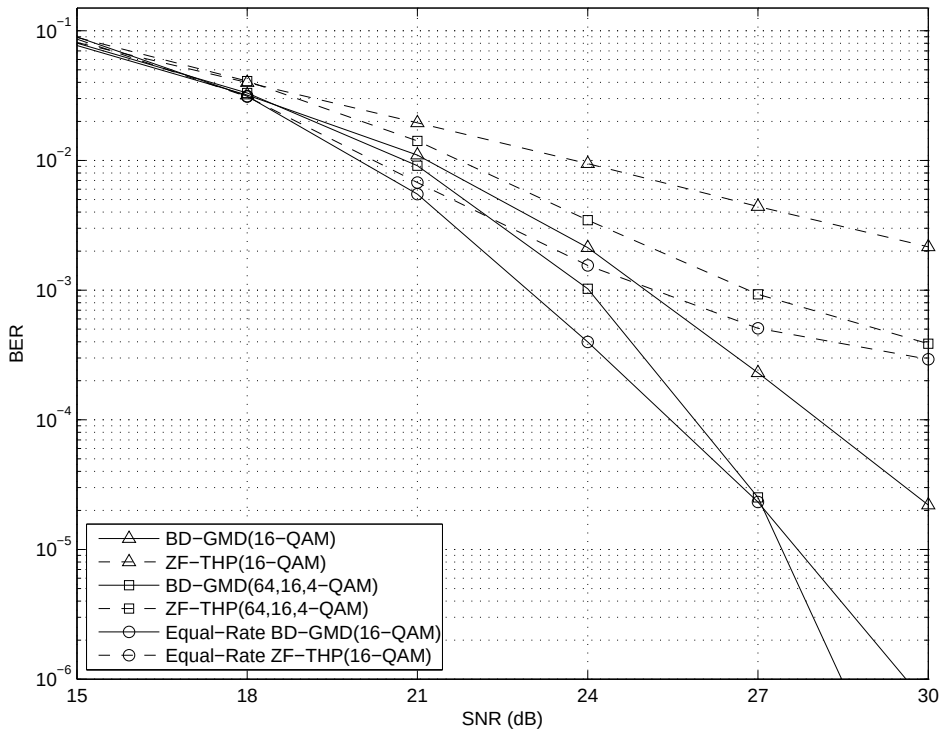

Figure 3.4: Effect of receiver equalization on BER performance of ZF-based schemes using THP and user ordering.

the new schemes over the conventional ones. The BD-GMD shows a gain of more than 6 dB at BER of 10^{-3} over the ZF-THP, because the BER performance is dominated by the weakest subchannel in the latter scheme. Also, the Equal-Rate BD-GMD also gained more than 6 dB at BER of 10^{-4} over the Equal-Rate ZF-THP. At high SNRs, the steeper gradients of the BER curves for the new schemes is evidence of the diversity gain which resulted from linear equalization at the receivers. Figure 3.5 shows that the achievable sum rates of the new schemes are negligibly less than that of the conventional schemes. While equalization at the mobile users' side help to increase the achievable sum rates for the block diagonal schemes, there is more freedom for row ordering in the conventional schemes ($12! \approx 4.8 \times 10^8$ possible permutations) than for user ordering in the block diagonal schemes ($3! = 6$ possible permutations). The gain from ordering slightly overrides the advantage from receiver equalization. Finally, the performance of

the equal-rate schemes is also compared with that of the block-equal-rate ones in Figure 3.4. The Equal-Rate BD-GMD shows a gain of 3 dB at BER of 10^{-5} over the BD-GMD. For the conventional Equal-Rate ZF-THP, the gain is even larger, with more than 6 dB improvement at BER of 10^{-3} over the ZF-THP. Note that for the equal-rate schemes, the BER performance of every user is the same as that shown in the figures, while for the block-equal-rate schemes, the BER curve is more indicative of the performance of the worst user. Thus, the gains described above represents the improvements experienced by the worst user when an equal-rate criterion is imposed. From Figure 3.5, the additional equal-rate criteria causes a slight loss of 1 dB in achievable sum rate. This loss is due to the allocation of more power to the worst user in order to fulfill the equal-rate criterion.

Another scheme can be obtained by performing successive SVDs and channel projections [94]. If the user ordering and subchannel selections are optimized, this MIMO scheme is expected to have a higher achievable sum rate than both the BD-GMD and the ZF-DPC schemes. This is because there are no equal rate constraints and multi-antenna equalization is permitted at each user's receiver. However, as mentioned in the beginning of this chapter, SVD-based schemes such as this generate subchannels, with diverse SNRs, for which variable-rate coding has to be applied. If the same MCS is used for all the subchannels, the BER performance would be dominated by the weakest subchannel.

Yet another multiuser MIMO scheme involves dominant eigenmode transmission [95]. Due to the use of only one data stream per user, this scheme would experience less sum rate than the BD-GMD and ZF-DPC schemes at high SNR. At low SNR, dominant eigenmode transmission may have higher sum rate than the BD-GMD scheme, if the latter scheme does not incorporate subchannel selection, which will be discussed in Chapter 4. The BER simulations for the BD-GMD scheme assumes 16 bit/sec/Hz for each user, so the performance of dominant

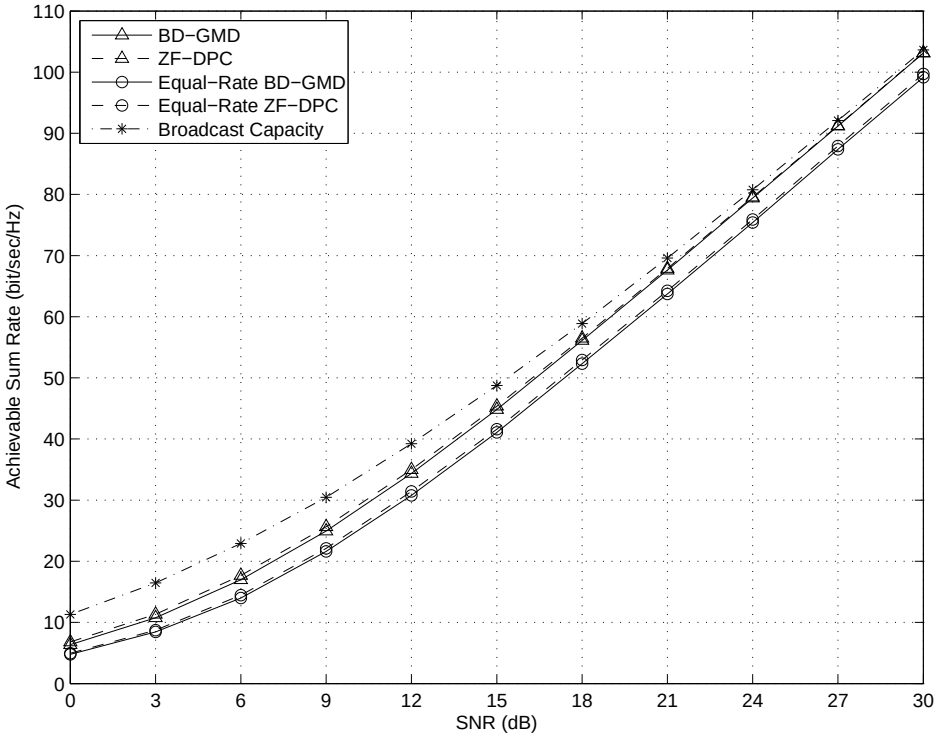

Figure 3.5: Achievable sum rate for ZF-based schemes with DPC and user ordering.

eigenmode transmission, requiring 65536-QAM, is expected to be poorer than the BD-GMD scheme.

3.4.2 MMSE-based Schemes

The MMSE schemes are the BD-UCD and the Equal-Rate BD-UCD. In Figures 3.6 and 3.7, the solid lines represent the ZF-based schemes, while the dashed lines represent the MMSE-based ones. Again, the triangles indicate the block-equal-rate schemes and the circles the equal-rate ones.

In Figure 3.6, there is only a tiny improvement in achievable sum rate of the BD-UCD over the MMSE-DPC. This can be understood by studying the effect of pre-equalization on the dual uplink channel capacity. The power loading aspect of pre-equalization has a much greater effect on capacity than the beam-forming aspect. Thus, in the dual broadcast case, although MMSE-DPC does not enjoy

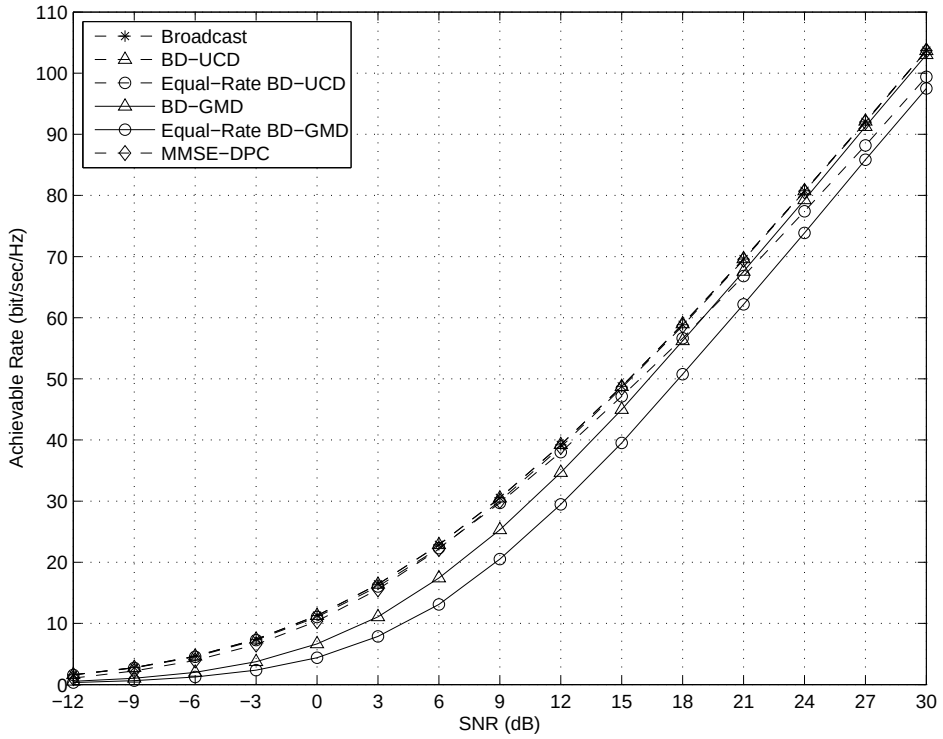

Figure 3.6: Comparison of achievable sum rate for ZF-based and MMSE-based schemes.

equalization at the receivers, it does not suffer any significant loss in capacity. However, in Figure 3.7, the BD-UCD shows a dramatic improvement in BER performance over the MMSE-THP, with more than 6 dB gain at BER of 10^{-3}, because BER performance is largely affected by the weakest subchannel in the latter scheme. The higher slope of the BD-UCD compared to the MMSE-THP is due to the diversity gain afforded by linear equalization at the receivers.

Next, the advantage of using a MMSE-based scheme against its ZF-based counterpart is shown. The BD-UCD enjoys a slight 1.5 dB gain in achievable sum rate over the BD-GMD at the low SNR region. As expected, their performance converges with increasing SNR. Similarly, the achievable sum rates of the Equal-Rate BD-GMD and Equal-Rate BD-UCD converge at high SNR. In terms of BER performance, the effect of error minimization is seen more clearly. In Figure 3.7, the BD-UCD consistently shows a 2 dB gain in BER performance over the BD-GMD

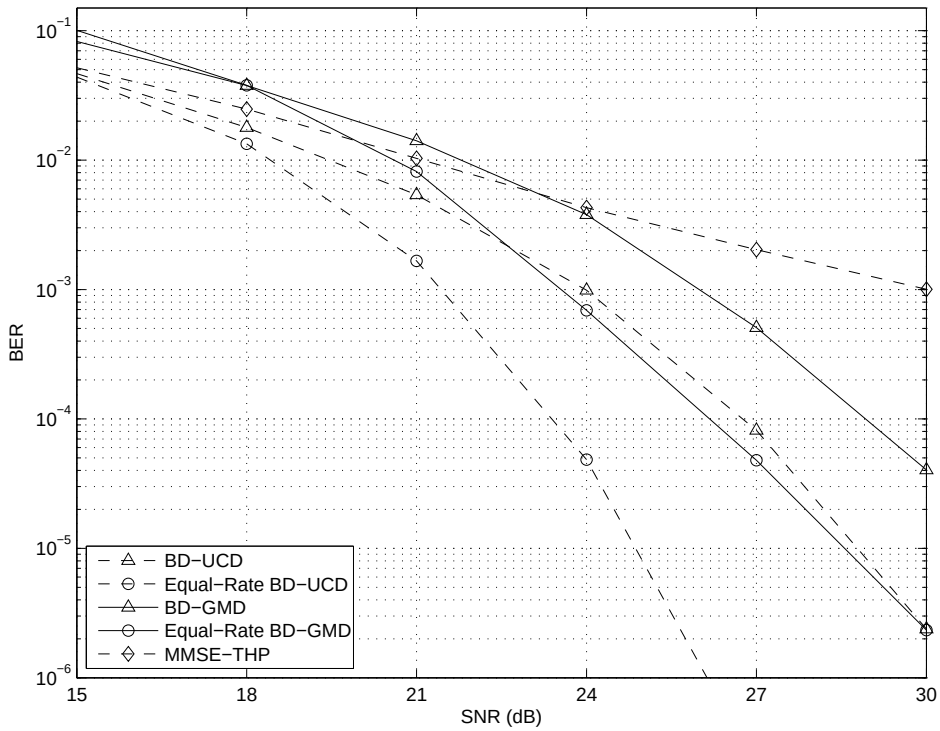

Figure 3.7: BER performance comparison for ZF-based and MMSE-based schemes using THP and 16-QAM.

at all SNRs. Meanwhile, the Equal-Rate BD-UCD shows an improvement of as much as 4.5 dB over the Equal-Rate BD-GMD at BER of 10^{-6}. Finally, the feasibility of providing equal rates for all users is studied. In Figure 3.6, it is seen that the Equal-Rate BD-UCD achieves the same sum rates as the BD-UCD at low SNR. Capacity in this SNR region is affected more by noise than by equal-rate constraints. At high SNR, the Equal-Rate BD-UCD only suffers a 1.5 dB loss. This also shows that the near-optimal iterative beamforming algorithm in Section 3.3.2 does not experience much performance loss. In Figure 3.7, the Equal-Rate BD-UCD demonstrates its superior BER performance over the BD-UCD, with about 4 dB gain at BER of 10^{-5}. This is because its worst subchannel is greatly elevated by the equal-rate constraint.

3.5 Summary

We have proposed a novel block diagonal geometric mean decomposition (BD-GMD) for the MIMO broadcast channel. Using this decomposition, each user obtains spatial subchannels with *identical* channel gains. This allows the use of equal-rate coding which has benefits for the system implementation, especially in the design of modulation and coding schemes. Four applications based on the BD-GMD were proposed: BD-GMD, Equal-Rate BD-GMD, BD-UCD, and Equal-Rate BD-UCD, all of which apply DPC at the transmitter for interference pre-subtraction. The first two schemes are ZF-based schemes, while the later two are MMSE-based. Also, for each ZF and MMSE case, the first scheme is block-equal-rate, where the channel gains for the subchannels of different users may be different, while the second scheme is equal-rate, where the channel gains are the same across all subchannels of all users. In the ZF schemes, user ordering is exploited to gain improvements in achievable sum rates and user fairness. The optimal power allocation needed to provide equal rates for every user was also derived. As for the MMSE schemes, the BD-UCD achieves the broadcast channel capacity, while the Equal-Rate BD-UCD provides all users with equal rates without much loss of sum rate. Simulation results have shown that the new schemes exhibit excellent BER properties as compared to conventional schemes.

Chapter 4

Efficient Power Minimization for MIMO Broadcast Channels

The previous chapter covered rate maximizing schemes given a sum power budget. The corresponding problem to be addressed in this chapter is power minimization given each user's data rate requirement. This problem is of significance because users normally subscribe to services of dissimilar data rates and users experience diverse channel strengths due to their random locations within the cell in a cellular system. Consequently, resource allocation is vital in ensuring that these users' requirements are met while keeping the transmit sum power low to minimize the interference ingress into neighbouring cells. Another benefit realized is the reduction of power consumption at the base station.

Given complete CSI at the transmitter, the problem of power minimization using DPC for the MIMO BC has been solved optimally in [87–89]. [88] solves the sum power minimization problem for the fading broadcast channel by using a dual decomposition. For an initial vector of Lagrange multipliers, the Lagrangian is minimized. Following that, the Lagrange multipliers are updated iteratively by the ellipsoid method. [87] obtains the differentiated capacity for an initial sum power. This involves a weighted sum rate maximization using a steepest-descent

algorithm [86]. A bisection search is then used to find the minimum sum power. [89] starts with a weighted sum rate maximization for an initial weight vector and an initial sum power. The iterations involve an inner loop, where the weight vector is updated, and an outer loop, where the power is updated by a one-dimensional bisection search. The oscillations near the end are used to derive the time-sharing rate points. For these papers, DFE is assumed at the BS for the dual uplink, and equivalently, DPC is used at the BS during the downlink. Time-sharing between the different decoding/encoding orders is required when the target rate-tuple lies on the convex hull of the respective vertices in the capacity region. The time-sharing scheme can be solved by a linear program [89]. Moreover, [90] satisfies both rate and BER requirements by considering the SNR gap-to-capacity and the concept of virtual rates.

These methods are known as interference-balancing (IB) because they take noise into account and allow interference between users/subchannels. Therefore, both IUI and ISI are present. A substantial number of iterations have to be performed before the optimal solution is found. Each iteration itself may contain a large amount of computation that may not be visible from a simple complexity order expression. Additionally, the number of iterations required for handling each channel realization is random and not easily predictable. The high complexities of these methods pose difficulties in designing real-time implementations. Therefore, the focus of this chapter is to design a non-iterative solution of low complexity. The problem of MIMO BC power minimization is formulated as a zero-forcing (ZF) DPC problem. As a result, all subchannels are decoupled and there exists no interference between the users or the subchannels. This ZF scenario is considered as it permits a closed-form solution for the power minimization.

Furthermore, subchannels with identical SNRs are created for each user. This allows for equal-rate modulation, which is useful where there is a restriction on

constellation size in wireless links. For example, very higher order modulation may be required for good subchannels when using a communication strategy based on SVD. On the other hand, balancing the SNRs across the subchannels enables the use of small QAM constellation for each subchannel, which is more practical in the presence of phase noise and synchronization errors.

There are two parts to this chapter. In the first part, MIMO BC power minimization without subchannel selection is studied. By doing so, it is shown that the optimum user encoding order can be found efficiently. Near-optimal user ordering can also be found with further reduced complexity. In the second part, MIMO BC power minimization with subchannel selection is studied. Thus, both user ordering and subchannel selection are derived to minimize the sum power subject to rate requirements. Simulations show that a sum power close to that of the optimal IB solution can be achieved using our efficient technique.

4.1 Power Minimization Without Subchannel Selection

Firstly, for a fixed user ordering, the problem of downlink power minimization using ZF-DPC is solved without the use of subchannel selection. Next, the optimal encoding order is derived. Although this may be suboptimal compared to the ordering found for the IB-optimal solution, the main advantage is that this ordering can be computed with a finite and predictable complexity, and has been shown to be computed much faster than that for the IB solution.

In order to reduce the complexity even further, three more simplified methods are proposed to find the user ordering that approach the performance of this ZF-optimal ordering. It is seen that by combining the three simplified methods, the power for the ZF-optimal solution can be reached very closely.

4.1.1 Channel Model

Given a cellular system with one BS and K mobile users, consider the *broadcast channel* from the BS to the mobile users. The BS is equipped with N_T antennas, and the k-th mobile user has n_k antennas. Let $N_R = \sum_{k=1}^{K} n_k$ be the total number of receive antennas, where $N_T \geq N_R$. The input-output relation can be represented as

$$\mathbf{y} = \mathbf{H}\mathbf{x} + \mathbf{u} \ , \tag{4.1}$$

where $\mathbf{x} \in \mathbb{C}^{N_T \times 1}$ is the transmit signal vector at the BS, $\mathbf{y} \in \mathbb{C}^{N_R \times 1}$ is the receive signal vector with $\mathbf{y} = [\mathbf{y}_1^T, \cdots, \mathbf{y}_K^T]^T$, and each $\mathbf{y}_k \in \mathbb{C}^{n_k \times 1}$ is the receive signal vector of user k. Multiplexing is considered, where user k has n_k data-bearing subchannels. The SNR for every subchannel of user k is set equal to γ_k. $\mathbf{H} = [\mathbf{H}_1^T, \ldots, \mathbf{H}_K^T]^T$, where each $\mathbf{H}_k \in \mathbb{C}^{n_k \times N_T}$ is the channel of user k. Assume that the noise vector $\mathbf{u}$ has independent and identically distributed (i.i.d.) zero-mean circularly symmetric complex Gaussian (CSCG) elements with $\mathbb{E}[\mathbf{u}\mathbf{u}^H] = N_0\mathbf{I}$, and $\mathbf{u}$ is independent of $\mathbf{x}$. Assume also that $\mathbb{E}[\|\mathbf{x}\|_2^2] = E_s$. Denote this downlink model by $N_T \times [n_1, \ldots, n_K]$.

4.1.2 Power Minimization for a Fixed Arbitrary Ordering

In this section, a ZF-based block-equal-rate transceiver scheme that applies DPC at the transmitter and allocates power according to SNR requirements is presented. Since there is a simple relationship between the rate and the SNR for each subchannel,

$$R_k = \log_2(1 + \rho_k) \ , \tag{4.2}$$

rate requirements can easily be translated into SNR requirements. First assume that the encoding order of the users has been determined. This scheme minimizes the transmit power with the constraint of zero IUI and zero ISI. Linear receive equalization is performed by a block diagonal matrix $\mathbf{A}$, where $\mathbf{A} = \text{blkdiag}(\mathbf{A}_1, \mathbf{A}_2, \ldots, \mathbf{A}_K)$, and each block $\mathbf{A}_k$ is the receive equalization matrix of user k. It has been shown in Section 3.1 that a BD-GMD can be done on a matrix $\mathbf{H}$ such that

$$\mathbf{H} = \mathbf{PLQ}^H \ , \tag{4.3}$$

where $\mathbf{P} = \text{blkdiag}(\mathbf{P}_1, \mathbf{P}_2, \ldots, \mathbf{P}_K)$, each $\mathbf{P}_k$ is $n_k \times n_k$ unitary, $\mathbf{Q}^H\mathbf{Q} = \mathbf{I}_{N_R}$, and $\mathbf{L}$ is a square lower triangular matrix with elements equal in blocks of $n_1, \ldots, n_K$ elements (termed "block-equal-diagonal").

The problem of power minimization can be formulated as

$$\begin{aligned} \text{minimize} \quad & \text{Tr}(\mathbf{F}^H\mathbf{F}) \\ \text{subject to} \quad & \mathbf{B} \in \mathbb{L} \ , \ \mathbf{A} \in \mathbb{B} \\ & \mathbf{AHF} = \sqrt{N_0}\mathbf{\Gamma}^{1/2}\mathbf{B} \\ & \|\mathbf{A}(i,:)\|_2 = 1 \qquad \text{for } 1 \le i \le N_R \ . \end{aligned} \tag{4.4}$$

where $\mathbb{L}$ is the set of all lower triangular matrices with unit diagonal and $\mathbb{B}$ is the set of all block diagonal matrices $\text{blkdiag}(\mathbf{A}_1, \mathbf{A}_2, \ldots, \mathbf{A}_K)$ in which $\mathbf{A}_k \in \mathbb{C}^{n_k \times n_k}$. $\mathbf{F}$ is the precoder and $\mathbf{\Gamma}$ is the diagonal matrix of SNR requirements. $\mathbf{\Gamma} = \text{blkdiag}(\mathbf{\Gamma}_1, \ldots, \mathbf{\Gamma}_K)$, where $\mathbf{\Gamma}_k = \gamma_k \mathbf{I}_{n_k}$.

Theorem 2. *Let* $\mathbf{H} = \mathbf{PLQ}^H$ *be the BD-GMD of* $\mathbf{H}$*, and let* $\mathbf{\Lambda} = \text{diag}(\mathbf{L})$.

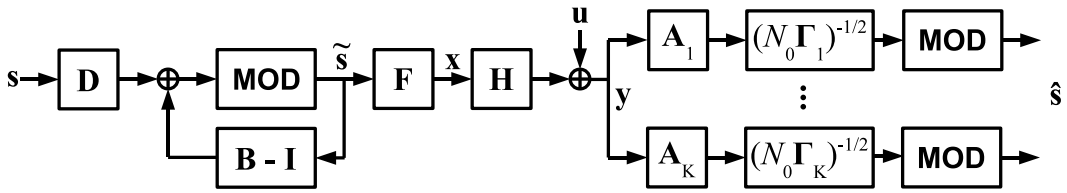

Figure 4.1: Block diagram of power-minimizing BD-GMD scheme that implements user ordering and THP.

$\mathbf{\Lambda} = \text{blkdiag}(\mathbf{\Lambda}_1, \ldots, \mathbf{\Lambda}_K)$, *where* $\mathbf{\Lambda}_k = r_k \mathbf{I}_{n_k}$ *for some* r_k. *Then, (4.4) is solved by*

$$\begin{aligned} \mathbf{\Omega} &= \sqrt{N_0}\mathbf{\Gamma}^{1/2}\mathbf{\Lambda}^{-1} \ , \quad \mathbf{F} = \mathbf{Q}\mathbf{\Omega} \ , \\ \mathbf{B} &= \mathbf{\Omega}^{-1}\mathbf{\Lambda}^{-1}\mathbf{L}\mathbf{\Omega} \ , \quad \mathbf{A} = \mathbf{P}^H . \end{aligned} \tag{4.5}$$

Proof. See Appendix B. □

Here, $\mathbf{\Omega}$ is the diagonal power allocation matrix, $\mathbf{\Omega} = \text{blkdiag}(\mathbf{\Omega}_1, \ldots, \mathbf{\Omega}_K)$, where $\mathbf{\Omega}_k = \omega_k \mathbf{I}_{n_k}$. The minimum power required is thus

$$E_s = \text{Tr}(\mathbf{F}^H\mathbf{F}) = \text{Tr}(\mathbf{\Omega}^2) \ . \tag{4.6}$$

The block diagram of the BD-GMD scheme that minimizes the sum power subject to user rate requirements is shown in Figure 4.1.

4.1.3 User Ordering

The encoding order of the users affects the total transmission power. Let $\{\pi_1, \pi_2, \ldots, \pi_K\}$ be the optimum encoding order, where the previous π_1-th user is now the first user, and so on. As the ordering of the users results in ordering the rows of $\mathbf{H}$, this can be represented by a multiplication by a permutation matrix, $\mathbf{D}$, such that $\mathbf{DH} = \mathbf{PLQ}^H$. Here, the k-th block $\mathbf{P}_k$ of $\mathbf{P}$ has dimensions $n_{\pi_k} \times n_{\pi_k}$.

To find the optimum user ordering that minimizes the transmit power, an exhaustive search over all ordering permutations can be applied. An "exhaustive

search" may seem like a large number, but the advantage of this method over other iterative methods is that the computations involved are much less. The best (ZF) ordering can be found over a hundred times faster than by using the optimum iterative method [87].

Yet, to reduce the complexity even further, three simple algorithms to find the near-optimal encoding order will be proposed. These can be done even before performing the BD-GMD or DPC. These methods are non-iterative, and do not involve convex optimization procedures. They proceed in a successive "top-down" manner, from user 1 to user K.

Method 1: Successive Closest Match

From (4.5), $\det(\mathbf{\Omega})$ is a constant determined by $\mathbf{\Gamma}$ and $\mathbf{H}$. Seeing from (4.6) that E_s is minimized when the diagonal values of $\mathbf{\Omega}$ are equal, $\mathbf{\Lambda}$ is designed such that it is close to a scalar multiple of $\mathbf{\Gamma}^{1/2}$. Let this desired matrix be $\mathbf{M}$, where $\mathbf{M} = \text{blkdiag}(\mathbf{M}_1, \ldots, \mathbf{M}_K)$, and $\mathbf{M}_k = m_k \mathbf{I}_{n_k}$. To ensure that the determinants of $\mathbf{H}\mathbf{H}^H$ and $\mathbf{M}^2$ match, define

$$\mathbf{M} = \mathbf{\Gamma}^{1/2} \cdot \sqrt[2N_R]{\frac{\det(\mathbf{H}\mathbf{H}^H)}{\det(\mathbf{\Gamma})}} \,. \tag{4.7}$$

Since $\mathbf{P}$ is block-diagonal unitary, $\mathbf{Q}$ is unitary and $\mathbf{L}$ is lower triangular, the diagonal elements in $\mathbf{\Lambda}_k$ is given by

$$r_k = \sqrt[2n_k]{\det(\mathbf{\Lambda}_k^2)} = \sqrt[2n_k]{\frac{\det(\widehat{\mathbf{H}}_k \widehat{\mathbf{H}}_k^H)}{\det(\widehat{\mathbf{H}}_{k-1} \widehat{\mathbf{H}}_{k-1}^H)}} \,, \tag{4.8}$$

where $\widehat{\mathbf{H}}_k = [\mathbf{H}_1^T, \ldots, \mathbf{H}_k^T]^T$. It is preferred that r_k be 'close' to m_k. From (4.8), it is seen that r_1 is independent of the ordering of the last $K-1$ users. Thus, $\mathbf{H}_1$ can first be chosen such that r_1 is close to m_1. Following this, $\mathbf{H}_2$ is chosen such that r_2 is close to m_2 and so on. A more precise method to determine 'closeness'

will be given next. From (4.7), the sum power required is

$$E_s = \mathrm{Tr}(\mathbf{\Omega}^2) = N_0 \sqrt[N_R]{\frac{\det(\mathbf{\Gamma})}{\det(\mathbf{H}\mathbf{H}^H)}} \mathrm{Tr}\left(\mathbf{M}^2\mathbf{\Lambda}^{-2}\right) \ . \tag{4.9}$$

Minimizing E_s is the same as minimizing

$$\mathrm{Tr}\left(\mathbf{M}^2\mathbf{\Lambda}^{-2}\right) = \mathrm{Tr}\left(\mathbf{M}_1^2\mathbf{\Lambda}_1^{-2}\right) + \mathrm{Tr}\left(\check{\mathbf{M}}_2^2\check{\mathbf{\Lambda}}_2^{-2}\right), \tag{4.10}$$

where $\check{\mathbf{M}}_k = \mathrm{blkdiag}(\mathbf{M}_k, \ldots, \mathbf{M}_K)$ and $\check{\mathbf{\Lambda}}_k = \mathrm{blkdiag}(\mathbf{\Lambda}_k, \ldots, \mathbf{\Lambda}_K)$. We have

$$\det\left(\mathbf{M}^2\mathbf{\Lambda}^{-2}\right) = 1 = \det\left(\mathbf{M}_1^2\mathbf{\Lambda}_1^{-2}\right) \cdot \det\left(\check{\mathbf{M}}_2^2\check{\mathbf{\Lambda}}_2^{-2}\right), \tag{4.11}$$

In general, for this "top-down" approach, the effect of choosing a particular $\mathbf{\Lambda}_1$ on the following $\mathbf{\Lambda}_k$'s is not known.

Let the best-case $\check{\mathbf{\Lambda}}_2$ to minimize (4.10) given $\mathbf{\Lambda}_1$ be $\widetilde{\mathbf{\Lambda}}_2$.

$$\check{\mathbf{M}}_2^2\widetilde{\mathbf{\Lambda}}_2^{-2} = \mathbf{I}_{\check{n}_2} \cdot \sqrt[\check{n}_2]{\det\left(\mathbf{\Lambda}_1^2\mathbf{M}_1^{-2}\right)} \tag{4.12}$$

where $\check{n}_k = \sum_{j=k}^{K} n_j$. Therefore (4.10) is equivalent to

$$n_1 \sqrt[n_1]{\det\left(\mathbf{M}_1^2\mathbf{\Lambda}_1^{-2}\right)} + \check{n}_2 \sqrt[\check{n}_2]{\det\left(\mathbf{\Lambda}_1^2\mathbf{M}_1^{-2}\right)}. \tag{4.13}$$

Since $\det(\mathbf{\Lambda}_1^2)$ can be found from $\mathbf{H}_1$ using (4.8), $\mathbf{H}_1$ is chosen to minimize (4.13). Next, the selection of users 2 to K will be described.

Define $\hat{\mathbf{M}}_k = \mathrm{blkdiag}(\mathbf{M}_1, \ldots, \mathbf{M}_k)$ and $\hat{\mathbf{\Lambda}}_k = \mathrm{blkdiag}(\mathbf{\Lambda}_1, \ldots, \mathbf{\Lambda}_k)$. For the k-th user, since $\hat{\mathbf{\Lambda}}_{k-1}$ has been determined, minimizing E_s is equivalent to minimizing

$$\mathrm{Tr}\left(\mathbf{M}_k^2\mathbf{\Lambda}_k^{-2}\right) + \mathrm{Tr}\left(\check{\mathbf{M}}_{k+1}^2\check{\mathbf{\Lambda}}_{k+1}^{-2}\right). \tag{4.14}$$

Again, we have

$$\begin{aligned} 1 &= \det\left(\mathbf{M}^2\mathbf{\Lambda}^{-2}\right) \\ &= \det\left(\hat{\mathbf{M}}_{k-1}^2\hat{\mathbf{\Lambda}}_{k-1}^{-2}\right)\cdot\det\left(\mathbf{M}_k^2\mathbf{\Lambda}_k^{-2}\right)\cdot\det\left(\check{\mathbf{M}}_{k+1}^2\check{\mathbf{\Lambda}}_{k+1}^{-2}\right), \end{aligned} \tag{4.15}$$

so the best-case $\check{\mathbf{\Lambda}}_{k+1}$ to minimize (4.14) is $\widetilde{\mathbf{\Lambda}}_{k+1}$, where

$$\check{\mathbf{M}}_{k+1}^2\widetilde{\mathbf{\Lambda}}_{k+1}^{-2} = \mathbf{I}_{\check{n}_{k+1}}\cdot\sqrt[\check{n}_{k+1}]{\det\left(\hat{\mathbf{\Lambda}}_{k-1}^2\hat{\mathbf{M}}_{k-1}^{-2}\right)\det\left(\mathbf{\Lambda}_k^2\mathbf{M}_k^{-2}\right)} \tag{4.16}$$

Therefore (4.14) is equivalent to

$$n_k\sqrt[n_k]{\det\left(\mathbf{M}_k^2\mathbf{\Lambda}_k^{-2}\right)} + \check{n}_{k+1}\sqrt[\check{n}_{k+1}]{\det\left(\hat{\mathbf{\Lambda}}_{k-1}^2\hat{\mathbf{M}}_{k-1}^{-2}\right)\det\left(\mathbf{\Lambda}_k^2\mathbf{M}_k^{-2}\right)} \tag{4.17}$$

Also, $\det(\mathbf{\Lambda}_k^2)$ can be calculated from $\mathbf{H}_k$ using (4.8), where the value $\det(\widehat{\mathbf{H}}_{k-1}\widehat{\mathbf{H}}_{k-1}^H)$ has already been found from the earlier step. $\mathbf{H}_k$ is chosen to minimize (4.17), and so on until user K, where there is only 1 choice. Thus, let this method be called *successive closest match* (SCM).

Method 2: Minimizing Diagonal Element

When users have equal channel strengths, the unordered BD-GMD, which is basically a QR decomposition, $\mathbf{P}^H\mathbf{H} = \mathbf{L}\mathbf{Q}^H$, usually has the first diagonal element of $\mathbf{L}$ much larger than the last element. If equal SNRs are desired for each user, which is usually the case, minimizing the first diagonal element tends to decrease the spread in the diagonal values of $\mathbf{L}$.

Therefore, this method can be stated simply. Starting from user 1, using (4.8), $\mathbf{H}_k$ is chosen to minimize r_k, and so on for users 2 to K.

Method 3: Minimizing Channel Strength

Consider the case where users are at different distances from the base station, resulting in different channel strengths. Suppose equal SNRs are desired for each user. In the dual uplink channel, it is expected that user with the weakest channel should be decoded last, in order to improve his achievable rate. In the downlink, this corresponds to encoding the user with the weakest channel first.

Thus, again starting from user 1, $\mathbf{H}_k$ is chosen to minimize $\mathrm{Tr}(\mathbf{H}_k\mathbf{H}_k^H)/n_k$, and so on until user K.

'Best Choice' Method

Simulations show that for different settings of user channel strengths, user antenna numbers and user SNR requirements, different methods are best for minimizing the total transmit power. Usually, method 1 (SCM) gives the best performance. Due to the reasons mentioned in sections 4.1.3 and 4.1.3, methods 2 or 3 may perform the best. In fact, there is a slight possibility that a particular original ordering is already optimal.

Therefore, it makes sense to select the best of methods 1 to 3 as well as the original ordering.

4.1.4 Computational Complexity

To find the optimum user ordering that minimizes the total transmit power, an exhaustive search across all the user permutations can be done. For K users, there are $K!$ permutations. For each permutation, K determinants has to be calculated based on (4.8), before the transmit power can be evaluated using (4.9), resulting in a total of $KK!$ determinant calculations. Since the value of r_k is independent of the ordering of the first $k-1$ users, the number of determinants to be calculated

can be reduced to

$$N_d = K! \sum_{i=0}^{K-1} \frac{1}{i!} \ . \tag{4.18}$$

On the other hand, the number of determinants to calculate for the proposed SCM method is

$$N_s = \sum_{i=1}^{K} i = \frac{K(K+1)}{2} \ . \tag{4.19}$$

Note that the calculation of the determinants of $\mathbf{M}_k^2$, $1 \leq k \leq K$, have been omitted as they are diagonal matrices. Also, in (4.17), $\det(\hat{\mathbf{\Lambda}}_{k-1}^2)$ can be found from

$$\det(\hat{\mathbf{\Lambda}}_{k-1}^2) = \det(\hat{\mathbf{\Lambda}}_{k-2}^2) \det(\mathbf{\Lambda}_{k-1}^2) \tag{4.20}$$

where the two terms on the right have already been calculated in the previous step.

Method 2 ($\min r_k$) also requires N_s number of determinant calculations. Method 3 (min chan) is the simplest, without requiring any determinant calculations.

The 'best choice' method is interesting. Since it is a composition of methods 1 to 3, the number of determinants to be computed is $2N_s$. An additional $4K$ determinants have to be calculated to find r_k using (4.8). Following that, (4.9) can be evaluated to find the minimum power of all these 4 orderings. Finally the BD-GMD is applied to the best ordering. The complexity of the BD-GMD is only K times as high as the GMD [72].

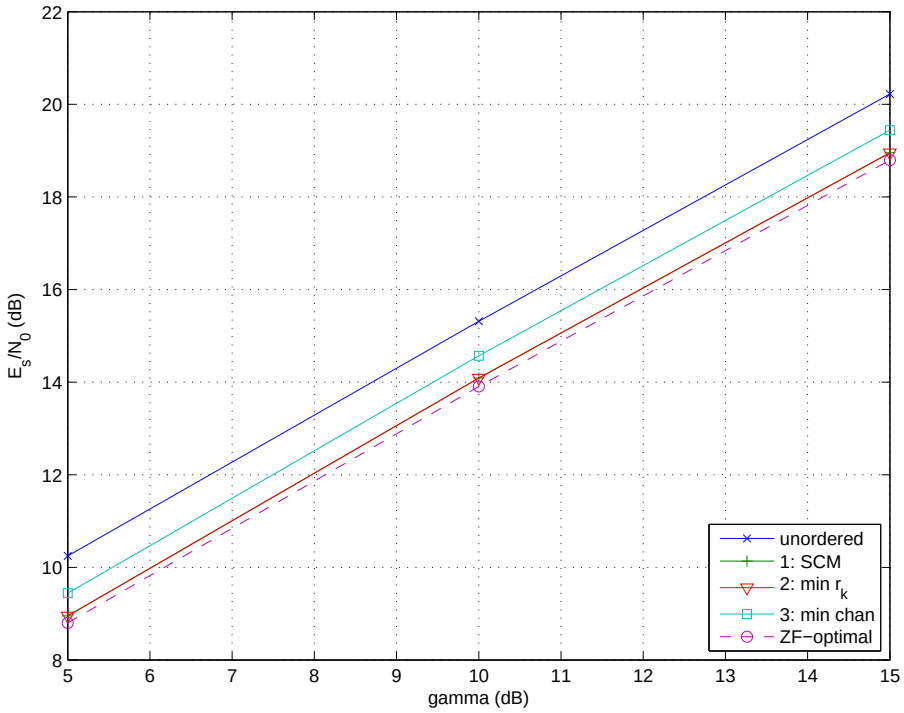

Figure 4.2: Transmit power vs SNR requirements for a $12 \times [2, 2, 2, 2, 2, 2]$ setup, $\boldsymbol{\gamma} = [\gamma, \gamma, \gamma, \gamma, \gamma, \gamma]$.

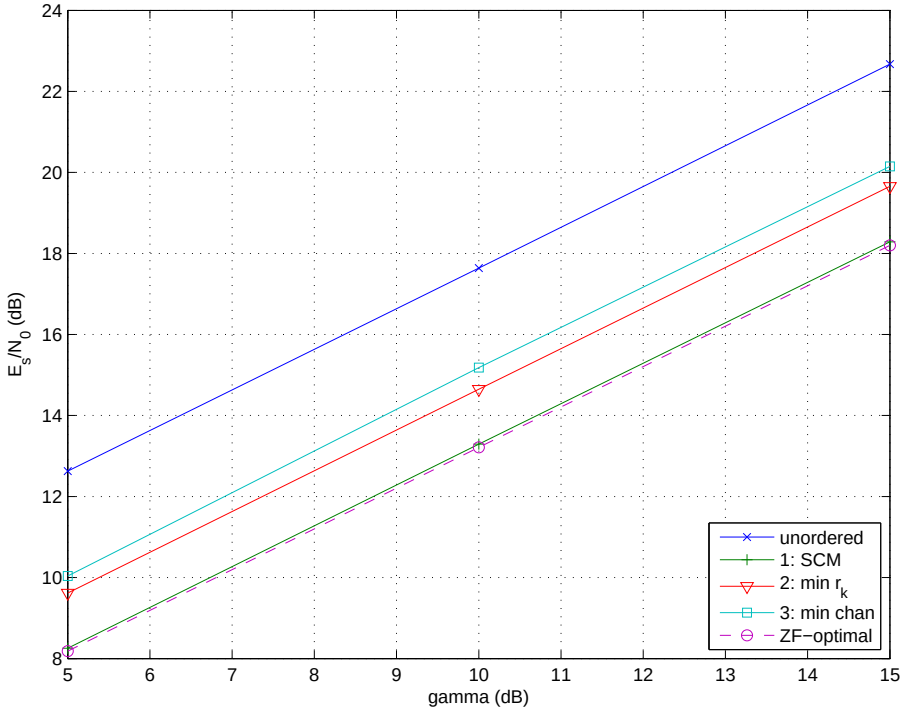

Figure 4.3: Transmit power vs SNR requirements for a $12 \times [2, 2, 2, 2, 2, 2]$ setup, $\boldsymbol{\gamma} = [\gamma/2, \gamma/2, \gamma, \gamma, 2\gamma, 2\gamma]$.

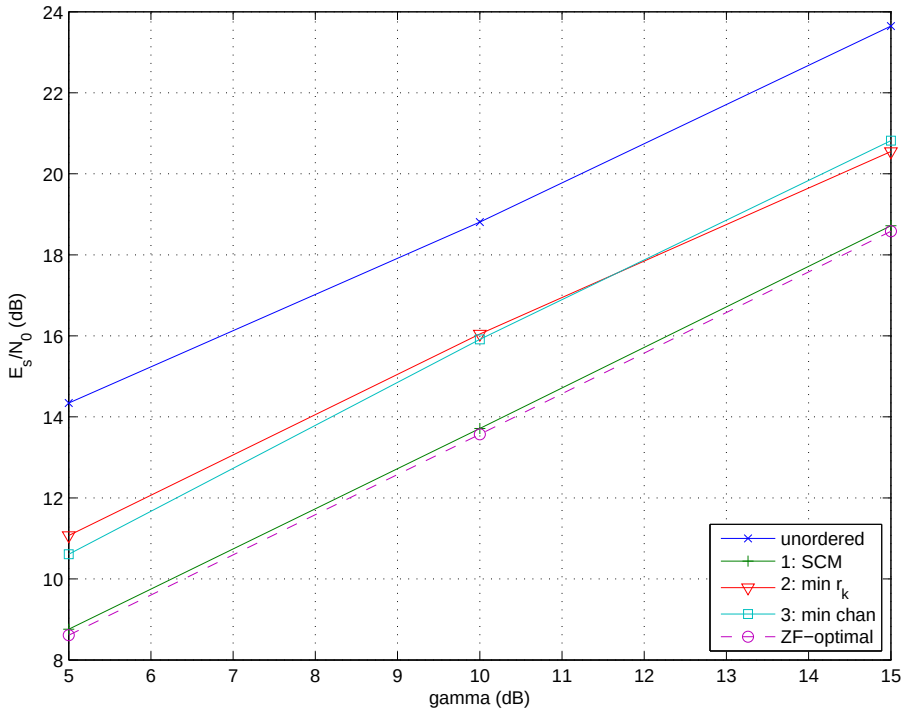

Figure 4.4: Transmit power vs SNR requirements for a $12 \times [4, 2, 2, 2, 1, 1]$ setup, $\boldsymbol{\gamma} = [\gamma, \gamma, \gamma, \gamma, \gamma, \gamma]$.

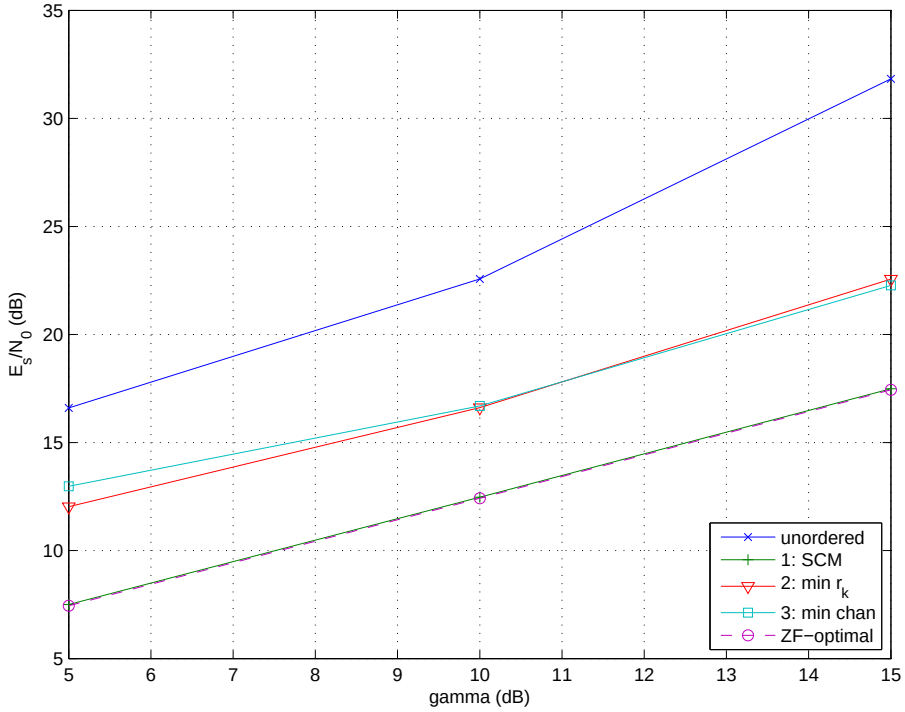

Figure 4.5: Transmit power vs SNR requirements for a $12 \times [4, 2, 2, 2, 1, 1]$ setup, $\boldsymbol{\gamma} = [\gamma/2, \gamma, \gamma, \gamma, 2\gamma, 2\gamma]$.

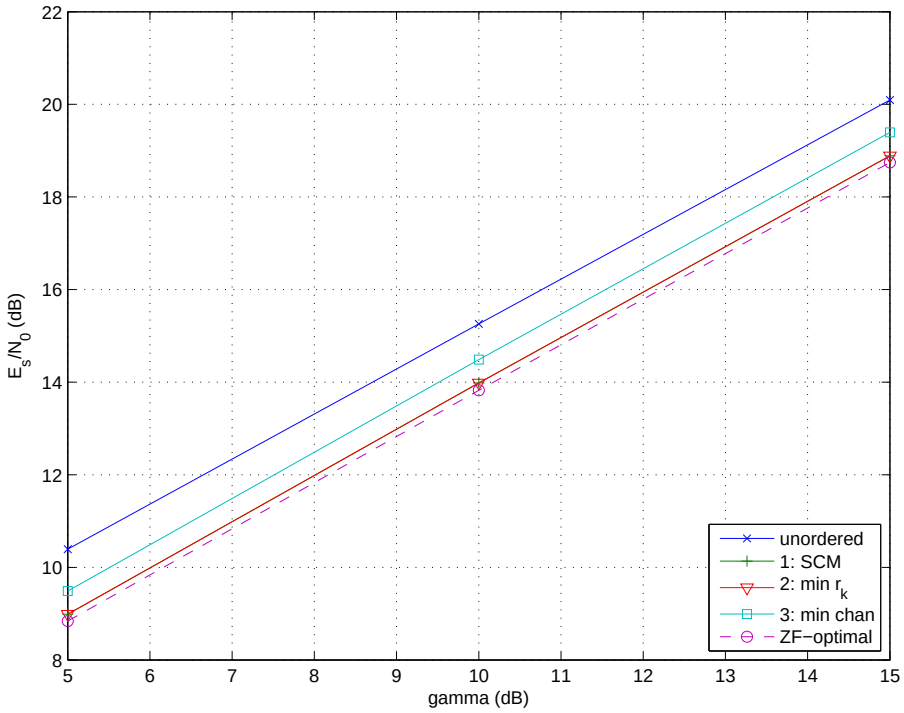

Figure 4.6: Transmit power vs SNR requirements for a $12 \times [2, 2, 2, 2, 2, 2]$ setup, $\boldsymbol{\gamma} = [\gamma, \gamma, \gamma, \gamma, \gamma, \gamma]$. $\mathbf{c} = [1.5, 1.5, 1, 1, 0.5, 0.5]$.

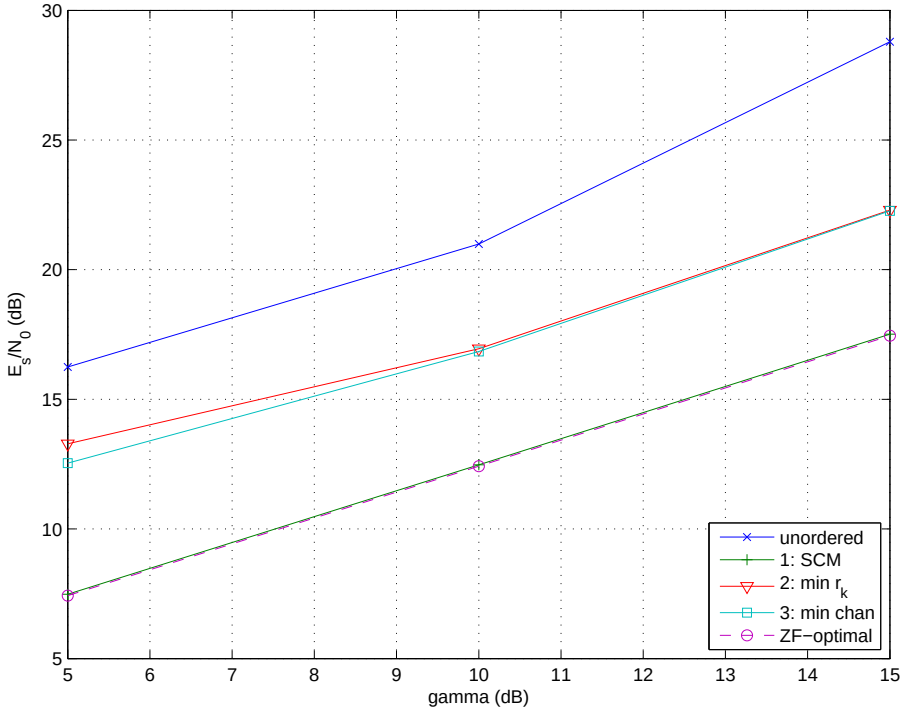

Figure 4.7: Transmit power vs SNR requirements for a $12 \times [4, 2, 2, 2, 1, 1]$ setup, $\boldsymbol{\gamma} = [\gamma/2, \gamma, \gamma, \gamma, 2\gamma, 2\gamma]$. $\mathbf{c} = [1, 1.5, 1, 0.5, 1.5, 0.5]$.

4.1.5 Simulation Results

Consider the $N_T \times [n_1, \ldots, n_K]$ downlink scenario. Let $\mathbf{n} = [n_1, \ldots, n_K]$ be the antenna numbers of the users. Let $\boldsymbol{\gamma} = [\gamma_1, \ldots, \gamma_K]$ be the vector of SNR requirements for each user. Let $\mathbf{c} = [c_1, \ldots, c_K]$ be the channel strengths of each user. The elements of the channel matrix of user k are modelled as i.i.d. zero-mean CSCG with variance c_k.

Figures 4.2 to 4.7 show the simulation results. 4000 Monte Carlo trials are performed for each value of γ. In general, method 1 (SCM) performs the best, followed by method 2 (min r_k), then method 3 (min chan), although settings have been found in which method 2 or method 3 performs best. The figures are chosen to give the most general settings encountered.

For these six figures, the IB scheme is not simulated because of the immense amount of time required. The schemes simulated are ZF-based, with no subchannel selection. It is expected that the optimal IB scheme would have a sizeable improvement over these ZF schemes, especially in the presence of channel correlation. In Section 4.2, ZF schemes with subchannel selection are implemented, resulting in a performance close to the optimal IB scheme.

For figures 4.2 to 4.5, the channel strengths for each user are set equal, i.e. $\mathbf{c} = [1, 1, 1, 1, 1, 1]$. Figure 4.2 represents the case of 2 antennas per user, and equal SNR requirements. Figure 4.3 shows the case where different users have different SNR requirements, for example if they have subscribed to plans of different data rates. Figure 4.4 is more general, when users can have 4, 2, or 1 antennas. In Figure 4.5, the user with more antennas is assigned a lower SNR requirement. This is reasonable because more data streams are permitted for this user, so each stream is allowed to have a lower data rate, if the rates for the different users are comparable. Figure 4.6 presents the case similar to Figure 4.2, but this time with varying channel strengths. This represents the practical scenario where users are

positioned at varying distances from the BS. Figure 4.7 is a generalization where users have different antenna numbers and different SNR requirements. In this scenario, the power reduction from the unordered case to the optimally ordered case is 8 dB, for requirement of γ=10 dB. Ordering methods 2 and 3 perform reasonably well, with a power saving of 4 dB each. Ordering method 1 (SCM) gives the best performance, which is only 0.1 dB higher than the optimally ordered case.

4.2 Power Minimization With Subchannel Selection

In the previous part of this chapter, we have seen that fast computation of the optimal (ZF case) user ordering is done with less than $KK!$ determinant calculations for a system with K users. Using a method called successive closest match (SCM), an ordering that is close to the optimal is found with only $K(K+1)/2$ determinant calculations. To do so, it was assumed that all available subchannels are used, meaning that the number of subchannels used for each user is equal to the number of its antennas.

For MIMO channels, a common phenomenon encountered is channel correlation. As the MIMO channels become rank deficient, it would be better to use only a selection of the available subchannels. For point-to-point communication using GMD, allowing subchannel selection may result in a lower transmit power for the same target rate. Correspondingly, for the MIMO broadcast channel, BD-GMD with subchannel selection (BD-GMD-SS) is proposed. In the multiuser scenario, there is an extra advantage of subchannel selection for a user because it frees up more spatial degrees of freedom for the later encoded users. This chapter describes techniques to find the best user ordering and subchannel selection for the BD-

GMD-SS. Simulations show that the minimum power solution using BD-GMD-SS can be be found over a hundred times faster than the optimal IB solution, with a sum power close to that. To reduce the complexity even further, a suboptimal ordering method is proposed with little performance loss.

The following sections are organized as follows. Section 4.2.1 gives the channel model. Following that, Section 4.2.2 describes a single-user GMD with subchannel selection. Next, the power minimization for a given user ordering and subchannel selection for the MIMO broadcast channel is derived in Section 4.2.3. The complexity of finding the best user ordering and subchannel selection is discussed in Section 4.2.4. Then in Section 4.2.5, an efficient method to find the user ordering and subchannel selection is proposed. Simulation results are provided in Section 4.2.6. The overall summary to this chapter is contained in Section 4.3.

4.2.1 Channel Model

The channel model is the same as in Section 4.1.1. However, since subchannel selection is applied, user k may not use all n_k subchannels. The number of subchannels used by user k is denoted by η_k. In contrast to Section 4.1, it is possible for $N_T < \sum_{k=1}^{K} n_k$. However, $N_T \geq \sum_{k=1}^{K} \eta_k$ must hold. Furthermore, η_k is limited by the rank of user k's equivalent channel.

4.2.2 Single-user GMD with Subchannel Selection

For a matrix $\mathbf{H}$, the single-user GMD is [72] $\mathbf{H} = \mathbf{PLQ}^H$. Here, $\mathbf{P}$ and $\mathbf{Q}$ are square unitary matrices, and $\mathbf{L}$ is a lower triangular matrix with all the diagonal elements equal, and given by the geometric mean of the singular values of $\mathbf{H}$, $\bar{s} = \prod_{i=1}^{N} s_i$, where N is the size of the smallest dimension of $\mathbf{H}$. When the channel is correlated, the last singular value becomes very small. As a result, the geometric mean of all the singular values, $\bar{s}$, also becomes very small. Since $\bar{s}$ is

the common channel gain of every subchannel, the total transmit power becomes very high, for a fixed rate requirement. In this case, subchannel selection allows a lower transmit power for a given target rate.

To do this, SVD is performed on the channel matrix. Next, GMD is applied to the first η singular values. For example, suppose that only the first 2 out of 3 singular values are used for a 3×3 channel matrix $\mathbf{H}$.

$$\mathbf{H} = \mathbf{U} \begin{bmatrix} \mathbf{S}' & \\ & s_3 \end{bmatrix} \mathbf{V}^H \tag{4.21}$$

$$= \begin{bmatrix} \mathbf{U}' & \mathbf{u}_3 \end{bmatrix} \begin{bmatrix} \mathbf{P}'\mathbf{L}\mathbf{Q}'^H & \\ & s_3 \end{bmatrix} \begin{bmatrix} \mathbf{V}'^H \\ \mathbf{v}_3^H \end{bmatrix} \tag{4.22}$$

$$= \begin{bmatrix} \mathbf{P} & \mathbf{u}_3 \end{bmatrix} \begin{bmatrix} \mathbf{L} & \\ & s_3 \end{bmatrix} \begin{bmatrix} \mathbf{Q}^H \\ \mathbf{v}_3^H \end{bmatrix} , \tag{4.23}$$

where the sizes of the respective matrices should be clear. Note that the first and last matrices of (4.23) are unitary. After pre- and post-multiplying (4.23) by $\mathbf{P}^H$ and $\mathbf{Q}$ respectively,

$$\mathbf{P}^H\mathbf{H}\mathbf{Q} = \mathbf{L} , \tag{4.24}$$

where $\mathbf{L}$ is a lower triangular matrix with diagonal elements all equal to the geometric mean of the first η singular values of $\mathbf{H}$. Let this equation (4.24) be called GMD-SS, where 'SS' refers to 'subchannel selection.'

4.2.3 Power Minimization for a Given User Ordering and Subchannel Selection

In Section 4.1, a ZF-based transceiver scheme that minimizes power without using subchannel selection has been proposed. In this section, a new power minimization using subchannel selection is presented. Firstly, assume that the encoding order of the users and the subchannel selection is fixed. Suppose the rate requirement for user k is R_k. Let η_k be the number of subchannels allocated to user k. Denote $N_D = \sum_{k=1}^{K} \eta_k$ as the total number of data streams. Then the SNR needed for each subchannel of user k is γ_k, where $\gamma_k = \left(2^{R_k/\eta_k} - 1\right)$. Denote $\mathbf{A} = \text{blkdiag}(\mathbf{A}_1, \mathbf{A}_2, \ldots, \mathbf{A}_K)$ as the block diagonal receive equalization matrix, $\mathbf{F}$ as the transmit pre-equalization matrix, and $\mathbf{B}$ as the interference matrix. The problem of power minimization is formulated as

$$\begin{aligned} \text{minimize} \quad & \text{Tr}(\mathbf{F}^H\mathbf{F}) \\ \text{subject to} \quad & \mathbf{AHF} = \sqrt{N_0}\mathbf{\Gamma}^{1/2}\mathbf{B} \\ & \mathbf{B} \in \mathbb{L} \ , \ \mathbf{A} \in \mathbb{B} \\ & \|\mathbf{A}(i,:)\|_2 = 1 \qquad \text{for } 1 \le i \le N_D \ . \end{aligned} \tag{4.25}$$

where $\mathbb{L}$ is the set of all $N_D \times N_D$ lower triangular matrices with unit diagonal, $\mathbb{B}$ is the set of all block diagonal matrices such that each block is $\mathbf{A}_k \in \mathbb{C}^{\eta_k \times n_k}$. $\mathbf{F} \in \mathbb{C}^{N_T \times N_D}$, and $\mathbf{\Gamma} \in \mathbb{C}^{N_D \times N_D}$ is the diagonal matrix of SNR requirements. $\mathbf{\Gamma} = \text{blkdiag}(\mathbf{\Gamma}_1, \ldots, \mathbf{\Gamma}_K)$, where $\mathbf{\Gamma}_k = \gamma_k \mathbf{I}_{\eta_k}$.

With subchannel selection for user k, $\mathbf{A}_k$ will not be square. Therefore $\mathbf{A}$ may not be unitary. The solution of Section 4.1.2 can be modified to this scenario. A

reformulation of the BD-GMD with subchannel selection is defined:

$$\mathbf{P}^H\mathbf{H}\mathbf{Q} = \mathbf{L} \ ,$$
$$\begin{bmatrix} \mathbf{P}_1^H & \mathbf{0} \\ \mathbf{0} & \check{\mathbf{P}}_2^H \end{bmatrix} \begin{bmatrix} \mathbf{H}_1 \\ \check{\mathbf{H}}_2 \end{bmatrix} \begin{bmatrix} \mathbf{Q}_1 & \check{\mathbf{Q}}_2 \end{bmatrix} = \begin{bmatrix} \mathbf{L}_1 & \mathbf{0} \\ \mathbf{X} & \check{\mathbf{L}}_2 \end{bmatrix} \ , \tag{4.26}$$

where $\mathbf{H}_1$ is the channel of user 1, and $\check{\mathbf{H}}_2$ contains the channels of user 2 onwards. $\mathbf{P}$ and $\mathbf{Q}$ are semi-unitary, i.e. $\mathbf{P}^H\mathbf{P} = \mathbf{I}$ and $\mathbf{Q}^H\mathbf{Q} = \mathbf{I}$. $\mathbf{L}$ is a lower triangular matrix which is block-equal-diagonal – the diagonal block corresponding to each particular user has equal diagonal elements.

Here, $\mathbf{L}_1$ can be obtained from $\mathbf{P}_1^H\mathbf{H}_1\mathbf{Q}_1 = \mathbf{L}_1$, which is the single-user GMD-SS. Since $\check{\mathbf{Q}}_2$ has to lie in the null space of $\mathbf{H}_1$, the projection matrix $(\mathbf{I} - \mathbf{Q}_1\mathbf{Q}_1^H)$ is used.

$$\check{\mathbf{P}}_2^H \left[\check{\mathbf{H}}_2 \left(\mathbf{I} - \mathbf{Q}_1\mathbf{Q}_1^H\right)\right] \check{\mathbf{Q}}_2 = \check{\mathbf{L}}_2 \ , \tag{4.27}$$

which is the same form as (4.26), so the algorithm proceeds recursively. Finally, $\mathbf{X}$ can be calculated as

$$\mathbf{X} = \check{\mathbf{P}}_2^H\check{\mathbf{H}}_2\mathbf{Q}_1 \ . \tag{4.28}$$

Let the resulting equation (4.26) be called BD-GMD-SS.

Let $\mathbf{P}^H\mathbf{H}\mathbf{Q} = \mathbf{L}$ be the BD-GMD-SS for $\mathbf{H}$, and let $\mathbf{\Lambda} = \mathrm{diag}(\mathbf{L})$. $\mathbf{\Lambda} = \mathrm{blkdiag}(\mathbf{\Lambda}_1, \ldots, \mathbf{\Lambda}_K)$, where $\mathbf{\Lambda}_k = \lambda_k\mathbf{I}_{\eta_k}$ for some λ_k. Then, similar to Section 4.1.2, to solve (4.25), the following is applied:

$$\mathbf{\Omega} = \sqrt{N_0}\mathbf{\Gamma}^{1/2}\mathbf{\Lambda}^{-1} \ , \quad \mathbf{F} = \mathbf{Q}\mathbf{\Omega} \ ,$$
$$\mathbf{B} = \mathbf{\Omega}^{-1}\mathbf{\Lambda}^{-1}\mathbf{L}\mathbf{\Omega} \ , \quad \mathbf{A} = \mathbf{P}^H. \tag{4.29}$$

The block diagram of the BD-GMD-SS scheme that minimizes the sum power while satisfying user target rates is shown in Figure 4.1.

4.2.4 Optimal User Ordering and Subchannel Selection

The optimal user ordering and subchannel selection can be found by an exhaustive search. However, the complexity here is much higher. In addition to searching through $K!$ orderings, all subchannel selection combinations have to be tested for each ordering. The BD-GMD-SS can be computed, to find the power, for each ordering and subchannel selection. The optimal case is chosen as the one that gives the minimum power.

To save on complexity, a 'power-test' version of the BD-GMD-SS can be used to find the transmit power, since that is the only relevant parameter of interest. As seen in section 4.2.3, $\mathbf{L}_1$ is obtained by the single-user GMD-SS. Therefore its diagonal elements are all equal to the geometric mean of the first η_k singular values, which can be obtained by a SVD. This gives $\mathbf{\Lambda}_1$. Next, as $\check{\mathbf{Q}}_2$ has to lie in the null space of $\mathbf{H}_1$, the projection matrix $(\mathbf{I} - \mathbf{V'}_1\mathbf{V'}_1^H)$ can be used, where the columns of $\mathbf{V'}_1$ are the first η_k right singular vectors of $\mathbf{H}_1$. Subsequently, the $\check{\mathbf{\Lambda}}_2$ can be found recursively, by applying the function on $\check{\mathbf{H}}_2(\mathbf{I} - \mathbf{V'}_1\mathbf{V'}_1^H)$. In this way, only K SVDs need to be carried out, instead of the complete BD-GMD.

Each user has at least one active subchannel, to satisfy its rate requirement. For each user ordering, the number of subchannel combinations to be tested is

$$N_c = \prod_{k=1}^{K} n_k \ . \tag{4.30}$$

If, however, $N_T < N_R$, we have $N_c < \prod_{k=1}^{K} n_k$, because the combinations where $\sum_{k=1}^{K} \eta_k > N_T$ are not valid and can be ignored.

The total number of tests would be $K!N_c$. This gives rise to a total of $KK!N_c$

SVDs.

4.2.5 Efficient Method to Obtain User Ordering and Subchannel Selections

When the number of users K is large, the complexity would be reduced if only a subset of all $K!$ orderings are tested. In this section, an efficient method to obtain a suboptimal ordering is proposed. Section 4.1.3 described 3 methods of ordering, assuming no subchannel selection. All three methods are non-iterative and do not involve convex optimization procedures. They select users in a "top-down" manner, from the first encoded user to the last encoded user. Method 1 is called successive closest match (SCM) which matches user SNR requirements with effective channel strengths after projection. Method 2 selects the user that gives the minimum λ_k. Method 3 selects the user that has the minimum channel strength $\text{trace}(\mathbf{H}_k\mathbf{H}_k^H)/n_k$. A total of $K(K+1)$ determinant calculations are required to obtain all these orderings.

For each of these orderings, as well as the original unordered case, the optimal subchannel selection is evaluated with KN_c SVDs. Therefore $4KN_c$ SVDs would be performed for all 4 orderings, compared to $KK!N_c$ SVDs in section 4.2.4. The ordering that gives the minimum power is chosen. Let this be called the 'best choice ordering.' This ordering is then used in the BD-GMD-SS to calculate the transmit and receive equalization matrices.

A limitation for the efficient method proposed in this subsection is that $N_T \geq N_R$ is required. Nevertheless, the solution in Section 4.2.4 can be used for the general case of $N_T \geq \sum_{k=1}^{K} \eta_k$. It would be interesting to derive efficient methods for this general case.

4.2.6 Simulation Results

Consider the $8 \times [2, 2, 2, 2]$ downlink scenario. Let each user have 2 antennas. Let $\mathbf{R} = [\rho_1, \ldots, \rho_K]$ be the vector of rate requirements for each user. Let $\mathbf{c} = [c_1, \ldots, c_K]$ be the channel strengths of each user. The elements of the channel matrix of user k are modelled as i.i.d. zero-mean CSCG with variance c_k.

For the scenario of channel correlation, the following model is employed. Correlation between the channel responses is seen for the transmit antennas, as the base station is usually located in a high and unobstructed position [39]. The transmit correlation matrix for each user is dependent on the nominal angle of departure (AoD), $\bar{\theta}_k$, and the angular spread. As each user is located in rich local scattering vicinity, its antennas see uncorrelated channel responses. Similarly, there is no correlation between different users' antennas, as they are usually far apart.

The channel for user k can be modelled as [101, 102]

$$\mathbf{H}_k = \mathbf{H}_{w,k}(\mathbf{R}_{T,k}^{1/2})^T \ , \tag{4.31}$$

where $\mathbf{H}_{w,k} \in \mathbb{C}^{n_k \times N_T}$, the elements of which are i.i.d., zero-mean CSCG with unit variance, and $\mathbf{R}_{T,k} \in \mathbb{C}^{N_T \times N_T}$ is the transmit correlation matrix for user k. The matrix square root $(\cdot)^{1/2}$ is defined such that $\mathbf{R}^{1/2}\mathbf{R}^{1/2} = \mathbf{R}$.

To construct the covariance matrices [68], consider a uniform linear array (ULA) at the base station, where the antenna spacing is denoted as d. For an AoD θ, the steering vector is given by

$$\mathbf{a}(\theta) = [1, e^{j2\pi d \sin(\theta)/\varpi}, \cdots, e^{j2\pi(N_T-1)d\sin(\theta)/\varpi}]^T. \tag{4.32}$$

where ϖ is the carrier wavelength. Let the cell served by the base station be

divided into S sectors. Then

$$\mathbf{R}_{T,k} = \int_{-\pi/S}^{\pi/S} \psi_k(\theta)\mathbf{a}(\theta)\mathbf{a}^H(\theta)d\theta, \tag{4.33}$$

where $\psi_k(\theta)$ is the ray-density function. The rays from the base station to each user are assumed to have a uniform density distribution. The nominal AoD is $\bar{\theta}_k$ and the angular spread is Δ_k. Thus

$$\psi_k(\theta) = \begin{cases} \frac{1}{\Delta_k} & \text{when } \bar{\theta}_k - \Delta_k/2 \leq \theta \leq \bar{\theta}_k + \Delta_k/2 \\ 0 & \text{otherwise.} \end{cases} \tag{4.34}$$

For all the figures, 'SS' means that BD-GMD with subchannel selection is used while 'no SS' means that subchannel selection is not used. 'u' denotes the unordered case, where the original user ordering is taken. 'no SS:opt' refers to the case where subchannel selection is not allowed but the optimal user ordering is found. The best subchannel selection for 'SS' is found by considering N_c cases. 'SS:u' denotes the unordered case with optimal subchannel selection applied. 'SS:opt' refers to the case where the optimal combination of user ordering and subchannel selection given by Section 4.2.4 is applied. For 'SS:bco,' the 'best choice ordering' described in Section 4.2.5 is used. The subchannel selection is also optimal in this case. 'IB:opt' shows the power obtained by the optimal IB solution. Although not a DPC technique, the graph for ZF linear block diagonalization (LBD) [82] is shown, for the sake of comparison. Optimal water-filling [70] is used for each user in the LBD scheme.

In Figure 4.8, the transmit power is plotted against the rate requirement ρ, where the rate requirement for each user is ρ bps/Hz. It can be seen that a large improvement can be obtained when subchannel selection is allowed, even for uncorrelated channels. As the rate requirement increases, this gain reduces because

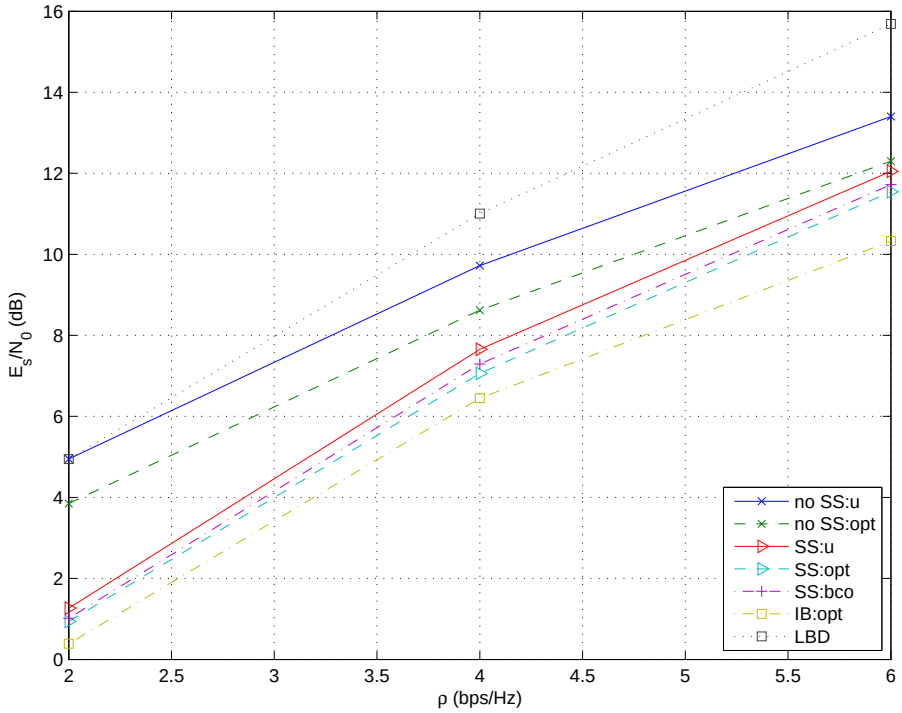

Figure 4.8: Sum power vs rate targets, $\mathbf{R} = [\rho, \rho, \rho, \rho]$. Uncorrelated channels.

more subchannels are used. Compared to the unordered schemes, ordering provides relatively small improvements. This is due to the similar channel strengths and similar rate requirements of all the users.

In Figure 4.9, sum power versus target rate ρ is shown for the case with differentiated user rate requirements. The target rate is given by $\mathbf{R} = [\rho/2, 2\rho, \rho/2, 2\rho]$ bps/Hz. Here, user ordering plays a major role. In fact, the optimal ordering with no subchannel selection already performs better than the unordered case with optimal subchannel selection, for $\rho = 4$ and $\rho = 6$. This can be explained by the fact that different orderings result in different effective channel strengths of the users and proper ordering is required to match each user's rate requirement with its effective channel strength.

Figure 4.10 shows the case of correlated channels and equal rate requirements. The nominal AoDs are set as $[-60^o, -20^o, 20^o, 60^o]$. The angular spread is set at 20^o for all users. Here the improvement from using subchannel selection is large,

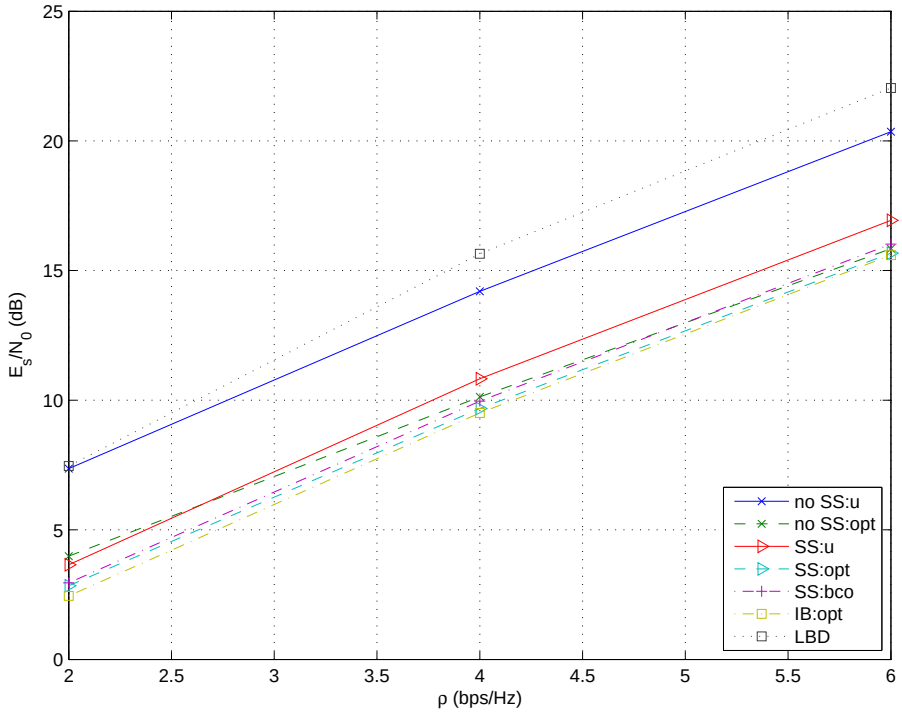

Figure 4.9: Sum power vs rate targets, $\mathbf{R} = [\rho/2, 2\rho, \rho/2, 2\rho]$. Uncorrelated channels.

about 5 dB for the unordered case. This is because in a rank deficient channel, the transmit power of each user can be reduced by choosing only a subset of available eigenchannels. In this case, optimal user ordering for the case of no subchannel selection is not able to compensate much for the effect due to correlation. This is reflected in the higher power of this method compared to the cases with subchannel selection allowed. This is due to the similar rate requirements of the users. Also, BD-GMD-SS has a transmit power around 0.5 dB higher than the optimal IB solution at $\rho = 4$ bps/Hz, whether or not user ordering is applied.

The effect of both differentiated rate requirements and correlated channels is plotted in Figure 4.11. Similar to the previous figure, there is a substantial reduction in power when subchannel selection is allowed, about 5 dB for the unordered case, due to the channel correlation. Furthermore, user ordering also provides a large benefit, as can be explained by the different target rates for different the users, which is also the phenomenon displayed in Figure 2. For example, there is a

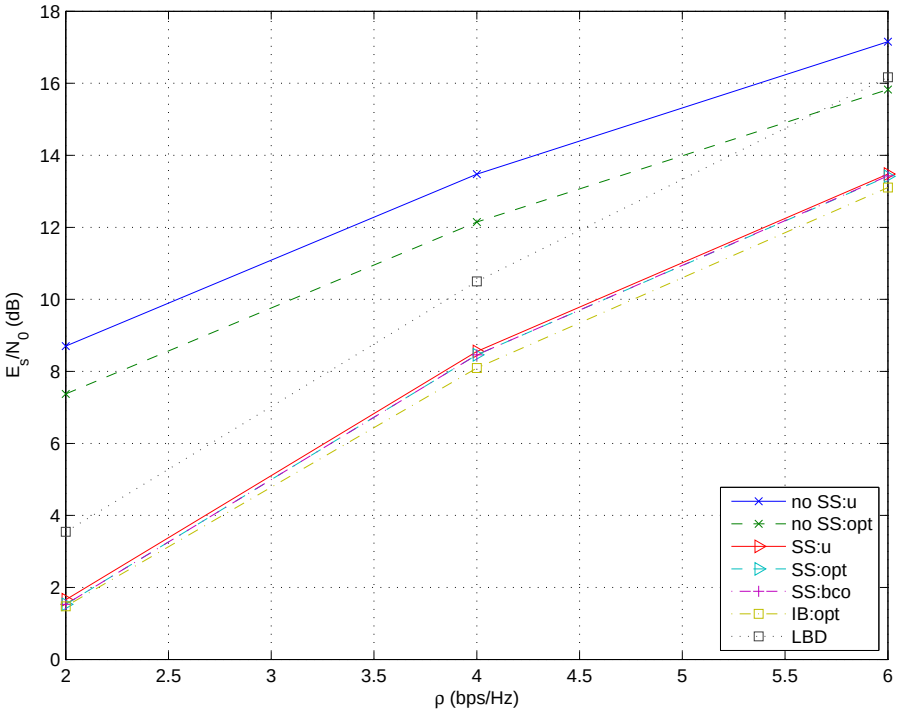

Figure 4.10: Sum power vs rate targets, $\mathbf{R} = [\rho, \rho, \rho, \rho]$. Correlated channels.

power reduction of 4 dB for the case of no subchannel selection at $\rho = 4$. Also, the gap between the BD-GMD-SS scheme with optimal user ordering and subchannel selection and the optimal IB scheme is less than 0.5 dB at $\rho = 4$.

Figure 4.12 illustrates the case where users have different channel strengths. This may be result of users being located at different distances from the base station. Even though the rate requirements are similar, there is a large improvement from ordering the users. This is because proper ordering matches the user rate requirements with the effective channel strengths after projection.

In all these graphs, it can be seen that by allowing subchannel selection, the transmit power can be reduced significantly. Optimal user ordering for the BD-GMD-SS scheme also improves the performance. It is able to provide a sum power close to the optimal IB solution but at a much lower complexity. Furthermore, the suboptimal method based on the 'best choice ordering' can be performed with even lesser computations without much loss in performance.

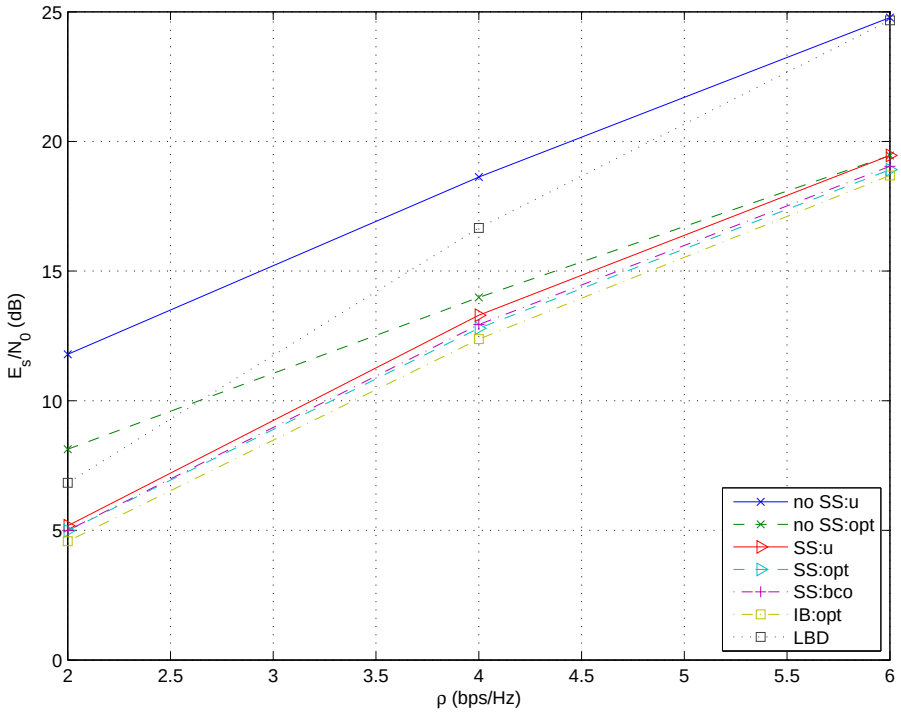

Figure 4.11: Sum power vs rate targets, $\mathbf{R} = [\rho/2, 2\rho, \rho/2, 2\rho]$. Correlated channels.

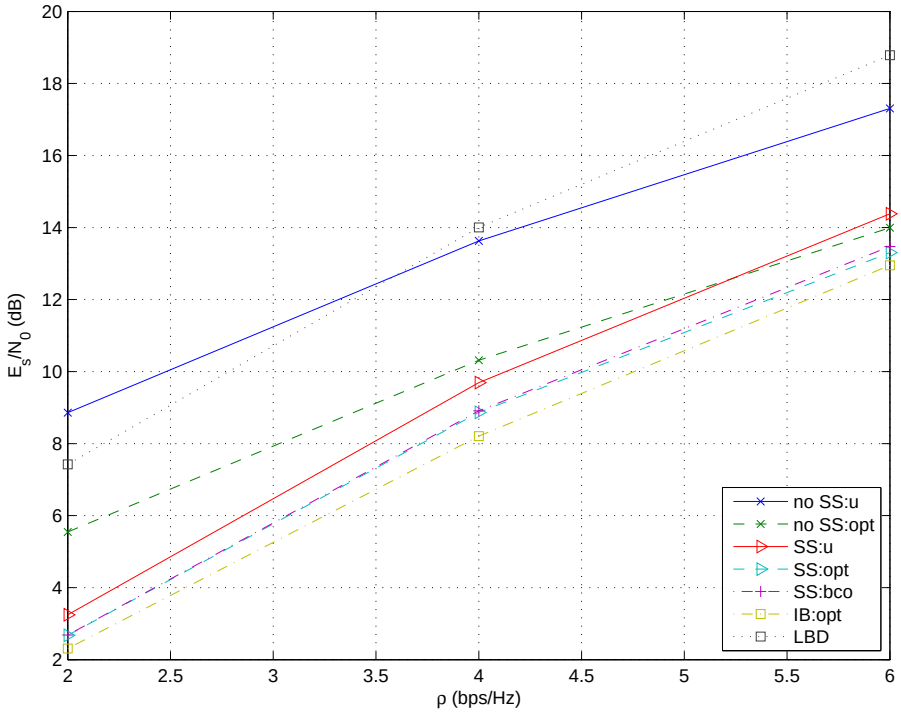

Figure 4.12: Sum power vs rate targets, $\mathbf{R} = [\rho, \rho, \rho, \rho]$. $\mathbf{c} = [1.5, 1.5, 0.5, 0.5]$. Uncorrelated channels.

4.3 Summary

The optimal solution to the MIMO BC power minimization problem given user SINR requirements has been solved optimally using iterative methods. However, these methods are computationally expensive, as explained in the start of this chapter. A major hurdle for MIMO systems is the high complexity involved.

In this chapter, the problem of the ZF-based power minimization using DPC has been formulated and solved with a closed-form expression, using the BD-GMD. The optimal ordering can be found efficiently. To speed up the process of obtaining the best ordering, suboptimal methods have been proposed. The methods have been shown to reach the ZF-optimal power very closely.

In the second half of this chapter, BD-GMD-SS has been proposed for ZF-based power minimization. This ZF-based solution with the optimal ordering and subchannel selection can be found much faster than the optimal IB solution. Simulations have shown that the sum power obtained with the optimal BD-GMD-SS is not far from that of the optimal IB solution. A suboptimal method of ordering with further reduced complexity has also been proposed and has shown minimal performance loss.

Chapter 5

Power Minimization for Multiuser MIMO-OFDM Systems

In orthogonal frequency division multiplexing (OFDM), a broadband frequency-selective channel is decoupled into multiple flat fading channels, through efficient fast fourier transform (FFT) operations. The combination of MIMO and OFDM technologies, termed MIMO-OFDM [103], is a strong candidate for next generation wireless systems, like 4th generation mobile communications. With the increase in the technology savvy population, there is now a huge demand for rich multimedia interactivity. Commercial cellular systems have to cope with not only an increase in the number of users, but also with an increase in the data rate requirement per user. MIMO-OFDM addresses these two concerns aptly. Not only is there an increase in overall throughput, there are also more degrees of freedom to accommodate a larger number of users. This is because users can be separated in space as well as frequency.

As mentioned in the previous chapter, users may be located at different distances from the base station (BS), resulting in different variances for each independent user's channel matrix. Furthermore, users may have subscribed to plans of different data rates. Therefore, practical resource allocation schemes have to take

those into consideration. Similar to the work in the previous chapter, an important question to answer is how to minimize the transmit power of each individual BS, while maintaining the rate requirements for the group of users currently served. This would help to reduce the interference that each BS produces to neighbouring cells, and as a result improve the whole cellular system's performance.

For a flat fading MIMO BC, the optimum solution [87–89] involves interference-balancing (IB) and nonlinear processing. In MIMO-OFDM, each subcarrier represents a flat fading MIMO channel. Using the nonlinear solutions above, each subcarrier may require a different decoding/encoding order, leading to an undesirable increase in complexity. While this is optimal in terms of minimizing the total transmit power, the demands on the hardware processing capability may far outweigh the benefit of the lower transmit power.

In contrast, linear schemes make use of only linear matrix multiplications for the components of the signal processing. The advantage of linear processing or beamforming is that the complexity is much reduced, leading to a decrease in hardware demand. In addition to reducing the complexity of this multicarrier system, linear processing tends to be more robust against channel uncertainty, than nonlinear processing like DPC. Also, in multicarrier systems, it is not necessary to support all the users on each subcarrier. When the numbers of antennas at the BS and each user's terminal are comparable, a linear strategy supporting only one or a few of the users on each subcarrier is not likely to suffer much performance loss from the optimum nonlinear strategy, due to the frequency diversity effect. Furthermore, for a flat fading MIMO broadcast channel, ZF beamforming with time division multiple access (TDMA) has been shown to achieve a sum rate close to the optimal DPC scheme when the number of users is large [109]. For the same reasons, the BD-GMD and BD-UCD schemes used in the earlier chapters are not considered here.

For the SISO case, orthogonal frequency division multiple access (OFDMA) downlink resource allocation has been developed via a dual decomposition approach in [107], which does not have the complexity of different encoding/decoding orders, since there can only be one user per subcarrier. [105] obtains subcarrier and bit allocations with a goal of minimizing the overall transmit power while maintaining a target BER for a multiuser MIMO-OFDM system. Similar to [107], in [105], there can only be one user per subcarrier. For each subcarrier, the user that achieves the maximum SNR is selected for this subcarrier. [105] and [107] are excellent for frequency-selective fading channels. However, frequency-flat fading channels, if they occur, may result in an inability to guarantee user rates because the decision to select a particular user for one subcarrier would be repeated for all the subcarriers.

In [108], users are classified according to the spatial separability, which is calculated from the correlation between the users' spatial signatures. By grouping the users in this manner, subcarriers can be allocated to the users while ensuring that the highly correlated users would not use the same subcarriers. More specifically, the correlation between any 2 users in different groups is set less than a predefined threshold. Therefore, parallel interference cancellation at the BS during the uplink is assumed to remove all the interference between the users.

In this chapter, an efficient method based on convex optimization theory is designed to minimize the total transmit power for MIMO-OFDM communications, subject to individual user rate constraints. This strategy requires only linear transmit and receive processing. Therefore it is applicable to both the downlink and the uplink. By considering the Lagrangian dual of the sum power objective function, the problem is broken down into M individual subproblems, where M is the number of subcarriers. The complexity is thus reduced from one exponential in M to one linear in M. Given that M is typically large for multicarrier systems, this

represents a huge amount of savings. The supergradient of the dual function is then used to update the Lagrange multipliers in finite step sizes. The step sizes are adjusted based on the convergence behaviour in order to speed up the convergence of the algorithm. Furthermore, the algorithm is able to adapt to changing channel conditions. It has been found that methods based on dual decomposition could possibly suffer from a uniformity among the subcarriers, resulting in large oscillations within the algorithm. A solution based on a *dual proportional fairness* is proposed to tackle the event of frequency-flat fading. Simulation results show that with reasonable number of subcarriers, the duality gap is effectively zero, thereby substantiating the proposed solution.

Section 5.1 describes the channel model and the strategy of linear block diagonalization (LBD) [82] that separates the users spatially via linear beamforming. The optimal solution to resource allocation for power minimization is given in Section 5.2. An efficient solution based on convex optimization is developed in Section 5.3. Adjustment of the step size for faster convergence and adaptation to changing channel conditions is discussed in Section 5.4. To handle the event of flat fading channels, a modification based on a dual proportional fairness is introduced in Section 5.5. Simulation results are given in Section 5.6. Finally, a summary is provided in Section 5.7.

5.1 Channel Model and Transmission Strategy

5.1.1 Channel Model

In this section, a general description of the channel model is given. Consider a cellular-based MIMO-OFDM system with a BS communicating with K user terminals via M subcarriers. Suppose the BS is equipped with N_T antennas and the k-th user terminal has n_k antennas. Denote $N_R = \sum_{k=1}^{K} n_k$ as the total number

of receive antennas. Let $\sigma_{k,m}$ indicate the presence of the k-th user on subcarrier m; $\sigma_{k,m} = 1$ if present and 0 if not. Therefore $\{\sigma_{k,m}\}$ represents the user selection on each subcarrier. Let the rank of the channel matrix of user k on subcarrier m be denoted by $\eta_{k,m}$, where $0 \leq \eta_{k,m} \leq \min(n_k, N_T), \forall m$. The diagram of downlink transmission is shown in Figure 5.1. The baseband input-output relationship is represented as

$$\mathbf{y}_d = \mathbf{H}_d \mathbf{x}_d + \mathbf{n}_d \ , \tag{5.1}$$

where $\mathbf{H}_d = \text{blkdiag}(\mathbf{H}_{d,1}, \ldots, \mathbf{H}_{d,M})$ is the channel, $\mathbf{x}_d = [\mathbf{x}_{d,1}^T, \ldots, \mathbf{x}_{d,M}^T]^T$ is the transmit signal vector, $\mathbf{y}_d = [\mathbf{y}_{d,1}^T, \ldots, \mathbf{y}_{d,M}^T]^T$ is the receive signal vector, and $\mathbf{n}_d$ is the $MN_R \times 1$ noise vector. Assume that the noise is zero-mean, circularly symmetric complex Gaussian (CSCG) with $\mathbb{E}[\mathbf{n}_d \mathbf{n}_d^H] = N_0 \mathbf{I}$, and $\mathbf{n}_d$ is independent of $\mathbf{x}_d$. For the m-th subcarrier, (5.1) can be interpreted as

$$\mathbf{y}_{d,m} = \mathbf{H}_{d,m} \mathbf{x}_{d,m} + \mathbf{n}_{d,m} \ , \tag{5.2}$$

where $\mathbf{H}_{d,m} = [\mathbf{H}_{d,1,m}^T, \ldots, \mathbf{H}_{d,K,m}^T]^T$ is the $N_R \times N_T$ random MIMO channel and $\mathbf{y}_{d,m} = [\mathbf{y}_{d,1,m}^T, \ldots, \mathbf{y}_{d,K,m}^T]^T$ is the $N_R \times 1$ receive signal vector on subcarrier m.

For the uplink, the block diagram is shown in Figure 5.2, where the received signal is given by

$$\mathbf{y}_u = \mathbf{H}_u \mathbf{x}_u + \mathbf{n}_u \ , \tag{5.3}$$

with $\mathbf{H}_u = \text{blkdiag}(\mathbf{H}_{u,1}, \ldots, \mathbf{H}_{u,M})$ being the uplink channel matrix. $\mathbf{x}_u = [\mathbf{x}_{u,1}^T, \ldots, \mathbf{x}_{u,M}^T]^T$ is the transmit signal vector and $\mathbf{n}_u$ is the $MN_T \times 1$ noise vector.

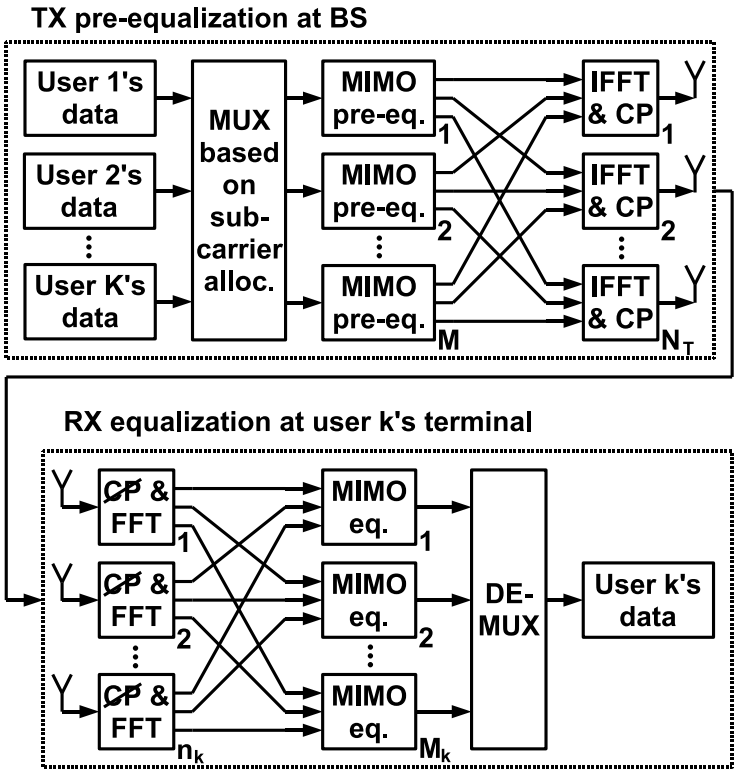

Figure 5.1: Block diagram of MIMO-OFDM downlink.

On the m-th subcarrier, we have

$$\mathbf{y}_{u,m} = \mathbf{H}_{u,m}\mathbf{x}_{u,m} + \mathbf{n}_{u,m} \ , \tag{5.4}$$

where $\mathbf{x}_{u,m} = [\mathbf{x}_{u,1,m}^T, \ldots, \mathbf{x}_{u,K,m}^T]^T$ is the $N_R \times 1$ transmit signal vector, $\mathbf{H}_{u,m}$ is the $N_T \times N_R$ uplink MIMO channel, and $\mathbf{y}_{u,m}$ is the $N_T \times 1$ receive signal vector on subcarrier m. Similar to the downlink case, the noise vector $\mathbf{n}_{u,m}$ is zero-mean CSCG with $\mathbb{E}[\mathbf{n}_{u,m}\mathbf{n}_{u,m}^H] = N_0\mathbf{I}_{N_T}$.

5.1.2 Equalization using Linear Block Diagonalization

This section describes the transmission scheme for the MIMO-OFDM channel, using linear transmit and receive equalization to block diagonalize the channel.

At each transmission slot, the BS decides on the subcarrier allocation and

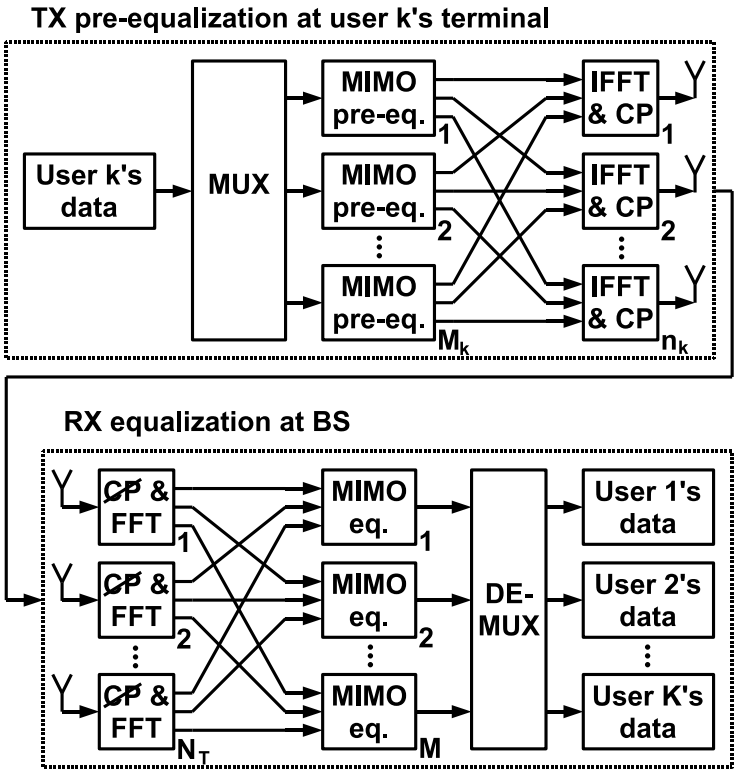

Figure 5.2: Block diagram of MIMO-OFDM uplink.

the transmit preprocessing for the downlink. When more than 1 user share a certain subcarrier, ZF linear block diagonalization (LBD) [82] can be used to separate the users spatially. This creates decoupled channels for all the users. The user terminals then perform channel estimation and receive processing, which can be based on ZF equalization. The user terminals are informed by the BS what transmit processing to employ for the uplink. The BS need only to perform ZF linear receive equalization, because all the user channels are completely decoupled.

Alternatively, if communication is by time division duplex (TDD), the reciprocity principle can be used at the BS to estimate the channel. The transmit matrix operations are identical to the receive matrix operations, greatly simplifying the communications procedure. Likewise, at the user terminals, each user can estimate its own channel because there is no interference between the users. The receive matrix operations are applied directly for the uplink transmission.

Downlink Case

Consider the transmission over one subcarrier during the downlink. For each user, singular value decomposition (SVD) is applied to the combined channel matrix of all the other users. The last few right singular vectors that correspond to zero singular values give the null space of this combined matrix. Next, each user's matrix is multiplied by the corresponding null space obtained earlier and SVD is performed on the resultant matrix. These two steps would give the transmit and receive equalization matrices. The different users' MIMO channels become completely decoupled, with no interference between the users.

When the number of users is large, all these mutual projections would make each user's subchannels very weak. The advantage of multicarrier MIMO communications is that all the users do not need to share the same subcarrier. An easy way to exploit this is to constrain the system such that only 1 user occupies each subcarrier. Consequently, no projections are required because the other users are not expecting any data on this subcarrier and would ignore whatever signals they receive. Due to low complexity, this design would be suitable for low cost hardware implementation.

When the number of BS antennas is relatively large, compared to the number of users, the performance may be improved by allowing more than 1 user to share the same subcarrier. Next, the algorithm to calculate the transmit and receive equalization matrices is illustrated for this general case.

Suppose that there are K_m users in subcarrier m. Let the downlink channel on this subcarrier be denoted by $\mathbf{H} = [\mathbf{H}_1^T, \ldots, \mathbf{H}_{K_m}^T]^T$. For user k, define $\tilde{\mathbf{H}}_k = [\mathbf{H}_1^T, \ldots, \mathbf{H}_{k-1}^T, \mathbf{H}_{k+1}^T, \ldots, \mathbf{H}_{K_m}^T]^T$. Perform SVD on each $\tilde{\mathbf{H}}_k$:

$$\tilde{\mathbf{H}}_k = \tilde{\mathbf{U}}_k \tilde{\mathbf{S}}_k \tilde{\mathbf{V}}_k^H = \tilde{\mathbf{U}}_k \tilde{\mathbf{S}}_k \left[\tilde{\mathbf{V}}_k^{(1)} \tilde{\mathbf{V}}_k^{(0)} \right]^H , \tag{5.5}$$

where $\tilde{\mathbf{U}}_k$ and $\tilde{\mathbf{V}}_k$ are unitary matrices in which the columns are the left and right singular vectors of $\tilde{\mathbf{H}}_k$ respectively. $\tilde{\mathbf{S}}_k$ is a diagonal matrix, which may be rectangular, containing the singular values of $\tilde{\mathbf{H}}_k$. The columns of $\tilde{\mathbf{V}}_k^{(1)}$ correspond to non-zero singular values whereas the columns of $\tilde{\mathbf{V}}_k^{(0)}$ correspond to the zero singular values of $\tilde{\mathbf{H}}_k$. Therefore $\tilde{\mathbf{V}}_k^{(0)}$ is the null space of $\tilde{\mathbf{H}}_k$. Each user's channel after mutual projections is

$$\check{\mathbf{H}}_k = \mathbf{H}_k \tilde{\mathbf{V}}_k^{(0)} = \check{\mathbf{U}}_k \check{\mathbf{S}}_k \check{\mathbf{V}}_k^H \ , \tag{5.6}$$

where the last equality represents the SVD of $\check{\mathbf{H}}_k$. As a result, on each subcarrier, for the group of users currently being served, their channels are completely decoupled and they observe no interference from one another. The transmit equalization matrix $\mathbf{F}$ is defined as

$$\mathbf{F} = [\mathbf{F}_1, \ldots, \mathbf{F}_{K_m}] \tag{5.7}$$

where $\mathbf{F}_k^H \mathbf{F}_k = \mathbf{I},\ 1 \leq k \leq K_m$. For each user here,

$$\mathbf{F}_k = \tilde{\mathbf{V}}_k^{(0)} \check{\mathbf{V}}_k \ . \tag{5.8}$$

The receive equalization matrix for this user is

$$\mathbf{W}_k = \check{\mathbf{U}}_k \ . \tag{5.9}$$

In sections 5.2 and 5.3, the user subcarrier allocation and the subchannel power loading will be derived. Let $\mathbf{P}$ be the diagonal power allocation matrix on a this subcarrier, where $\mathbf{P} = \text{blkdiag}(\mathbf{P}_1, \ldots, \mathbf{P}_k, \ldots, \mathbf{P}_{K_m})$ and $\mathbf{P}_k$ is the power allocation matrix for user k. Depending on where the diagonal elements of $\mathbf{P}_k$ are zero, some spatial subchannels may not be used. The final input-output relationship for

each user on this subcarrier may be expressed as

$$\begin{aligned}\mathbf{z}_k &= \mathbf{W}_k^H \mathbf{y}_k \\ &= \mathbf{W}_k^H (\mathbf{H}_k \mathbf{x}_k + \mathbf{n}_k) \\ &= \mathbf{W}_k^H (\mathbf{H}_k \mathbf{F}_k \mathbf{P}_k^{1/2} \mathbf{a}_k + \mathbf{n}_k) \\ &= \check{\mathbf{S}}_k \mathbf{P}_k^{1/2} \mathbf{a}_k + \mathbf{W}_k^H \mathbf{n}_k \ . \end{aligned} \tag{5.10}$$

Therefore, the data streams for each user are decoupled:

$$z_{k,l} = s_{k,l} \sqrt{\tilde{p}_{k,l}} a_{k,l} + \tilde{n}_{k,l} \ , \tag{5.11}$$

where $a_{k,l}$ is the transmitted data symbol on subchannel l, $s_{k,l}$ and $\tilde{p}_{k,l}$ are the l-th diagonal elements of $\check{\mathbf{S}}_k$ and $\mathbf{P}_k$ respectively, $z_{k,l}$ is the received signal, and $\tilde{n}_{k,l}$ is the zero-mean CSCG noise with variance N_0. Overall, for this subcarrier, we have

$$\begin{aligned}\mathbf{z} &= \mathbf{W}^H \mathbf{y} \\ &= \mathbf{W}^H (\mathbf{H}\mathbf{x} + \mathbf{n}) \\ &= \mathbf{W}^H (\mathbf{H}\mathbf{F}\mathbf{P}^{1/2}\mathbf{a} + \mathbf{n}) \\ &= \check{\mathbf{S}}\mathbf{P}^{1/2}\mathbf{a} + \mathbf{W}^H \mathbf{n} \ , \end{aligned} \tag{5.12}$$

where $\mathbf{a} = [\mathbf{a}_1^T, \ldots, \mathbf{a}_{K_m}^T]^T$ is the transmit data vector in which $\mathbb{E}[\mathbf{a}\mathbf{a}^H] = \mathbf{I}$, $\mathbf{W} = \text{blkdiag}(\mathbf{W}_1, \ldots, \mathbf{W}_{K_m})$ is the receive equalization matrix, $\check{\mathbf{S}} = \text{blkdiag}(\check{\mathbf{S}}_1, \ldots, \check{\mathbf{S}}_{K_m})$ is the equivalent channel, and $\mathbf{z} = [\mathbf{z}_1^T, \ldots, \mathbf{z}_{K_m}^T]^T$ is the equalized signal vector at the receiver.

Uplink Case

The equalization scheme for the uplink can be derived by considering the *dual downlink*. For an uplink channel over one subcarrier, $\mathbf{H}_u$, define the dual downlink

channel as

$$\mathbf{H}_d = \mathbf{H}_u^H \ . \tag{5.13}$$

The same steps as in the previous subsection can be used to derive $\mathbf{F}$ and $\mathbf{W}$, by considering $\mathbf{H}_d$ as $\mathbf{H}$. However, in this case, $\mathbf{W}$ is the transmit equalization matrix while $\mathbf{F}$ is the receive equalization matrix. The input-output relationship for this subcarrier is

$$\begin{aligned} \mathbf{z}_u &= \mathbf{F}^H \mathbf{y}_u \\ &= \mathbf{F}^H (\mathbf{H}_u \mathbf{x}_u + \mathbf{n}_u) \\ &= \mathbf{F}^H (\mathbf{H}_d^H \mathbf{W} \mathbf{P}^{1/2} \mathbf{a}_u + \mathbf{n}_u) \\ &= \check{\mathbf{S}} \mathbf{P}^{1/2} \mathbf{a}_u + \mathbf{F}^H \mathbf{n}_u \ , \end{aligned} \tag{5.14}$$

Again, the data streams of all the users are decoupled, just as in (5.11). The same power allocation can be used, giving the same data rates for all the users, be it the downlink or the uplink.

5.2 Optimal Solution for Power Minimization

In this section, the problem of power minimization given user rate requirements is formulated mathematically and the optimal solution is derived. While this is optimal, the complexity is huge because of an exhaustive search over a large set of possible subcarrier allocations.

The objective is to find the optimal subcarrier allocation $\{\sigma_{k,m}\}$ and power allocation $\{p_{k,m}\}$ that minimize the overall transmit power subject to satisfying each user's normalized data rate requirement $\bar{R}_k$ bits per sec per Hz (bps/Hz). [1]

[1]For M subcarriers, each with bandwidth ω, the overall rate for user k is $M\bar{R}_k\omega$ bps. $M\bar{R}_k$ bits are transmitted for user k in the duration of one OFDM symbol i.e. one channel use.

Mathematically, the optimization can be expressed as

$$\begin{aligned} \underset{\{\sigma_{k,m}\},\{p_{k,m}\}}{\text{minimize}} \quad & \sum_{m=1}^{M}\sum_{k=1}^{K} p_{k,m} \\ \text{subject to} \quad & \sum_{m=1}^{M} r_{k,m} \geq M\bar{R}_k \ , \quad \forall k \\ & p_{k,m} \geq 0 \ , \quad \forall k, m \end{aligned} \tag{5.15}$$

where $r_{k,m}$ is the rate of user k on subcarrier m and it can be written as

$$r_{k,m} = \sum_{l=1}^{\eta_{k,m}} \log_2 \left(1 + \frac{\tilde{p}_{k,m,l} s_{k,m,l}^2}{\Gamma N_0}\right) \ , \tag{5.16}$$

where $s_{k,m,l}$ is the l-th diagonal element of user k's equivalent channel $\check{\mathbf{S}}_{k,m}$ on subcarrier m as in (5.11). Therefore $\{s_{k,m,l}\}$ is dependent on the user selection $\{\sigma_{k,m}\}$ on subcarrier m, where $\sigma_{k,m}$ is as defined in Section 5.1.1. $\tilde{p}_{k,m,l}$ is the power loading on subchannel l for user k on the m-th subcarrier, and $p_{k,m} = \sum_{l=1}^{\eta_{k,m}} \tilde{p}_{k,m,l}$. If $\sigma_{k,m} = 0$, we set $p_{k,m} = 0$, $s_{k,m,l} = 0 \forall l$, and $r_{k,m} = 0$. In (5.16), Γ is the SNR gap which can be represented as

$$\Gamma = -\frac{\ln(5 \text{ BER})}{1.5} \tag{5.17}$$

for an uncoded M-QAM modulation with a specified BER [104]. For practical systems that use error-correction coding, the SNR gap can be much smaller. If the subcarrier assignment $\{\sigma_{k,m}\}$ is fixed, the power allocation can be found for

each user separately. If user k is of interest, the problem becomes

$$\begin{aligned} \underset{\{p_{k,m}\}}{\text{minimize}} \quad & \sum_{m=1}^{M} p_{k,m} \\ \text{subject to} \quad & \sum_{m=1}^{M} r_{k,m} \geq M\bar{R}_k \\ & p_{k,m} \geq 0 \ , \quad \forall m \\ & p_{k,m} = 0 \ , \quad \text{if } \sigma_{k,m} = 0 \ . \end{aligned} \tag{5.18}$$

Water-filling can be then carried out over user k's eigen-channels across all the subcarriers to find the optimal power and rate allocation:

$$\tilde{p}_{k,m,l} = \max\left\{\frac{\mu_k}{\ln 2} - \frac{\Gamma N_0}{s_{k,m,l}^2} \ , \ 0\right\} \ , \tag{5.19}$$

$$\tilde{r}_{k,m,l} = \log_2\left(\max\left\{\frac{\mu_k s_{k,m,l}^2}{\ln 2 \ \Gamma N_0} \ , \ 1\right\}\right) \ , \tag{5.20}$$

where $\frac{\mu_k}{\ln 2}$ is the water level such that

$$\sum_{m=1}^{M}\sum_{l=1}^{\eta_{k,m}} \tilde{r}_{k,m,l} = M\bar{R}_k \ . \tag{5.21}$$

To illustrate the water-filling, $\frac{\mu_k}{\ln 2}$ can be interpreted as the common water level of the power or water poured over channels with river beds equal to $\frac{\Gamma N_0}{s_{k,m,l}^2}$. Starting with the maximum number of streams, $\frac{\mu_k}{\ln 2}$ is evaluated for a decreasing number of streams until the point where the water level is above the highest river bed.

In order to obtain the globally optimal solution, an exhaustive search is needed over all the subcarrier assignments $\{\sigma_{k,m}\}$ to find the minimum transmit sum power. Thus, K water-filling procedures over Mn_k singular values have to be carried out for each of 2^{KM} possibilities. Even if a constraint is imposed such that only 1 user occupies each subcarrier, there would be K^M possibilities to test.

5.3 Efficient Solution for Power Minimization

In this section, an efficient solution to the power minimization problem is derived based on a Lagrange dual decomposition. First, let us write the problem of (5.15) as the following optimization problem:

$$\begin{aligned} \underset{\{r_{k,m}\}}{\text{minimize}} \quad & f(\mathbf{r}) \\ \text{subject to} \quad & \sum_{m=1}^{M} \mathbf{r}_m \geq M\bar{\mathbf{R}} \ , \end{aligned} \tag{5.22}$$

where $\mathbf{r} = [\mathbf{r}_1^T, \ldots, \mathbf{r}_m^T, \ldots, \mathbf{r}_M^T]^T$, in which $\mathbf{r}_m = [r_{1,m}, \ldots, r_{K,m}]^T$, is the rate allocation to be optimized. $f(\cdot)$ is a $\mathbb{R}^{MK} \rightarrow \mathbb{R}$ function that is not necessarily convex. The rate requirements are represented by the $\bar{\mathbf{R}} = [\bar{R}_1, \ldots, \bar{R}_K]^T$ and "$\geq$" denotes a set of elementwise inequalities. Even though the objective function is not convex, it is still possible to transform this problem into a convex one, by forming the Lagrangian dual of the objective function. This is called the *dual method*. The original optimization is known as the *primal* problem, while the transformed problem is known as the *dual* problem. In the dual method, the Lagrangian of (5.22) is first evaluated:

$$\mathcal{L}(\mathbf{r}, \boldsymbol{\mu}) = f(\mathbf{r}) + \boldsymbol{\mu}^T \left(M\bar{\mathbf{R}} - \sum_{m=1}^{M} \mathbf{r}_m \right) \ . \tag{5.23}$$

where $\boldsymbol{\mu} = [\mu_1, \ldots, \mu_K]^T$ is the vector of Lagrange multipliers. The dual function $g(\boldsymbol{\mu})$ is defined as the unconstrained minimization of the Lagrangian.

$$g(\boldsymbol{\mu}) = \min_{\mathbf{r}} \mathcal{L}(\mathbf{r}, \boldsymbol{\mu}) = \mathcal{L}(\mathbf{r}^\star, \boldsymbol{\mu}) \ . \tag{5.24}$$

where $\mathbf{r}^\star = \arg\min_{\mathbf{r}} \mathcal{L}(\mathbf{r}, \boldsymbol{\mu})$. The dual problem is therefore

$$\begin{aligned} \underset{\boldsymbol{\mu}}{\text{maximize}} \quad & g(\boldsymbol{\mu}) \\ \text{subject to} \quad & \boldsymbol{\mu} \geq \mathbf{0} \ . \end{aligned} \tag{5.25}$$

The dual function is always concave, independent of the convexity of $f(\cdot)$. Therefore efficient convex optimization techniques can be used to maximize $g(\boldsymbol{\mu})$. If the function $f(\cdot)$ is convex, it turns out that solving the dual problem is equivalent to solving the primal problem, and both solutions are identical [99]. In our optimization of (5.15), the objective function is a pointwise minimum of several convex functions. This is clearly not convex. However, the solution to the dual problem is a lower bound for the optimal primal objective function value. The difference between the optimal primal and dual function values is termed the "duality gap." It has been shown that for multicarrier systems with large M, the duality gap is negligible [110].

From the previous section, the Lagrangian of the optimization problem (5.15) is

$$\mathcal{L}_1 = \sum_{m=1}^{M} \sum_{k=1}^{K} p_{k,m} + \sum_{k=1}^{K} \mu_k \left(M \bar{R}_k - \sum_{m=1}^{M} r_{k,m} \right) \ , \tag{5.26}$$

where μ_k are the Lagrange multipliers as in (5.23) and $r_{k,m}$ is given by (5.16). If the μ_k are fixed, the user selection can be done on a per subcarrier basis as follows. Write (5.26) as

$$\mathcal{L}_1 = \sum_{m=1}^{M} \mathcal{L}_2(m) + \sum_{k=1}^{K} \mu_k M \bar{R}_k \ , \tag{5.27}$$

where

$$\mathcal{L}_2(m) = \sum_{k=1}^{K} (p_{k,m} - \mu_k r_{k,m}) \ . \tag{5.28}$$

Consequently, the problem is decomposed into M independent subproblems. Assume that the user selection $\{\sigma_{k,m}\}$ has been fixed. Considering one subcarrier,

$$\mathcal{L}_2(m) = \sum_{k=1}^{K} \sum_{l=1}^{\eta_k} \left(\tilde{p}_{k,m,l} - \mu_k \log_2 \left(1 + \frac{\tilde{p}_{k,m,l} s_{k,m,l}^2}{\Gamma N_0} \right) \right) \ . \tag{5.29}$$

$\mathcal{L}_2(m)$ can then be minimized for each user separately in order to calculate $\tilde{p}_{k,m,l}$. By applying the water-filling procedure, the power allocation and rate for the l-th subchannel of user k can be found:

$$\tilde{p}_{k,m,l} = \max \left\{ \frac{\mu_k}{\ln 2} - \frac{\Gamma N_0}{s_{k,m,l}^2} \ , \ 0 \right\} \ , \tag{5.30}$$

$$\tilde{r}_{k,m,l} = \log_2 \left(\max \left\{ \frac{\mu_k s_{k,m,l}^2}{\ln 2 \ \Gamma N_0} \ , \ 1 \right\} \right) \ . \tag{5.31}$$

Consequently, a search over 2^K possible user selections $\{\sigma_{k,m}\}$ on subcarrier m can be carried out to find the best user selection that minimizes $\mathcal{L}_2(m)$.

A constraint of only one user per subcarrier would greatly simplify the search, since there would only be K possible selections to choose from. The user that minimizes $\mathcal{L}_2(m)$ is selected. If $\mathcal{L}_2(m) \geq 0$, this user is dropped and eventually no users are allowed on this subcarrier. This is because a positive value of $\mathcal{L}_2(m)$ does not serve to minimize $\mathcal{L}_1$. Overall, for M subcarriers, there would only be MK possibilities to test.

In a more general case, more than one user is allowed per subcarrier. On each subcarrier, once a certain user has been selected, the algorithm proceeds by finding the minimum $\mathcal{L}_2(m)$ for $\binom{K}{2}$ possible pairs of users. If this value of $\mathcal{L}_2(m)$ is more than the value of $\mathcal{L}_2(m)$ for a single user, the search stops here and only one user is

selected for this subcarrier. However, if this value of $\mathcal{L}_2(m)$ is lower than that of a single user, these two users are confirmed to be using the current subcarrier. The algorithm then proceeds to test all $\binom{K}{3}$ possible triplets of users. The maximum number of user selections to examine would be 2^K. Over all M subcarriers, there would be $M \cdot 2^K$ possibilities to test.

When the number of subcarriers M is large, the duality gap is negligible [110]. For a certain channel realization, if the duality gap happens to be zero, the efficient solution offered in this section coincides exactly with the optimal solution. The resource allocation would therefore be optimal, resulting in the least possible power. On the other hand, if the duality gap is not zero, this efficient solution is near-optimal in terms of sum power minimization for target rates.

On each subcarrier, a suboptimal search based on the greedy algorithm can be used to simplify the user selection process given above. As before, $\mathcal{L}_2(m)$ is evaluated for each of the K users and the user that gives the minimum $\mathcal{L}_2(m)$ is selected. Next, $\mathcal{L}_2(m)$ is calculated for the case where one of the remaining $K-1$ users is added to the set. The user that gives the minimum value of $\mathcal{L}_2(m)$ is selected. If this value of $\mathcal{L}_2(m)$ is higher than the $\mathcal{L}_2(m)$ found previously for a single user, this second user is dropped and eventually only one user would occupy this subcarrier.

However, if the current $\mathcal{L}_2(m)$ value is lower than the previous $\mathcal{L}_2(m)$ for a single user, these two users are confirmed to use the current subcarrier. The algorithm then proceeds to test if a third user is able to use this subcarrier and so on.

Finally, to complete this power minimization solution, the optimal Lagrange multipliers $\boldsymbol{\mu}$ that maximize the dual function $g(\boldsymbol{\mu})$ need to be found. $g(\boldsymbol{\mu})$ can be maximized by updating $\boldsymbol{\mu}$ along some search direction, all components at a time. The concavity of $g(\boldsymbol{\mu})$ guarantees that the maximum can be found by a gradient-

based search. Although $g(\boldsymbol{\mu})$ is concave, it may not be differentiable at all points, so a gradient may not always exist. In spite of this, it is still possible to obtain a search direction by finding a supergradient [111], which is a generalization of a gradient. A supergradient at a point $\hat{\boldsymbol{\mu}}$ is a vector $\bar{\mathbf{d}}$ that satisfies

$$g(\tilde{\boldsymbol{\mu}}) \leq g(\hat{\boldsymbol{\mu}}) + \bar{\mathbf{d}}^T (\tilde{\boldsymbol{\mu}} - \hat{\boldsymbol{\mu}}) \ . \tag{5.32}$$

for every $\tilde{\boldsymbol{\mu}} \neq \boldsymbol{\mu}$.

Proposition 3. *For the optimization problem (5.15) with a dual function value* $g(\hat{\boldsymbol{\mu}}) = \mathcal{L}(\mathbf{r}^\star, \hat{\boldsymbol{\mu}})$ *at* $\hat{\boldsymbol{\mu}}$*, where* $\mathbf{r}^\star = \arg\min_{\mathbf{r}} \mathcal{L}(\mathbf{r}, \hat{\boldsymbol{\mu}})$*, a valid supergradient at the point* $\hat{\boldsymbol{\mu}}$ *is given by*

$$\bar{\mathbf{d}} = M\bar{\mathbf{R}} - \sum_{m=1}^{M} \mathbf{r}_m^\star \ . \tag{5.33}$$

Proof.

$$\begin{aligned}
g(\tilde{\boldsymbol{\mu}}) &= \min_{\mathbf{r}} \mathcal{L}(\mathbf{r}, \tilde{\boldsymbol{\mu}}) \\
&= \min_{\mathbf{r}} \sum_{m=1}^{M} f_m(\mathbf{r}_m) + \tilde{\boldsymbol{\mu}}^T \left(M\bar{\mathbf{R}} - \sum_{m=1}^{M} \mathbf{r}_m \right) \\
&\leq \sum_{m=1}^{M} f_m(\mathbf{r}_m^\star) + \tilde{\boldsymbol{\mu}}^T \left(M\bar{\mathbf{R}} - \sum_{m=1}^{M} \mathbf{r}_m^\star \right) \\
&= \sum_{m=1}^{M} f_m(\mathbf{r}_m^\star) + \hat{\boldsymbol{\mu}}^T \left(M\bar{\mathbf{R}} - \sum_{m=1}^{M} \mathbf{r}_m^\star \right) + (\tilde{\boldsymbol{\mu}} - \hat{\boldsymbol{\mu}})^T \left(M\bar{\mathbf{R}} - \sum_{m=1}^{M} \mathbf{r}_m^\star \right) \\
&= g(\hat{\boldsymbol{\mu}}) + \left(M\bar{\mathbf{R}} - \sum_{m=1}^{M} \mathbf{r}_m^\star \right)^T (\tilde{\boldsymbol{\mu}} - \hat{\boldsymbol{\mu}}) \ ,
\end{aligned} \tag{5.34}$$

thereby satisfying the supergradient definition (5.32). □

A supergradient can be represented as a supporting hyperplane defined by the vector $(-\bar{\mathbf{d}}, 1)$ that touches the graph of $g(\boldsymbol{\mu})$ at the point $\hat{\boldsymbol{\mu}}$ such that the graph

$g(\boldsymbol{\mu})$ lies below this hyperplane for all $\boldsymbol{\mu}$.

In practice, a scaled version of the supergradient, $\mathbf{d} = [d_1, \ldots, d_K]^T = \frac{\bar{\mathbf{d}}}{M}$, can be used, where

$$d_k = \bar{R}_k - \frac{1}{M} \sum_{m=1}^{M} r_{k,m} \ . \tag{5.35}$$

Therefore, starting from an initial value, the Lagrange multipliers are updated in the positive supergradient direction in order to maximize the dual function.

$$\mu_k(\tau + 1) = \max \{\mu_k(\tau) + \delta \ d_k \ , \ 0\} \ , \tag{5.36}$$

where τ represents the iteration number and δ is a small step size. μ_k can be interpreted as the reward for user k to increase its rate. The direction of (5.36) suggests that if the rate of user k falls below its target rate, its rate reward μ_k should be increased. On the other hand, if user k exceeds its rate requirement, μ_k should be decreased. Furthermore, the rate reward should not fall below zero. Note that for minimization of a convex function, the corresponding generalization of the gradient is the subgradient, in which case, the update is in the negative subgradient direction.

During the optimization process, the dual rates for the users,

$$r_k = \sum_{m=1}^{M} r_{k,m} \ , \tag{5.37}$$

gradually approach the rate requirements $M\bar{R}_k$. However, at any point in time, the current subcarrier selections $\{\sigma_{k,m}\}$ can be captured to solve for the optimal minimum power solution given target rates. As the optimization proceeds, this power value for guaranteed rates will tend to decrease and approach the dual function $\mathcal{L}_1$. Unlike algorithms such as steepest-descent, the dual function is not

guaranteed to increase monotonically with each iteration. Therefore, the algorithm keeps track of the the subcarrier selection $\{\sigma_{k,m}\}$ that provides the minimum sum power over all the previous iterations.

5.4 Adaptation for Efficient Solution

The previous section has shown how efficient power minimization can be done using convex optimization techniques. For the Lagrange multiplier update, while any initial value of $\boldsymbol{\mu}$ can be used, it would be better to start with an estimate of $\boldsymbol{\mu}$ to shorten the convergence time. Furthermore, a good value of the step size δ would also improve the convergence. Too small a step size would result in slow convergence while too large a step size results in low precision. In this section, algorithms are provided to estimate an initial value of $\boldsymbol{\mu}$ and to update the step size adaptively for faster convergence.

An initial value of $\boldsymbol{\mu}$ can be found if the subcarrier allocation is fixed cyclicly. Let user k take subcarriers $qK + k$, $q = 0, 1, 2, \ldots$. Then $\mathcal{L}_1$ can be minimized by considering each user separately.

$$\mathcal{L}_1 = \sum_{k=1}^{K} \mathcal{L}_3(k) \ , \text{ where} \tag{5.38}$$

$$\begin{aligned} \mathcal{L}_3(k) &= \sum_{m=1}^{M} p_{k,m} + \mu_k \left(M\bar{R}_k - \sum_{m=1}^{M} r_{k,m} \right) \\ &= \sum_{m=1}^{M} \sum_{l=1}^{\eta_{k,m}} \tilde{p}_{k,m,l} + \mu_k \left(M\bar{R}_k - \sum_{m=1}^{M} \sum_{l=1}^{\eta_{k,m}} \tilde{r}_{k,m,l} \right) \ . \end{aligned} \tag{5.39}$$

Water-filling can be applied to calculate the power allocation:

$$\tilde{p}_{k,m,l} = \max \left\{ \frac{\mu_k}{\ln 2} - \frac{\Gamma N_0}{s_{k,m,l}^2} \ , \ 0 \right\} \ , \tag{5.40}$$

$$\tilde{r}_{k,m,l} = \log_2 \left(\max \left\{ \frac{\mu_k s_{k,m,l}^2}{\ln 2 \ \Gamma N_0} \ , \ 1 \right\} \right) \ , \tag{5.41}$$

where $\frac{\mu_k}{\ln 2}$ is the water level such that

$$\sum_{m=1}^{M} \sum_{l=1}^{\eta_{k,m}} \tilde{r}_{k,m,l} = M \bar{R}_k \ . \tag{5.42}$$

Let these values of μ_k be the initial values $\mu_k(1)$. The initial step size can be chosen as

$$\delta(1) = \xi_1 \frac{\sum_{k=1}^{K} \mu_k(1)}{\sum_{k=1}^{K} \bar{R}_k} \ . \tag{5.43}$$

where ξ_1 is a positive constant. The step size is adjusted adaptively as the algorithm proceeds, based on the performance of the convergence. Before going into the adaptation algorithm, thresholds are set for the maximum and minimum step size.

$$\delta_{\max} = \xi_{\max} \ \delta(1) \ , \tag{5.44}$$

$$\delta_{\min} = \xi_{\min} \ \delta(1) \ . \tag{5.45}$$

where the constants are such that $\xi_{\max} > 1$ and $0 < \xi_{\min} < 1$. When the dual rates for all the users are observed to be moving in one direction, the step size δ is increased:

$$\delta(\tau + 1) = \delta(\tau) \times \xi_2 \ , \tag{5.46}$$

where the constant $\xi_2 > 1$, or else if a user's dual rate is oscillating, the step size δ is decreased:

$$\delta(\tau + 1) = \delta(\tau) \ / \ \xi_3 \ , \tag{5.47}$$

where the constant $\xi_3 > 1$. The conditions for these two actions can be defined

mathematically. When

$$\begin{aligned} &[d_k(\tau-1) > 0 \text{ and } d_k(\tau) > 0] \\ \text{or } &[d_k(\tau-1) < 0 \text{ and } d_k(\tau) < 0] \end{aligned} \tag{5.48}$$

for all the users, the step size is increased. Else, when

$$\begin{aligned} &\left[\begin{array}{l} r_k(\tau) - r_k(\tau-1) < 0 \text{ and} \\ r_k(\tau-1) - r_k(\tau-2) > 0 \\ \text{for at least one user} \end{array}\right], \\ \text{or } &\left[\begin{array}{l} r_k(\tau) - r_k(\tau-1) > 0 \text{ and} \\ r_k(\tau-1) - r_k(\tau-2) < 0 \\ \text{for at least one user} \end{array}\right], \end{aligned} \tag{5.49}$$

the step size is decreased. If these two conditions are not satisfied, the step size remains as it is.

While any values of the parameters ξ_1, $\xi_{\max}$, $\xi_{\min}$, ξ_2, and ξ_3 could work theoretically, specific values may be chosen to speed up the convergence. A suggested combination of the parameters is $\xi_1 = 0.1$, $\xi_{\max} = 5$, $\xi_{\min} = 0.1$, $\xi_2 = 1.1$, and $\xi_3 = 2$. The rationale for choosing these is as follows. A large initial value of ξ_1 would result in large oscillations in the beginning, which would tend to stabilize as the step size is reduced. It is found that the given value of ξ_1 would also result in a fast convergence except without large initial oscillations. In the initial stage of the algorithm, the dual rates are relatively far from the rate requirements and would approach the rate requirements without oscillations. This means that it makes sense to increase the step size to speed up the convergence. Once the dual rates are close to the rate requirements, they tend to oscillate around the rate requirements. Therefore the step size is reduced to increase the precision. How-

ever, oscillations generally do not eventually disappear in methods based on the supergradient, so a lower limit $\xi_{\min}$ is set on the step size. In the trivial case of only one user, there are no oscillations during convergence. To prevent the step size from increasing without bound, an upper limit $\xi_{\max}$ is set. As for the step size adaptation, a small value of ξ_2 ensures that the algorithm would not suddenly go into large oscillations, and if oscillations do occur, a large value of ξ_3 allows the oscillations to be brought down quickly. These benefits have to be traded off with the advantage of a large step size.

It is interesting to see how well this adaptive method based on the supergradient can perform. In the following, we will investigate how close the algorithm can get to the maximum of the dual function, $g(\boldsymbol{\mu}^\star)$. When the Lagrange multipliers $\boldsymbol{\mu}$ approach the optimal value $\boldsymbol{\mu}^\star$, the dual rates $\mathbf{r}$ tend to hover about the target rates $M\bar{\mathbf{R}}$, resulting in oscillations. It is therefore expected that the step size would be close to the minimum threshold $\delta_{\min}$ due to the adaptation above. Furthermore, the Euclidean distance between $\mathbf{r}/M$ and $\bar{\mathbf{R}}$, or equivalently the supergradient norm $\|\mathbf{d}^{(\tau)}\|_2$, would normally be small for a large iteration number τ.

Theorem 4. *Assume that* $\|\mathbf{d}^{(\tau)}\|_2 < d_1, \forall \tau > \tau_1$ *and* $\delta^{(\tau)} < \delta_1, \forall \tau > \tau_2$ *for some positive real numbers* d_1 *and* δ_1*, and some positive integers* τ_1 *and* τ_2*. Also, assume* $\delta^{(\tau)} \geq \delta_{\min}, \forall \tau$*. Denote the maximum dual function value over all the previous iterations as* $g\left(\boldsymbol{\mu}_{\text{best}}^{(\tau)}\right)$*. For any* $\epsilon > 0$*, it can be shown that* $\exists\ \tau_3$ *such that*

$$g(\boldsymbol{\mu}^\star) - g\left(\boldsymbol{\mu}_{\text{best}}^{(\tau)}\right) < \frac{M\delta_1^2 d_1^2}{2\delta_{\min}} + \epsilon\ , \quad \forall \tau > \tau_3 \tag{5.50}$$

Proof.

$$\|\boldsymbol{\mu}^{(\tau+1)} - \boldsymbol{\mu}^\star\|_2^2 = \|\boldsymbol{\mu}^{(\tau)} - \boldsymbol{\mu}^\star\|_2^2 + 2\delta^{(\tau)}\mathbf{d}^{(\tau)T}\left(\boldsymbol{\mu}^{(\tau)} - \boldsymbol{\mu}^\star\right) + \delta^{(\tau)2}\|\mathbf{d}^{(\tau)}\|_2^2 \quad (5.51)$$

$$\leq \|\boldsymbol{\mu}^{(\tau)} - \boldsymbol{\mu}^\star\|_2^2 + \frac{2}{M}\delta^{(\tau)}\left(g\left(\boldsymbol{\mu}^{(\tau)}\right) - g\left(\boldsymbol{\mu}^\star\right)\right) + \delta^{(\tau)2}\|\mathbf{d}^{(\tau)}\|_2^2 , \quad (5.52)$$

from the definition of the supergradient. Due to recursion, we have

$$\|\boldsymbol{\mu}^{(\tau+1)} - \boldsymbol{\mu}^\star\|_2^2 \leq \|\boldsymbol{\mu}^{(1)} - \boldsymbol{\mu}^\star\|_2^2 - \frac{2}{M}\sum_{t=1}^{\tau}\delta^{(t)}\left(g\left(\boldsymbol{\mu}^\star\right) - g\left(\boldsymbol{\mu}^{(t)}\right)\right) + \sum_{t=1}^{\tau}\delta^{(t)2}\|\mathbf{d}^{(t)}\|_2^2 . \quad (5.53)$$

Let $\beta = \|\boldsymbol{\mu}^{(1)} - \boldsymbol{\mu}^\star\|_2$. Then

$$0 \leq \beta^2 - \frac{2}{M}\sum_{t=1}^{\tau}\delta^{(t)}\left(g\left(\boldsymbol{\mu}^\star\right) - g\left(\boldsymbol{\mu}^{(t)}\right)\right) + \sum_{t=1}^{\tau}\delta^{(t)2}\|\mathbf{d}^{(t)}\|_2^2 . \quad (5.54)$$

Since $g\left(\boldsymbol{\mu}^\star\right) - g\left(\boldsymbol{\mu}_{\text{best}}^{(t)}\right) \leq g\left(\boldsymbol{\mu}^\star\right) - g\left(\boldsymbol{\mu}^{(t)}\right)$,

$$\frac{2}{M}\sum_{t=1}^{\tau}\delta^{(t)}\left(g\left(\boldsymbol{\mu}^\star\right) - g\left(\boldsymbol{\mu}_{\text{best}}^{(t)}\right)\right) \leq \beta^2 + \sum_{t=1}^{\tau}\delta^{(t)2}\|\mathbf{d}^{(t)}\|_2^2 , \quad (5.55)$$

$$\left(g\left(\boldsymbol{\mu}^\star\right) - g\left(\boldsymbol{\mu}_{\text{best}}^{(\tau)}\right)\right)\frac{2\tau\delta_{\min}}{M} \leq \beta^2 + \sum_{t=1}^{\tau}\delta^{(t)2}\|\mathbf{d}^{(t)}\|_2^2 . \quad (5.56)$$

Denote $\tau_4 = \max\{\tau_1, \tau_2\}$ and define τ_3 as

$$\tau_3 = \left\lceil \max\left\{ \frac{M\beta^2}{\delta_{\min}\epsilon} , \frac{M\sum_{t=1}^{\tau_4}\delta^{(t)2}\|\mathbf{d}^{(t)}\|_2^2}{\delta_{\min}\epsilon} \right\} \right\rceil . \quad (5.57)$$

Then

$$g\left(\boldsymbol{\mu}^{\star}\right)-g\left(\boldsymbol{\mu}_{\text{best}}^{(\tau)}\right) \leq \frac{M\beta^2}{2\tau\delta_{\min}}+\frac{M\sum_{t=1}^{\tau_4}\delta^{(t)2}\|\mathbf{d}^{(t)}\|_2^2}{2\tau\delta_{\min}}+\frac{M\sum_{t=\tau_4+1}^{\tau}\delta^{(t)2}\|\mathbf{d}^{(t)}\|_2^2}{2\tau\delta_{\min}} \tag{5.58}$$

$$\leq \frac{\epsilon}{2}+\frac{\epsilon}{2}+\frac{M\tau\delta_1^2 d_1^2}{2\tau\delta_{\min}}\ , \quad \forall\tau>\tau_3 \tag{5.59}$$

$$= \frac{M\delta_1^2 d_1^2}{2\delta_{\min}}+\epsilon\ , \quad \forall\tau>\tau_3\ . \tag{5.60}$$

□

With the mentioned adaptations in place, the optimization algorithm in the previous section can be applied for time-varying channels without a need to re-initialize $\boldsymbol{\mu}$. This is because the relative channel strengths of different users would not tend to change drastically. μ_k, which represents the rate reward for user k, would update to track the channel conditions. Similarly, μ_k adapts to track user k's rate requirements. When there is a change in the channel or the rate requirements, the thresholds $\delta_{\max}$ and $\delta_{\min}$ are recalculated and the last known best subcarrier allocation is reset. $\boldsymbol{\mu}$ and δ are not re-initialized. It is suggested that the algorithm be run for a certain number of iterations before the actual usage of the subcarrier allocation, because it may take a few iterations for the sum power to fall, below that of a fixed subcarrier allocation for example.

5.5 Dual Proportional Fairness

The optimization algorithm in Section 5.3 is immediately applicable to harsh wireless channels. As the MIMO channel is frequency-selective in this case, the user selection on each subcarrier is optimized to provide the minimum overall transmit power. However, a problem arises for frequency-flat fading channels, if they ever occur. In a perfectly flat fading channel, user selection on one subcarrier is re-

peated for all the subcarriers. When this happens, only one or a few of the users are allocated subcarriers at any one time. This has serious consequences for the algorithm. The subcarrier allocation $\{\sigma_{k,m}\}$ given by the optimization is unable to guarantee all the users' rate requirements.

In this section, a solution based on convex optimization theory is developed that can tackle the event of frequency-flat fading. This flat fading management is based on a concept that will be called *dual proportional fairness*. This is inspired by the principle of proportional fairness (PF) [84] in which there is a certain randomness to be exploited. While in PF, the nature of the fluctuating channel is used to design the time schedules, in dual PF, the nature of the fluctuating dual rates is utilized to design the subcarrier allocation.

5.5.1 Principle of Dual Proportional Fairness

In the dual method of convex optimization, for example in power minimization, the Lagrange multipliers $\boldsymbol{\mu}$ represent a tangent plane in a graph of power versus user rates. In this graph, there are several power surfaces, each representing a different subcarrier allocation. The pointwise minimum of all these power surfaces represent the minimum sum power for any given tuple of user rate requirements. When the number of subcarriers is large, there are more power surfaces corresponding to various subcarrier allocations and the pointwise minimum of these power surfaces tend to assume a convex shape. During the optimization process, the tangent plane is in contact with this minimum surface. The coordinates at this contact point give the current dual rates for all the users. As the Lagrange multipliers get updated, the tangent plane adjusts and the point of contact shifts such that the dual rates approach the users' target rates. Convergence occurs when the dual rates hit the target rates and the minimum sum power is achieved.

Frequency-flat fading channels pose a problem because the points where the

power surfaces can touch the tangent plane are collinear. For now, assume that only one user occupies each subcarrier. Consider the case of 2 users. In simulations, it is impossible for the tangent plane to touch the centre power surface, corresponding to a subcarrier allocation of 50% to user 1 and 50% to user 2, without touching the other power surfaces. As a result, the algorithm oscillates between giving all the subcarriers to user 1 or all to user 2. Consequently, each user's rate swings between zero and a value larger than its rate requirement.

Based on this understanding, a flat fading management based on *dual proportional fairness* is proposed. In a flat fading scenario, the power allocations and rates for user k on all the subcarriers are identical:

$$p_{k,m} = \hat{p}_k \ , \quad \forall m \tag{5.61}$$

$$r_{k,m} = \hat{r}_k \ , \quad \forall m \tag{5.62}$$

$$p_k = M_k \hat{p}_k \tag{5.63}$$

$$r_k = M_k \hat{r}_k \ , \tag{5.64}$$

where M_k is the number of subcarriers allocated to user k and $\sum_{k=1}^{K} M_k = M$. Consider the case of two users. The possible coordinates given by the optimization algorithm are

$$(M\hat{r}_1 \ , \ 0 \ , \ M\hat{p}_1) \tag{5.65}$$

$$(0 \ , \ M\hat{r}_2 \ , \ M\hat{p}_2) \ . \tag{5.66}$$

Another coordinate, not given by the original optimization, is also possible:

$$(M_1\hat{r}_1 \ , \ M_2\hat{r}_2 \ , \ M_1\hat{p}_1 + M_2\hat{p}_2) \ . \tag{5.67}$$

It can be seen that these three coordinates are collinear. This concept can be

extended to more than 2 users. The trick is now to find the right combination of $\{M_k\}$ that minimizes the sum power. This can be found in the following three steps:

1. Identify the flat fading users.
2. Identify the flat fading groups.
3. Distribute the subcarriers proportionally for each fading group.

5.5.2 Algorithm for Flat Fading Management

In this subsection, a three-step algorithm is provided to automatically detect and deal with the scenario of flat fading.

1. Identify the flat fading users

Flat fading users are identified as users with rates that oscillate largely or drop to zero:

$$\begin{aligned} \{ \quad [\quad & r_k > 1.2\ M\bar{R}_k \text{ at least once} \\ & \text{and } r_k < 0.8\ M\bar{R}_k \text{ at least once }] \\ & \text{or } r_k = 0 \text{ at least once} \qquad \} \end{aligned} \tag{5.68}$$

in the current and previous 9 iterations. Assume there are K_{ff} such users.

2. Identify the flat fading groups

For each flat fading user, look back to see when he had received a dual rate higher than his rate requirement. (If he had not, the flat fading management cannot be done right now.) Find out the minimum number of subcarriers user k needs to just fulfill his rate requirement. Let this be $\bar{M}_k$.

Next, consider all users pairwise. Take user 1 and user 2 for example. Find

out where the subcarriers allocated to user 1, $\mathbf{\Sigma}_1$, overlaps with the subcarriers of user 2, $\mathbf{\Sigma}_2$. If they do overlap, users 1 and 2 are in the same group G_v. The union of subcarriers is taken as the flat fading subcarriers of this group, $\mathbf{\Sigma}_{G_v}$. Continue this process for all K_{ff} flat fading users. Users that are not interlinked in this manner are placed in separate flat fading groups. Assume there are K_v users in each fading group G_v.

3. Distribute the subcarriers proportionally for each fading group

Let there be $\tilde{M}_v$ flat fading subcarriers in G_v. First assume the special case of flat fading over all the subcarriers. Users are allocated subcarriers cyclically until user k gets a maximum of

$$\text{round}\left[\frac{\bar{M}_k}{\sum_{k\in G_v}\bar{M}_k}\tilde{M}_v\right] \tag{5.69}$$

subcarriers. To make sure all the subcarriers get allocated, the last user can get all the remaining subcarriers.

An additional modification to (5.69) allows the algorithm to handle the most general case of partially frequency-selective channels. Take for example the case of two users. In the graph of power versus user rates, only a subset of subcarrier allocations result in collinear points of contact with the tangent plane. This time, oscillations do occur but they are not between zero and very high rates. Instead, each user's dual rate oscillates above and below its rate requirement while its dual rate does not drop to zero. Practically, taking the current subcarrier allocation $\{\sigma_{k,m}\}$ still allows the user rates to be guaranteed, but this is at an expense of higher transmit power that also oscillates largely. In the following, a modification to (5.69) is developed that allows smooth convergence for the general case of partially frequency-selective channels.

For each user, find the subcarriers that were allocated to this user for the

current and previous 9 iterations. Let there be $M_{k,\min}$ such subcarriers. Let $\tilde{\mathbf{\Sigma}}_{G_v}$ be the subcarriers of group G_v with the subcarriers corresponding to $M_{k,\min}$ of all flat fading users removed. Let there be $\tilde{\bar{M}}_v$ flat fading subcarriers in $\tilde{\mathbf{\Sigma}}_{G_v}$. These subcarriers are distributed in a similar manner as in the previous section. All flat fading users get allocated their respective $M_{k,\min}$ subcarriers. The initial estimated number of subcarriers each flat fading user would get from $\tilde{\mathbf{\Sigma}}_{G_v}$ is

$$\bar{\bar{M}}_k = \max\left\{\bar{M}_k - M_{k,\min}\ ,\ 0\right\}\ . \tag{5.70}$$

Users are allocated subcarriers cyclically until user k gets a maximum of

$$\text{round}\left[\frac{\bar{\bar{M}}_k}{\sum_{k\in G_v}\bar{\bar{M}}_k}\tilde{\bar{M}}_v\right] \tag{5.71}$$

subcarriers. Again, to handle any rounding errors, the last user is allocated all the remaining subcarriers. Subcarriers that are not affected by the flat fading management are assigned the same subcarriers as given by the original solution without any flat fading management. For the purpose of adaptation, when the channel or rate requirements change, this algorithm is restarted. As in Section 5.4, $\boldsymbol{\mu}$ and δ are not re-initialized.

5.6 Simulation Results

This section first shows the convergence behaviour of the proposed algorithm for certain typical scenarios. Following that, the performance of the efficient subcarrier allocation versus a fixed subcarrier allocation is examined. Other heuristic algorithms are also included for comparison.

Unless otherwise stated, the setup is a $3 \times [3, 3, 3]$ MIMO system, where the base station has 3 antennas and there are 3 user terminals with 3 antennas each,

and the rate requirement is $\bar{R}_k = 3$ bps/Hz $\forall k$, with an SNR gap of 3 dB. The number of subcarriers is $M = 64$. It is assumed that each subcarrier is occupied by at most one user only. The channel is frequency-selective with 17 taps and has a uniform power delay profile. The algorithm in Section 5.5.2 is used in all the simulations. Step 1 involves an automatic identification of flat fading users. If there are flat fading users detected, steps 2 and 3 are then employed for flat fading management. For the graphs, the SNR is defined as $\frac{\sum_{m=1}^{M}\sum_{k=1}^{K} p_{k,m}}{MN_0} = \frac{E_s}{MN_0}$, where total transmitted signal energy is divided by total noise energy. Therefore the dual function is also scaled by $\frac{1}{MN_0}$ for comparison.

Figure 5.3 illustrates the typical convergence behaviour for these default settings. As can be seen, the sum power required for the efficient subcarrier allocation quickly drops to a near-optimal value, in just 2 iterations for this example. Note that this sum power is for *guaranteed* rates, as shown by the '+' symbols in the second subgraph. The dual function, on the other hand, corresponds to the dual rates, which are the coordinates of the point of contact between the tangent plane and the objective function. In the second subgraph, each curve represents the dual rate for each user. The power for the efficient allocation approaches the dual function value, showing that the duality gap is almost zero.

To see the concept of dual proportional fairness at work, consider a flat fading channel, i.e. a channel with only 1 tap. In Figure 5.4, the dual rates fluctuate between zero and about 9 bps/Hz. Because the decision to select a particular user is repeated for all the subcarriers, only 1 user is allocated all the subcarriers at each iteration. However, the flat fading management is automatically started, and the algorithm is able to attain a near-optimal sum power in just 4 iterations, while satisfying all user rate requirements, denoted by the '+' marks in the second subgraph. This is because the nature of the fluctuating dual rates are used to balance the subcarrier assignment between the users. The vertical lines in the first

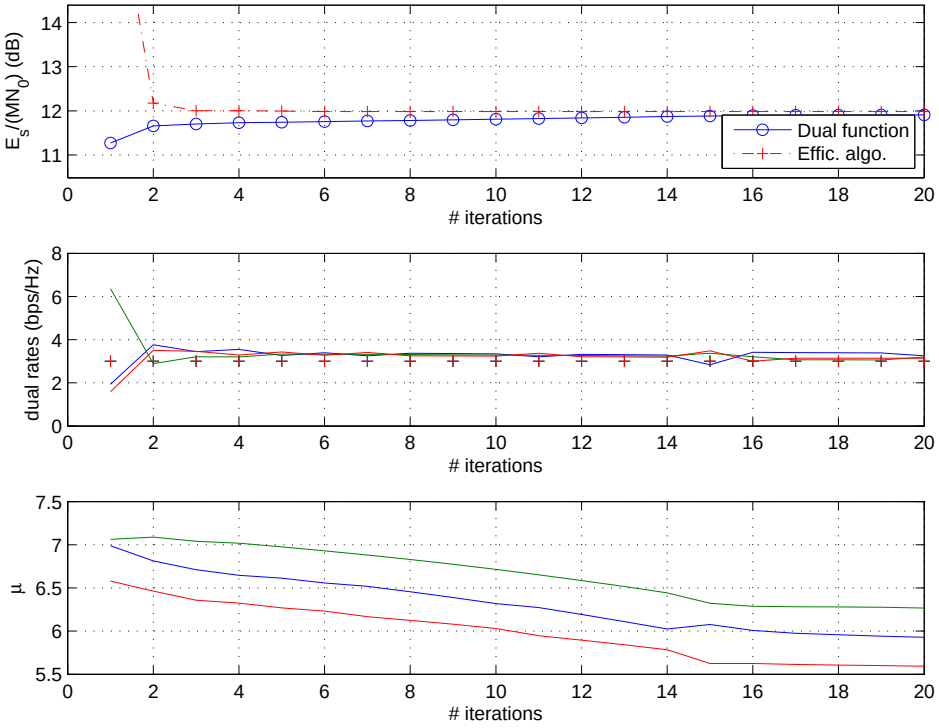

Figure 5.3: Typical convergence behaviour of the efficient algorithm applied to a $3 \times [3, 3, 3]$ MIMO system with $M = 64$ subcarriers.

3 iterations represent the instances where the proposed algorithm cannot give the solution as it is still evaluating the subcarrier allocation based on dual proportional fairness.

Next, consider a partially frequency-selective fading channel, with flat fading over 20 out of 64 subcarriers. As expected, the dual rates in Figure 5.5 fluctuate over a wide range, suggesting that the sum power would be far from optimal. However, with the flat fading management, the algorithm easily obtains a near-optimal sum power in only 11 iterations.

Figure 5.6 shows the convergence behaviour of the algorithm applied to a channel with a power delay profile with only 2 taps: 0.999 and 0.001. This is an example of a channel with almost flat fading. Again, the dual rates fluctuate wildly, and the flat fading management is automatically started. Without flat fading management, it is often impossible to guarantee user rates because at least one user

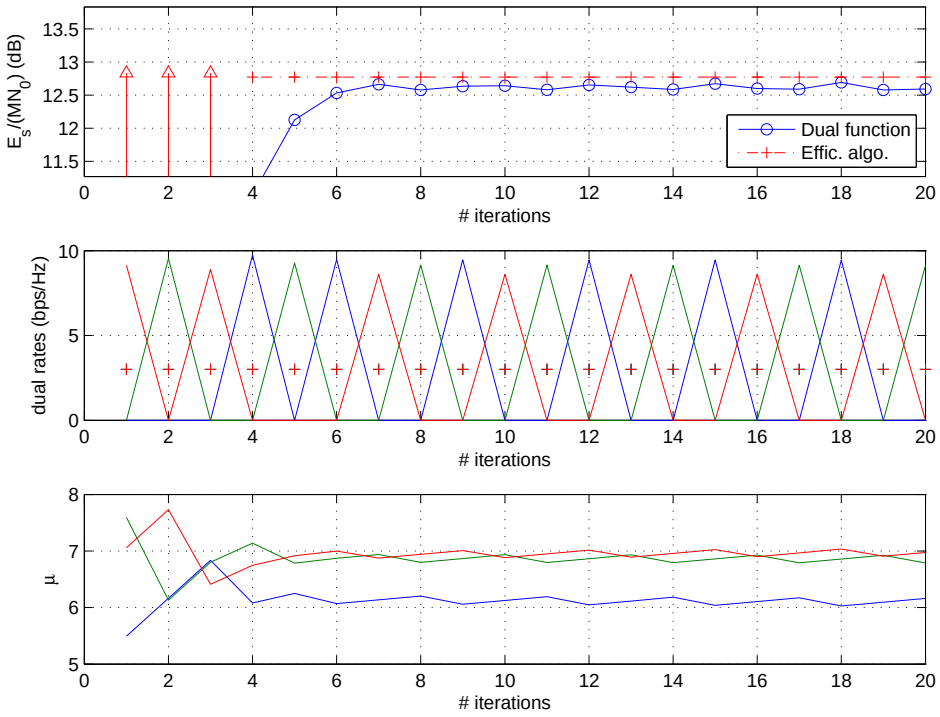

Figure 5.4: Sample convergence for a channel with flat fading over all subcarriers.

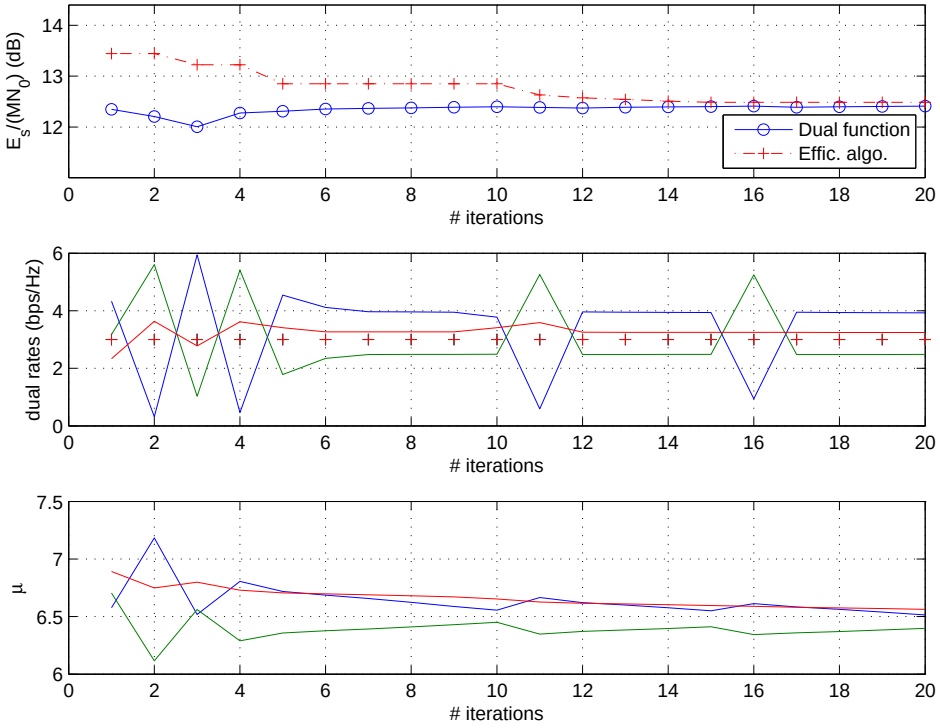

Figure 5.5: Sample convergence for a partially frequency-selective channel, with flat fading over subcarriers 21 to 40.

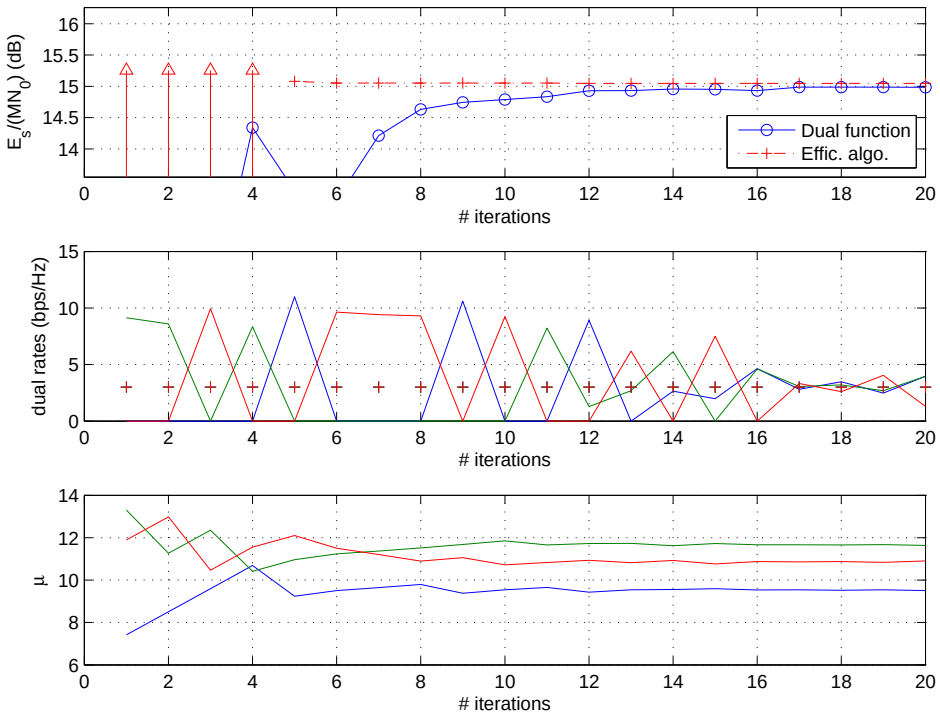

Figure 5.6: Convergence behaviour for a weakly frequency-selective channel.

is not allocated any subcarriers, as can be seen by the zero dual rates. However, the proposed efficient allocation is able to attain a satisfactory sum power in just 5 iterations.

In the absence of prior channel knowledge, an equal number of subcarriers should be allocated to each user in a fixed scheme. To obtain some frequency diversity, a distributed cyclic subcarrier allocation is chosen due to its robustness to frequency-selective fading. In this fixed allocation scheme, user k takes subcarriers $qK + k$, $q = 0, 1, 2, \ldots$. Another scheme, the "amplitude-craving greedy" (ACG) algorithm of [106] allocates subcarriers intelligently based on users' rate requirements as well as channel strengths, for SISO-OFDM. In order to extend this heuristic algorithm to the MIMO-OFDM case, we modify the algorithm by substituting the SISO channel strength of [106] with the mean of the squared absolute values of the MIMO channel matrix elements i.e. $\tilde{c}_{k,m} = \frac{\mathrm{Tr}(\mathbf{H}_{k,m}^H \mathbf{H}_{k,m})}{N_T n_k}$. This will be referred to as "ACG2" in the graphs.

A simple allocation scheme takes the form of localized transmission, where a block of consecutive subcarriers is allocated to each user. To achieve some multiuser diversity, the assignment is adapted based on the channel conditions of the different users. The first $\hat{M} = \lfloor \frac{M}{K} \rfloor$ subcarriers are given to the user with the highest average channel strength $\bar{c}_{k,1} = \frac{\sum_{m=1}^{\hat{M}} \tilde{c}_{k,m}}{\hat{M}}$. The next $\hat{M}$ subcarriers are allocated to one of the remaining users with the highest channel strength, and so on. Finally, the last user gets all the remaining subcarriers. This is labelled "Localized TX" in the graphs.

The graphs include the "Lower bound" i.e. $\frac{g(\boldsymbol{\mu})}{MN_0}$ for the solution obtained with optimal resource allocation, based on the fact that the value of the dual function $g(\boldsymbol{\mu})$ from (5.24) is always a lower bound to the minimum transmit power $\sum_{m=1}^{M} \sum_{k=1}^{K} p_{k,m}$. Therefore, the solution $\frac{E_s}{MN_0}$ achieved with optimal resource allocation is upper and lower bounded by the proposed "Effic. alloc." and "Lower bound" respectively. If these two bounds coincide, the duality gap is zero and the proposed efficient allocation is also optimal.

In Figure 5.7, the transmit power is plotted against the rate requirement ρ, where the rate requirement vector is $\bar{R}_k = \rho$ bps/Hz $\forall k$. As expected, the sum power increases with the rate requirements while the efficient allocation performs uniformly better than the fixed allocation. At a common rate requirement of 4 bps/Hz for each user, the gain of the efficient subcarrier allocation over a fixed allocation is 1.4 dB.

Figure 5.8 shows the graph of BER requirement versus the sum power. An uncoded M-QAM modulation is assumed in this case. At a BERs of 10^{-3} to 10^{-5}, the SNR gain appears relatively constant at 1.2 dB. This is due to the similar effect of the SNR gap on both the efficient and fixed allocation schemes.

The effect of channel frequency selectivity is tested in Figure 5.9. The number of taps is varied from 1 to 15. The gain of the efficient subcarrier allocation

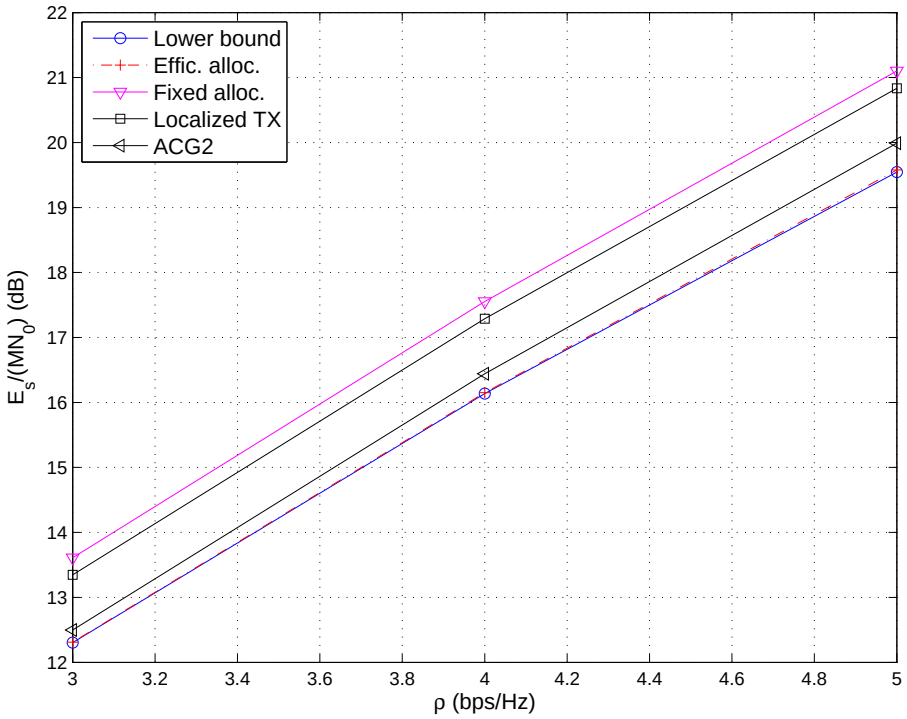

Figure 5.7: Required total transmit power for various data rate requirements.

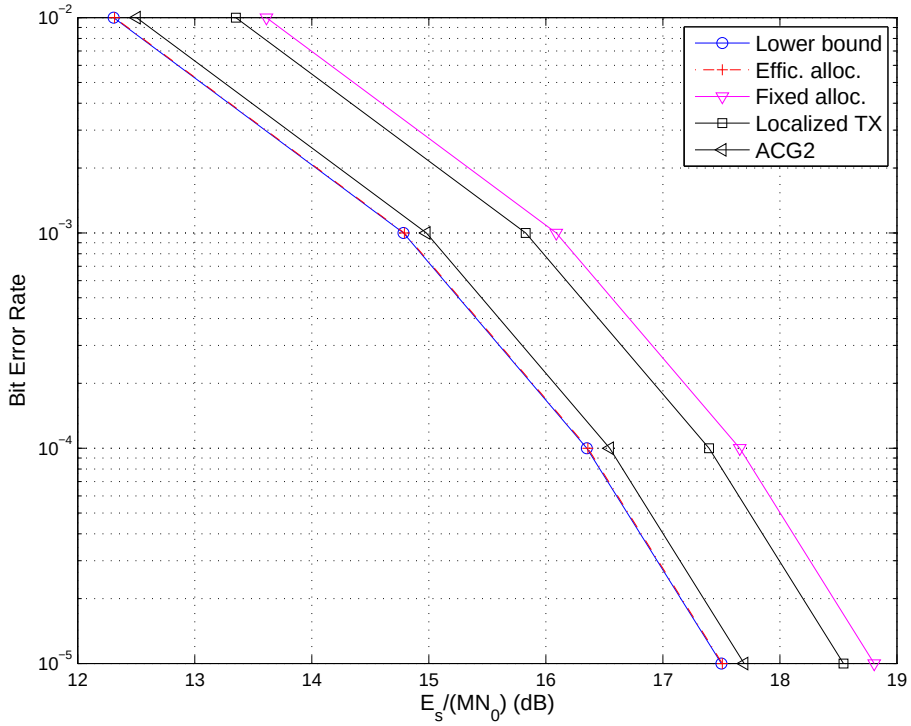

Figure 5.8: BER versus sum power for the different subcarrier allocation schemes.

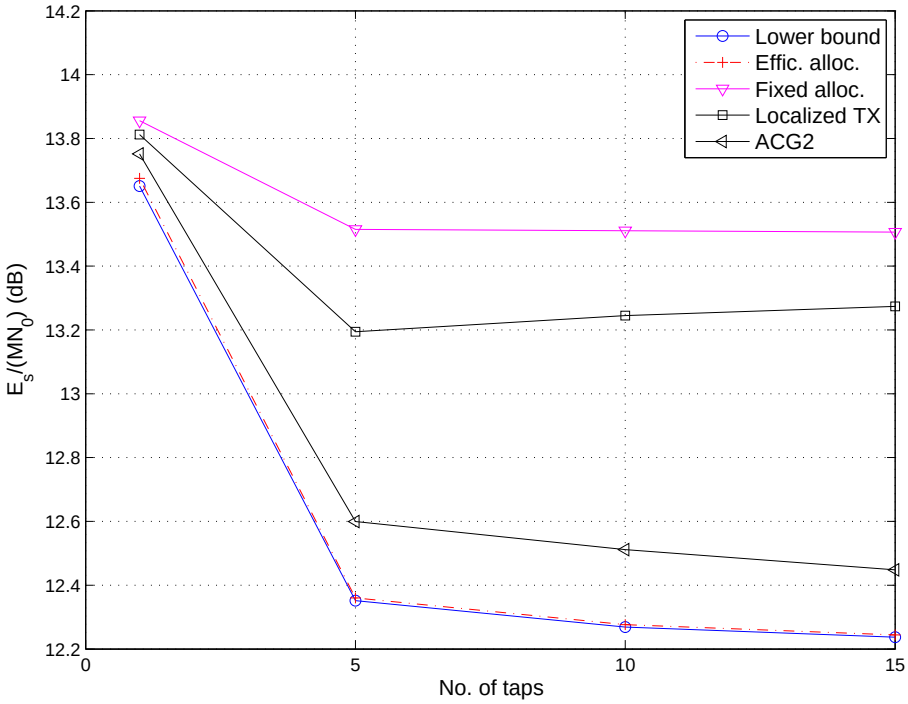

Figure 5.9: Graph of sum power versus number of taps in power delay profile, showing the effect of channel frequency selectivity.

grows as the channel becomes more frequency-selective. This is because a fixed subcarrier allocation would not be able to adapt to take advantage of the diverse channel conditions. With a flat fading channel, the gain is rather small, about 0.2 dB. This can be explained by the fact that with similar rate requirements and similar channel strengths among the users, a fixed allocation of subcarriers would serve just as well to distribute the subcarriers equally for all the users in a flat fading scenario.

Figure 5.10 shows the effect of the number of antennas. The setup here is $\bar{n} \times [\bar{n}, \bar{n}, \bar{n}]$, where $\bar{n}$ is varied from 1 to 4. As the number of antennas increase, the sum power required decreases, for the same target rates. This graph clearly shows the advantage of MIMO communications over SISO communications. Even by just increasing the number of antennas $\bar{n}$ from 1 to 2, the sum power can be decreased by over 10 dB.

Figure 5.11 plots the performance with different number of users. Values of

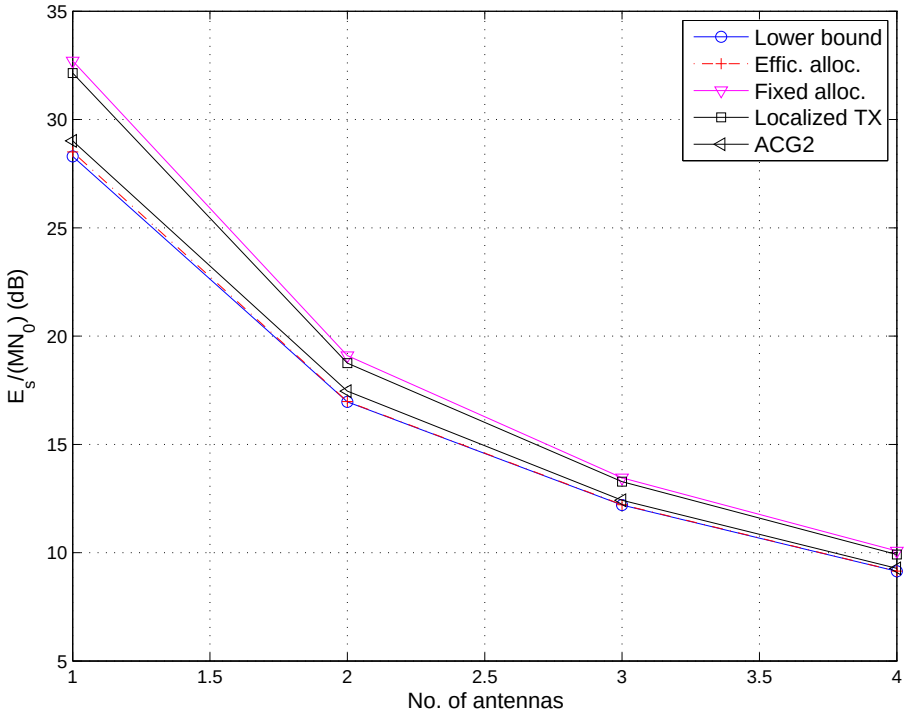

Figure 5.10: Transmit power versus number of antennas $\bar{n}$, for a $\bar{n} \times [\bar{n}, \bar{n}, \bar{n}]$ MIMO setup.

K range from 3 to 5. As the number of users increases, the sum power increases due to a higher sum rate requirement. It can be seen that the gain over a fixed subcarrier allocation also increases. This is because there is greater potential to exploit the multiuser diversity as there are more users introduced into the system. For example, with 5 users, the gain is 2 dB, compared to 1.2 dB with only 3 users.

For the performance comparisons so far, localized TX has a lower sum power than the fixed allocation. This is because by selecting the user with the highest channel strength for each block of subcarriers, some multiuser diversity is exploited. The ACG2 shows a further improvement from localized TX because both the number and positions of the subcarriers are adapted for each user.

In a general setting, users have differentiated rate requirements if they subscribe to services of different data rates. Additionally, for practical scenarios, user terminals may be placed at varying distances from the base station. This effect is

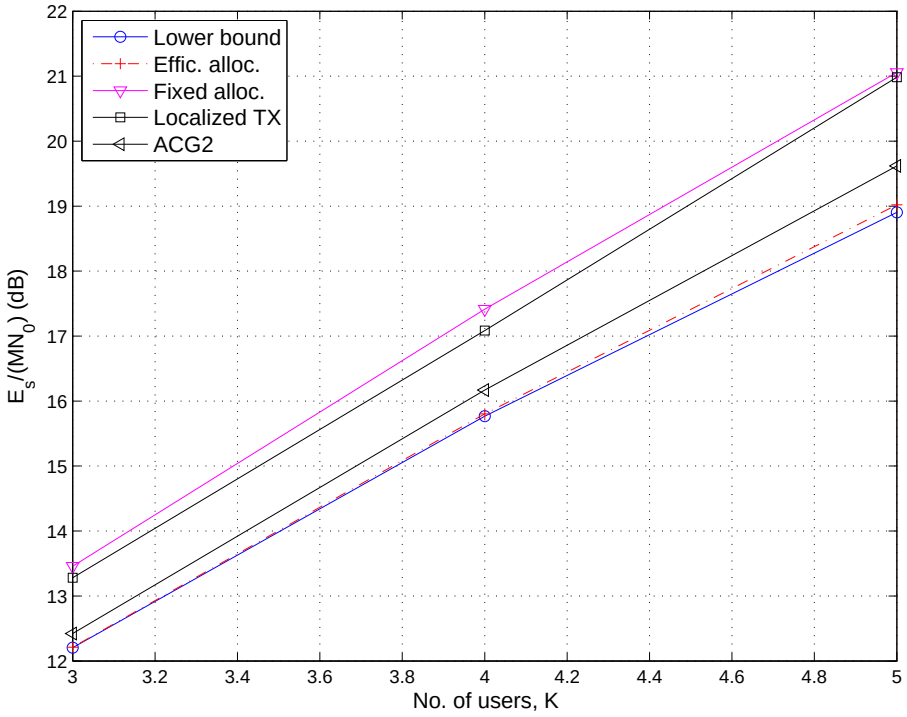

Figure 5.11: Sum power for 3, 4, and 5 users in the system.

represented by $\mathbf{c} = [c_1, c_2, c_3]$, where the variance of the channel matrix elements are scaled by c_1, c_2, and c_3 respectively for users 1, 2, and 3. Figure 5.12 plots sum power versus $\Delta\rho$, where the target rate vector is $\bar{\mathbf{R}} = [3, 3-\Delta\rho, 3+\Delta\rho]^T$ bps/Hz, and the channel strengths are $\mathbf{c} = [0.5, 1.5, 1]$. When $\Delta\rho = 2$, the gain of the proposed allocation is large, over 4 dB. This because the fast adaptive subcarrier allocation is able to optimize the number and positions of subcarriers for each user. This time, the localized TX does not perform better than the fixed scheme because the large difference in channel strengths result in the users being selected in a fixed pattern. However, the ACG2 is still able to provide a low sum power because the number of subcarriers each user gets is decided by the users' target rates.

In Figure 5.13, the channel strengths are given by $\mathbf{c} = [1-\Delta c, 1+\Delta c, 1]$, while the rate requirements are $\bar{\mathbf{R}} = [3, 2, 4]^T$ bps/Hz. The transmit power is plotted against the variation in channel strength Δc. When $\Delta c = 0.9$, the gain over a fixed

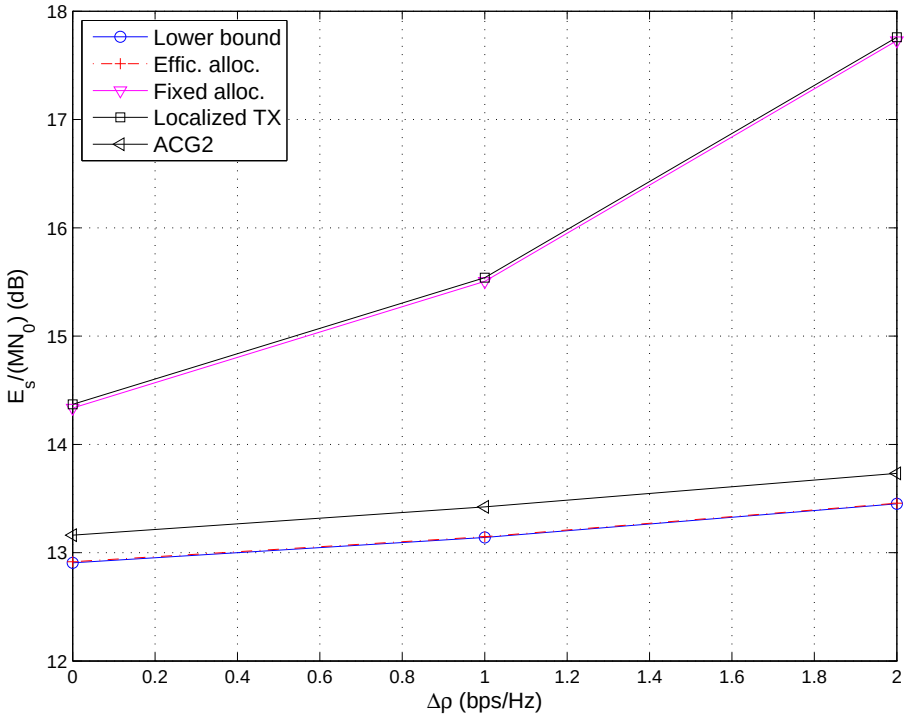

Figure 5.12: Transmit power for differentiated rate requirements given by $\bar{\mathbf{R}} = [3, 3-\Delta\rho, 3+\Delta\rho]^T$ bps/Hz, with channel strengths $\mathbf{c} = [0.5, 1.5, 1]$.

allocation is as large as 3 dB. Again, this is because under the optimal scheme, more subcarriers would be allocated to the user with the weaker channel in order to minimize the total transmit power, whereas the fixed allocation is not able to compensate for the different channel strengths. Figure 5.14 examines the sum power as the number of subcarriers M increases. It can be seen that even with only 16 subcarriers, the duality gap is negligible. When $M = 128$, the duality gap becomes zero, and the proposed efficient algorithm is optimal.

In all these simulations, it can be seen that the efficient subcarrier allocation yields a large gain over a fixed subcarrier allocation. The gain tends to increase with a more frequency-selective channel or a greater number of users. The gains are largest for practical scenarios where there can be varied channel strengths or differentiated rate requirements. In general, the localized TX performs better than the fixed allocation, while the ACG2, in turn, performs better than the localized

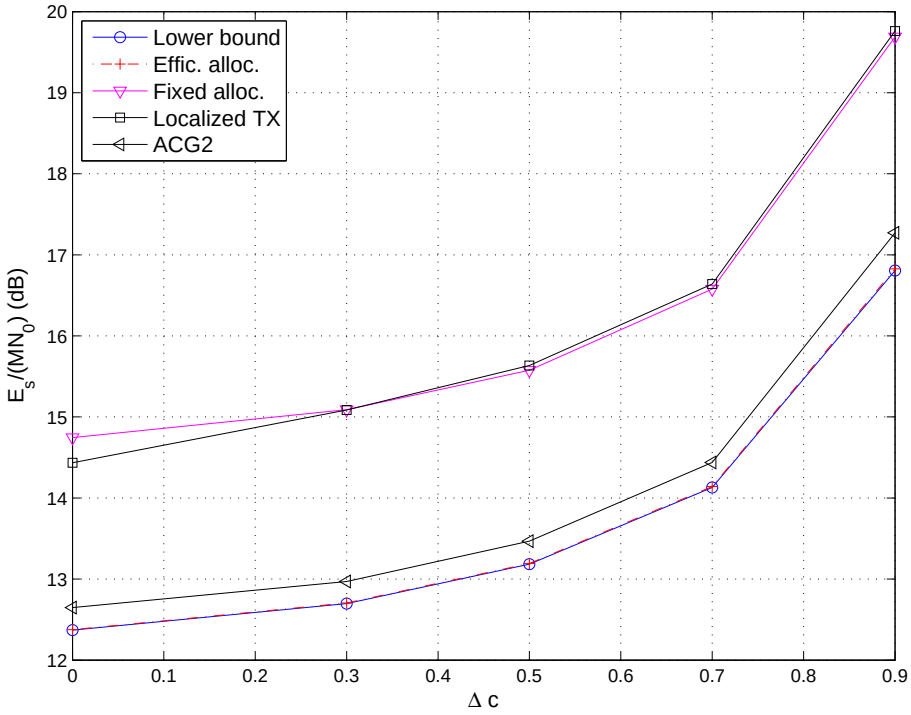

Figure 5.13: Effect of different channel strengths among the users, where $\mathbf{c} = [1 - \Delta c, 1 + \Delta c, 1]$, with $\bar{\mathbf{R}} = [3, 2, 4]^T$ bps/Hz.

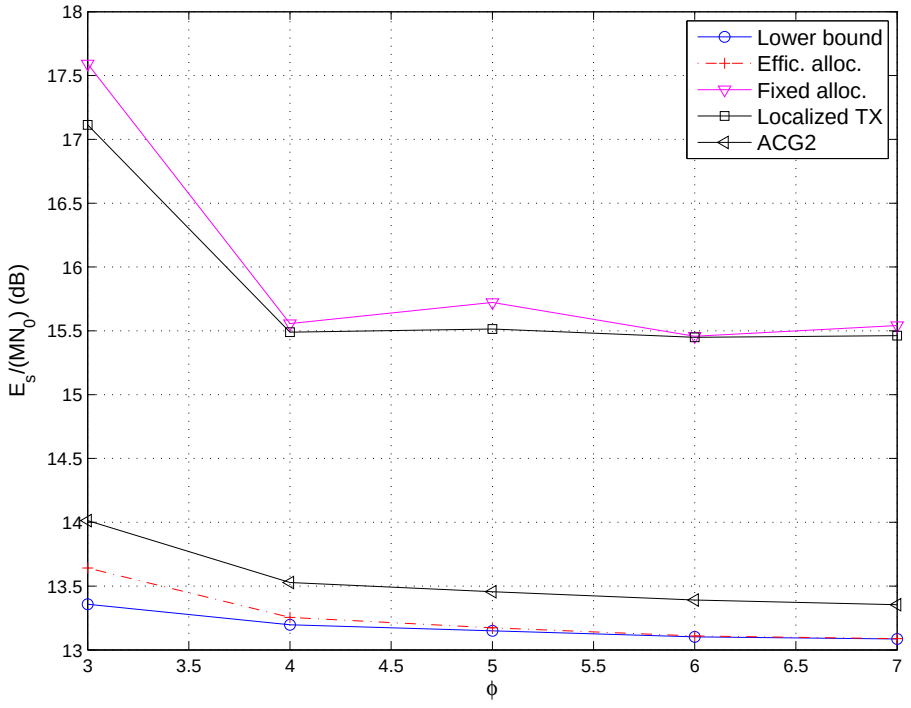

Figure 5.14: Performance for different numbers of subcarriers $M = 2^{\phi}$, where number of taps=M/4+1, $\bar{\mathbf{R}} = [3, 2, 4]^T$ bps/Hz, and $\mathbf{c} = [0.5, 1.5, 1]$.

TX. Finally, the proposed efficient allocation consistently outperforms all the other schemes.

5.7 Summary

High data rate communication is one of the key benefits of MIMO-OFDM. In order to utilize the system resources efficiently, fast and adaptive optimization algorithms are required. This chapter has addressed the issue of optimal resource allocation to minimize the total transmit power while satisfying users' target rates. An efficient and adaptive algorithm, based on convex optimization theory, is proposed to obtain the subcarrier, power, and rate allocations that exploit the diversities of the system. To provide a low complexity implementation, only linear beamforming is carried out at the transmitter and the receiver. Therefore, this solution is immediately applicable to both the downlink and the uplink. Adaptation for this efficient resource allocation allows for fast power convergence. When the duality gap for a particular channel realization is zero, this efficient solution coincides with the optimal minimum power solution, else this solution is near-optimal. To handle the event of a flat fading channel, a technique termed *dual proportional fairness* is employed to give good performance even in this scenario. Simulation results show a large performance improvement over a fixed subcarrier allocation.

Chapter 6

Summary of Contributions and Future Work

In this chapter, we summarize the main contributions and present some suggestions for future work.

6.1 Summary of Contributions

Space-time or MIMO wireless communications offer the advantages of increased throughput as well as higher reliability. These advantages compared to SISO communications can be realized without the need to use a larger transmit power or to consume additional bandwidth, two vital and limited resources. Meanwhile, the population of users demanding global connectivity is expanding at a tremendous rate. Apart from telephone calls and text messaging, there is an increasing number applications that require high data rates. Such applications include multimedia messaging service (MMS), streaming of high definition television (HDTV) content, video chat, digital video broadcasting (DVB), and wireless broadband internet access. Accordingly, there is much interest and research on the incorporation of MIMO technology into future wireless systems, to meet the rising demand of data

rate.

Despite having the above mentioned benefits of MIMO transmission, there is a trade-off between good performance and low hardware complexity. Wireless technology is predominantly used in mobile devices such as cellular phones, personal digital assistants (PDAs), and laptops. A high hardware complexity requires more processing power and drains the source of energy quickly, reducing the battery life per charge. As a result, the benefits of MIMO may be seriously diminished. Therefore the design of low-complexity schemes for MIMO communications is crucial in the development of practical hardware implementations. This thesis has presented both optimal and efficient schemes for multiuser MIMO communications. Specifically, the problems of rate maximization subject to a sum power budget and sum power minimization subject to individual rate requirements have been considered. While the optimal schemes are of higher complexity, the efficient schemes proposed in this thesis were evaluated using the optimal schemes as the benchmarks.

This thesis first gave an overview of MIMO communications. Following that, rate maximizing transceiver designs were proposed for the flat fading MIMO BC. A decomposition termed the BD-GMD [174, 177] was proposed to create equal SNRs for the subchannels of each user, thereby allowing the use of the same MCS for the subchannels. The BD-GMD was also extended to the BD-UCD [175], which is MMSE-based and obtains identical SINRs for the subchannels of each user. While the BD-UCD-based DPC scheme is optimal in the sense of achieving the MIMO BC capacity, the BD-GMD-based DPC scheme is an efficient ZF scheme that offers a good trade-off between performance and low complexity. It has been found that the proposed schemes demonstrate excellent BER properties compared to conventional schemes. Recently, the Tunable Channel Decomposition (TCD) scheme [97] has been proposed by Jiang et. al. for the single-user MIMO channel, based on the Generalized Triangular Decomposition [96]. The TCD scheme decomposes

a MIMO channel into multiple data streams with prescribed capacities, without loss of sum capacity. The TCD scheme is useful for applications in which the data streams, sharing the same MIMO channel, have different qualities-of-service (QoS). As the GTD is a generalization of the UCD, it may be possible to design a multiuser version of the GTD, for use in the MIMO BC.

Next, for the MIMO BC, sum power is minimized subject to user target rates. The optimal (IB) power minimization requires an iterative solution of high complexity, with possible time-sharing between different user encoding orders. With a view to create an efficient algorithm for practical real-time implementation, the ZF-DPC problem was considered. By doing so, a closed-form solution was obtained, thus permitting a low-complexity implementation [176]. Furthermore, subchannels with identical SNRs are created for each user. Subchannel selection was then incorporated into the transceiver design. The user encoding order and the subchannel selection for each user can be evaluated efficiently [179]. Simulations have shown the a sum power close to the optimal IB-DPC solution can be achieved.

Following that, broadband communications was studied. The sum power for multiuser MIMO-OFDM transmission is minimized, while satisfying user rate requirements [178, 180]. Using convex optimization techniques, an efficient algorithm has been developed that achieves a lower transmit power than conventional schemes. By using a Lagrange dual decomposition, the complexity is reduced from one exponential in the number of subcarriers to one that is only linear in the number of subcarriers. Although frequency-flat fading may adversely affect decomposition-based techniques, a concept called dual proportional fairness was proposed to give good performance in all fading scenarios. By comparing the sum power achieved with the theoretical lower bound, it has been shown that the efficient algorithm obtains near-optimal performance for more than 16 subcarriers.

Wi-Fi is a popular technology that is used in WLAN devices around the world.

This technology is based on the 802.11 standard. An improved version of this technology, known as IEEE 802.11n amendment, promises much higher throughput and transmission range [112, 113] by utilizing MIMO transmission. MIMO-enabled Wi-Fi devices are beginning to emerge in the consumer mass markets [114]. The efficient MIMO-OFDM resource allocation described in Chapter 5 could be applied in the 802.11n, although this amendment is about to be finalized. The techniques proposed in Chapters 3 and 4, the BD-GMD and BD-UCD schemes, are not applicable to the 802.11n because it does not support SDMA. However, it is likely that newer amendments to the 802.11 standard will support multiuser MIMO communications via SDMA.

WiMAX networks, based on the IEEE 802.16 standard, also have MIMO functionality [115, 116], and are being set up worldwide. The Virtual Antenna feature allows more than one user to share the same subcarrier via SDMA. Amendments to this IEEE standard, which allow SDMA, could incorporate the BD-GMD and BD-UCD schemes for improved BER performance.

Additionally, the Long Term Evolution (LTE) is being developed by the 3rd Generation Partnership Project (3GPP) for the next generation mobile networks [117, 118]. The LTE makes use of MIMO transmission for the downlink and the uplink. The efficient MIMO-OFDM resource allocation in Chapter 5 is applicable to the LTE, when only 1 user transmits on each subcarrier. All fading scenarios are handled seamlessly. If more than one user is allowed to share the same subcarrier via SDMA, the proposed MIMO-OFDM resource allocation can also be applied. However, an encumbrance of the proposed algorithm that handles flat fading is that SDMA is not currently supported. Where virtual MIMO / SDMA is used, the BD-GMD and BD-UCD schemes proposed in this thesis could also be applied. These schemes allow the use of small signal constellations without much loss of sum rate. If the same constellation is used for the subchannels of each user, these

schemes have remarkable BER improvement compared to conventional SVD-based schemes.

Overall, this thesis has established some efficient schemes for multiuser MIMO wireless communications to reduce the complexity of MIMO systems. While the methods proposed are applicable to the MIMO BC and MIMO MAC, the concepts could be extended to future wireless systems using relays and cognitive radio networks [119, 120].

6.2 Future Work

In the following sections, some proposals for future work are mentioned.

6.2.1 THP and Other DPC Methods

For the proposed BD-GMD scheme, THP has been considered as a suboptimal form of DPC. THP suffers from precoding losses, like shaping loss, modulo loss and power loss [121, 122]. More research could be done on mitigating these losses. The performance of MMSE-THP and ZF-THP are identical at high SNR, and both suffer from the shaping loss of 1.53 dB due to the peak constraint at the transmitter [123]. At low SNR, the loss from capacity for THP is predominantly due to power and modulo losses.

The V-BLAST presents the optimal ordering for DFE in the uplink. For the downlink, the reverse ordering for THP is close to optimal. However, the optimal ordering is data dependent [124], and has to be found by an exhaustive search. Methods to find the optimal ordering is still an area of research.

On the other hand, combination of BD-GMD with other forms of DPC techniques could be developed. By performing quantization using k-dimensional lattices, the precoding loss goes to zero as the dimension k goes to infinity, with a

proper choice of lattice. This vector quantization is able to approach the capacity of the AWGN channel [54, 55]. A useful application of lattice strategies would be in achieving the capacity of the MIMO BC.

Trellis precoding [125, 126] is another DPC technique. It achieves a shaping gain of 1.53 dB compared to a Tomlinson-Harashima precoder. Trellis precoding can be applied to the wireless broadcast channel.

The vector-perturbation technique is a multi-dimensional extension of THP [127, 128]. It can be used on the regularized inverse of the channel matrix. The transmitted signal is perturbed, in finite step sizes determined by a lattice, in such a way as to minimize the transmit power. [129] proposes an efficient method to find the perturbation vector.

6.2.2 Precoding with Limited or Imperfect Feedback

The BD-GMD-based schemes developed in this thesis assume perfect and instantaneous CSI at the transmitter. In TDD systems, channel reciprocity may be used to estimate the downlink channel. In FDD systems, additional processing such as frequency calibration [68, 173] may be used to estimate the downlink channel based on uplink measurements. Otherwise, feedback of downlink CSI is required from the user terminals back to the BS.

This overhead consumes the system resources and reduces the effective data throughput during the uplink. Therefore, it is vital to reduce the amount of CSI feedback to the BS.

DPC techniques are adversely affected by imperfect CSI at the transmitter. DPC schemes that handle limited or imperfect feedback is an active area of research [130–133]. DFE may even be incorporated to improve robustness to imperfect CSI.

6.2.3 Application to Relays

The concepts introduced in Chapter 5 could be extended to relays [134–136]. [139] solves the power allocation for an amplify-and-forward (AF) relay through a sequence of convex feasibility problems using the bisection method. Other forwarding schemes include the decode-and-forward (DF) and compress-and-forward (CF) [138].

[140–143] consider the design of MIMO AF relay. While only the relay amplification matrix is optimized in [141, 143], both the source covariance matrix and the relay forwarding matrix are optimized to maximize the achievable rate in [140, 142]. Due to the non-convexity of the latter problem, only suboptimal iterative solutions have been proposed. Moving to broadband communications, multicarrier MIMO relaying is considered in [37, 144].

In contrast to the one-way relay, two-way relaying involves the exchange of information between two terminals, via a relay node [145]. Network coding [137] has been given a new light due to its application in the recent physical layer network coding (PNC) results [146–151]. In PNC, two terminals send signals to the relay simultaneously. The relay simply amplifies the combined signal before transmitting. Given complete CSI, each terminal is able to cancel its own self interference. In other words, nulling to suppress interference is not required at the relay. This is opposed to the case where interference suppression is performed at the base station [152, 153] with little or no interference cancellation at the destination terminals. Apart from AF, two-way relaying can also make use of the DF scheme [154, 155].

6.2.4 Transmission based on Statistical CSI

In this thesis, perfect instantaneous CSI was assumed. In practice, the propagation delay of the feedback link may render this CSI invalid for the next downlink

transmission. However, statistical CSI is valid for a longer period of time than instantaneous CSI. The use of statistical CSI for communications in multiple antenna systems also helps in reducing the amount of feedback required.

While the performance of schemes using statistical CSI is poorer than those using instantaneous CSI, the performance improves with increasing channel correlation. Multiuser space-time communications based on statistical CSI is an interesting area to be investigated.

Pre-filtering based on statistical CSI at the transmitter has been considered in [156–167, 173]. The eigenvectors for the optimal source covariance matrix was derived for the MISO case [156], then for the MIMO case [157, 159]. Next, progress has been made in determining the eigenvalues of the optimal source covariance matrix [160, 163–165].

Coming back to the relay channel, AF relaying based on partial CSI is considered in [169]. For the AF scheme, statistical properties of the SISO [171] and MIMO [170] relay channel have been analyzed.

[172] makes use of statistical CSI to design the spatial filter at the relay station, for the one-way relay. Next, in [181], we have proposed both optimal and efficient schemes for the multi-antenna two-way relay which exploits statistical CSI. The extension to multicarrier communications is also an interesting avenue of research.

For vector block-fading channels, the optimal schemes for rate maximization are water-filling to achieve ergodic capacity, and generalized water-filling to achieve delay-limited capacity. Suboptimal schemes take the form of constant power transmission or channel inversion to obtain identical receive SNR for all subchannels over all time frames. Subchannel grouping [168] has lower complexity compared to optimal water-filling schemes, but have higher rates than conventional suboptimal schemes. In each frame, subchannels are sorted based on their channel gains, and subchannels in the same sorted position over all frames are grouped together.

Different groups have different fading characteristics and therefore are assigned different targets (i.e. transmission power or receive SNR). The results in Chapter 5 could be extended to the block-fading scenario, together with the consideration of subchannel grouping for reduced complexity.

Bibliography

[1] C. E. Shannon, "A Mathematical Theory of Communication," *The Bell System Technical Journal,* vol. 27, pp. 379–423, 623–656, Jul., Oct., 1948.

[2] I. E. Telatar, "Capacity of Multi-antenna Gaussian Channels," *Bell Labs Technical Memorandum,* Jun. 1995.

[3] G. J. Foschini and M. J. Gans, "On Limits of Wireless Communications in a Fading Environment when Using Multiple Antennas," *Wireless Personal Commun.,* vol. 6, no. 3, pp. 311–335, Mar. 1998.

[4] H. Yang, "A road to future broadband wireless access: MIMO-OFDM-Based air interface," *IEEE Commun. Mag.,* vol. 43, no. 1, pp. 53–60, Jan. 2005.

[5] G. Li and H. Liu, "On the optimality of downlink OFDMA MIMO systems," *Asilomar Conf. Signals, Systems, Computers,* vol. 1, pp. 324–328, Nov. 2004.

[6] D. P. Palomar, J. M. Cioffi, and M. A. Lagunas, "Joint Tx-Rx Beamforming Design for Multicarrier MIMO Channels: A Unified Framework for Convex Optimization," *IEEE Trans. Signal Processing*, vol. 51, no. 9, pp. 2381–2401, Sep. 2003.

[7] H. Huang, H. Viswanathan and G. J. Foschini, "Multiple antennas in cellular CDMA systems: transmission, detection, and spectral efficiency," *IEEE Trans. Wireless Commun.,* vol. 1, no. 3, pp. 383–392, Jul. 2002.

[8] Y.-C. Liang, F. P. S. Chin, and K. J. R. Liu, "Downlink Beamforming for DS-CDMA Mobile Radio with Multimedia Services," *IEEE Trans. Commun.*, vol. 49, no. 7, pp. 1288–1298, Jul. 2001.

[9] E. G. Larsson and P. Stoica, *Space-Time Block Coding for Wireless Communications,* Cambridge University Press, 2003.

[10] H. Jafarkhani, *Space-Time Coding: Theory and Practice,* Cambridge University Press, 2005.

[11] B. Vucetic, J. Yuan, *Space-Time Coding,* John Wiley & Sons, 2003.

[12] L. Zheng and D. Tse, "Diversity and multiplexing: A fundamental tradeoff in multiple-antenna channels," *IEEE Trans. Inform. Theory,* vol. 49, no. 5, pp. 1073–1096, May. 2003.

[13] M. Cicerone, O. Simeone, and U. Spagnolini, "Channel Estimation for MIMO-OFDM Systems by Modal Analysis/Filtering," *IEEE Trans. Commun.*, vol. 54, no. 11, pp. 2062–2074, Nov. 2006.

[14] D. Guo, S. Shamai (Shitz), and S. Verdu, "Mutual Information and Minimum Mean-Square Error in Gaussian Channels," *IEEE Trans. Inform. Theory*, vol. 51, no. 4, pp. 1261–1282, Apr. 2005.

[15] A. M. Tulino and S. Verdu, *Random Matrix Theory and Wireless Communications*, Now Publishers Inc, 2004.

[16] A. Goldsmith, S. A. Jafar, N. Jindal and S. Vishwanath "Capacity limits of MIMO channels," *IEEE J. Select. Areas Commun.,* vol. 21, no. 5, pp. 684–702, Jun. 2003.

[17] G. J. Foschini, D. Chizhik, M. J. Gans, C. Papadias, and R. A. Valenzuela, "Analysis and performance of some basic space-time architectures," *IEEE J. Select. Areas Commun.,* vol. 21, no. 3, pp. 303–320, Apr. 2003.

[18] D. Gesbert, M. Shafi, D.-S. Shiu, P. J. Smith, and A. Naguib, "From Theory to Practice: An Overview of MIMO Space-Time Coded Wireless Systems," *IEEE J. Select. Areas Commun.*, vol. 21, no. 3, pp. 281–302, Apr. 2003.

[19] Y. Li, B. Vucetic, and M. Dohler, "A Space-Time Trellis Coding Scheme for Vector Gaussian Broadcast Channels," *IEEE Commun. Lett.*, vol. 9, no. 5, pp. 388–390, May. 2005.

[20] N. Al-Dhahir, C. Fragouli, A. Stamoulis, W. Younis, and R. Calderbank, "Space-time processing for broadband wireless access," *IEEE Commun. Mag.,* vol. 40, no. 9, pp. 136–142 Sep. 2002.

[21] A. Scaglione, P. Stoica, S. Barbarossa, G. B. Giannakis and H. Sampath, "Optimal designs for space-time linear precoders and decoders," *IEEE Trans. Signal Processing* vol. 50, no. 5, pp. 1051–1064, May 2002.

[22] L. Collin, O. Berder, P. Rostaing, and G. Burel, "Optimal Minimum Distance-Based Precoder for MIMO Spatial Multiplexing Systems," *IEEE Trans. Signal Processing*, vol. 52, no. 3, pp. 617–627, Mar. 2004.

[23] S. Catreux, V. Erceg, D. Gesbert, and R. W. Heath, "Adaptive modulation and MIMO coding for broadband wireless data networks," *IEEE Commun. Mag.,* vol. 40, no. 6, pp. 108–115, Jun. 2002.

[24] A. Forenza, M. Airy, M. Kountouris, R. W. Heath Jr., D. Gesbert, and S. Shakkottai, "Performance of the MIMO Downlink Channel with Multi-Mode Adaptation and Scheduling," *Proc. IEEE SPAWC*, pp. 695–699, Jun. 2005.

[25] K.-B. Song, A. Ekbal, S. T. Chung, and J. M. Cioffi, "Adaptive Modulation and Coding (AMC) for Bit-Interleaved Coded OFDM (BIC-OFDM)," *IEEE Trans. Wireless Commun.*, vol. 5, no. 7, pp. 1685–1694, Jul. 2006.

[26] H. V. Poor, "Iterative multiuser detection," *IEEE Signal Processing Mag.*, vol. 21, no. 1, pp. 81–88, Jan. 2004.

[27] Y.-C. Liang, S. Sun, and C. K. Ho, "Block-Iterative Generalized Decision Feedback Equalizers for Large MIMO Systems: Algorithm Design and Asymptotic Performance Analysis," *IEEE Trans. Signal Processing*, vol. 54, no. 6, pp. 2035–2048, Jun. 2006.

[28] S. K. Yong, and J. S. Thompson, "A Three-Dimensional Spatial Fading Correlation Model for Uniform Rectangular Arrays," *IEEE Antennas Wireless Propag. Lett.*, vol. 2, no. 1, pp. 182–185, 2003.

[29] Q. H. Spencer, C. B. Peel, A. L. Swindlehurst and M. Haardt, "An introduction to the multi-user MIMO downlink," *IEEE Commun. Mag.*, vol. 42, no. 10, pp. 60–67, Oct. 2004.

[30] J. Mitola III, "Cognitive Radio - An Integrated Agent Architecture for Software Defined Radio," Ph.D. dissertation, Royal Institute of Technology (KTH), Stockholm, Sweden, 2000.

[31] N. Devroye, P. Mitran, and V. Tarokh, "Achievable Rates in Cognitive Radio Channels," *IEEE Trans. Inform. Theory*, vol. 52, no. 5, pp. 1813–1827, May 2006.

[32] A. N. Mody, S. R. Blatt, D. G. Mills, T. P. McElwain, N. B. Thammakhoune, J. D. Niedzwiecki, M. J. Sherman, C. S. Myers, and P. D. Fiore, "Recent Advances in Cognitive Communications," *IEEE Commun. Mag.*, vol. 45, no. 10, pp. 54–61, Oct. 2007.

[33] M. Gastpar, "On Capacity Under Receive and Spatial Spectrum-Sharing Constraints," *IEEE Trans. Inform. Theory*, vol. 53, no. 2, pp. 471–487, Feb. 2007.

[34] L. Zhang, Y.-C. Liang, and Y. Xin, "Joint Beamforming and Power Allocation for Multiple Access Channels in Cognitive Radio Networks," *IEEE J. Select. Areas Commun.*, vol. 26, no. 1, pp. 38–51, Jan. 2008.

[35] L. B. Thiagarajan, S. Attallah, and Y.-C. Liang, "Reconfigurable Transceivers for Wireless Broadband Access Schemes," *IEEE Wireless Commun.*, vol. 14, no. 3, pp. 48–53, Jun. 2007.

[36] D. Soldani and S. Dixit, "Wireless Relays for Broadband Access," *IEEE Commun. Mag.*, vol. 46, no. 3, pp. 58–66, Mar. 2008.

[37] T. C.-Y. Ng and W. Yu, "Joint Optimization of Relay Strategies and Resource Allocations in Cooperative Cellular Networks," *IEEE J. Select. Areas Commun.*, vol. 25, no. 2, pp. 328–339, Feb. 2007.

[38] B. Allen, W. Q. Malik, P. J. Smith, and D. J. Edwards, "Antenna technology - Demystifying MIMO," *IET Commun. Engineer*, vol. 4, no. 6, pp. 38–42, Dec./Jan. 2006/07.

[39] D. S. Shiu, G. J. Foschini, M. J. Gans and J. M. Kahn, "Fading correlation and its effect on the capacity of multielement antenna systems," *IEEE Trans. Commun.,* vol. 48, no. 3, pp. 502–513, Mar. 2000.

[40] G. Barriac and U. Madhow, "Characterizing outage rates for space-time communication over wideband channels," *IEEE Trans. Commun.,* vol. 52, no. 12, pp. 2198–2208, Dec. 2004.

[41] Z. Hong, K. Liu, R. W. Heath, Jr., A. M. Sayeed, "Spatial multiplexing in correlated fading via the virtual channel representation," *IEEE J. Select. Areas Commun.,* vol. 21, no. 5, pp. 856–866, Jun. 2003.

[42] D. Gesbert, H. Bolcskei, D. A. Gore, A. J. Paulraj, "Outdoor MIMO wireless channels: Models and performance prediction," *IEEE Trans. Commun.,* vol. 50, no. 12, pp. 1926–1934, Dec. 2002.

[43] D. Chizhik, J. Ling, P. W. Wolniansky, R. A. Valenzuela, N. Costa and K. Huber, "Multiple-input-multiple-output measurements and modeling in Manhattan," *IEEE J. Select. Areas Commun.,* vol. 21, no. 3, pp. 321–331, Apr. 2003.

[44] G. Ginis and J. M. Cioffi, "On the relation between V-BLAST and the GDFE," *IEEE Commun. Lett.,* vol. 5, no. 9, pp. 364–366, Sep. 2001.

[45] M. K. Varanasi and T. Guess, "Optimum decision feedback multiuser equalization with successive decoding achieves the total capacity of the Gaussian multiple-access channel," *Asilomar Conf. Signals, Systems, Computers,* vol. 2, pp. 1405–1409, Nov. 1997.

[46] M. Costa, "Writing on dirty paper," *IEEE Trans. Inform. Theory,* vol. 29, no. 3, pp. 439–441, May. 1983.

[47] C. B. Peel, "On "Dirty-Paper coding"," *IEEE Signal Processing Mag.,* vol. 20, no. 3, pp. 112–113, May. 2003.

[48] M. Tomlinson, "New automatic equaliser employing modulo arithmetic," *Electron. Lett.,* vol. 7, no. 5, pp. 138–139, Mar. 1971.

[49] H. Harashima and H. Miyakawa, "Matched-transmission technique for channels with intersymbol interference," *IEEE Trans. Commun.,* vol. 20, no. 4, pp. 774–780, Aug. 1972.

[50] G. Ginis and J. M. Cioffi, "A multi-user precoding scheme achieving crosstalk cancellation with application to DSL systems," *Asilomar Conf. Signals, Systems, Computers,* vol. 2, pp. 1627–1631, Nov. 2000.

[51] C. Windpassinger, R. Fischer, T. Vencel and J. B. Huber, "Precoding in multiantenna and multiuser communications," *IEEE Trans. Wireless Commun.*, vol. 3, no. 4, pp. 1305–1316, Jul. 2004.

[52] G. H. Golub and C. F. Van Loan, *Matrix Computations,* 3rd Edition, The John Hopkins University Press, 1996.

[53] R. A. Horn and C. R. Johnson, *Matrix Analysis,* Cambridge University Press, 1985.

[54] U. Erez and S. ten Brink, "A close-to-capacity dirty paper coding scheme," *IEEE Trans. Inform. Theory,* vol. 51, no. 10, pp. 3417–3432, Oct. 2005.

[55] U. Erez, S. Shamai and R. Zamir, "Capacity and lattice strategies for canceling known interference," *IEEE Trans. Inform. Theory,* vol. 51, no. 11, pp. 3820–3833, Nov. 2005.

[56] Q. H. Spencer and A. L. Swindlehurst, "A hybrid approach to spatial multiplexing in multiuser MIMO downlinks," *EURASIP J. Wireless Commun. and Networking*, vol. 2004, pp. 236–247, 2004.

[57] M. Bengtsson, "A pragmatic approach to multi-user spatial multiplexing," *IEEE Sensor Array and Multichannel Signal Processing Workshop*, pp. 130–134, Aug. 2002.

[58] J. H. Chang, L. Tassiulas and F. Rashid-Farrokhi, "Joint transmitter receiver diversity for efficient space division multiaccess," *IEEE Trans. Wireless Commun.*, vol. 1, no. 1, pp. 16–27, Jan. 2002.

[59] M. Schubert and H. Boche "Solution of the multiuser downlink beamforming problem with individual SINR constraints," *IEEE Trans. Vehicular Technology*, vol. 53, no. 1, pp. 18–28, Jan. 2004.

[60] D. Wang, E. A. Jorswieck, A. Sezgin and E. Costa, "Joint Tomlinson-Harashima precoding with diversity techniques for multiuser MIMO systems," *Proc. IEEE Vehicular Technology Conf.*, vol. 2, pp. 1017–1021, May. 2005.

[61] R. Fischer, C. Windpassinger, A. Lampe and J. B. Huber, "MIMO precoding for decentralized receivers," *Proc. Int. Symp. Inform. Theory*, pp. 496, 2002.

[62] F. Boccardi and H. Huang, "Optimum power allocation for the MIMO-BC zero-forcing precoder with per-antenna power constraints," *Conf. Inform. Sciences and Systems*, Mar. 2006.

[63] T. Lan and W. Yu, "Input optimization for multi-antenna broadcast channels with per-antenna power constraints," *Proc. Global Commun. Conf.*, vol. 1, pp. 420–424, Nov. 2004.

[64] R. Doostnejad, T. J. Lim and E. Sousa, "Joint precoding and beamforming design for the downlink in a multiuser MIMO system," *Proc. IEEE WiMob*, vol. 1, pp. 153–159, Aug. 2005.

[65] T. Haustein, M. Schubert and Holger Boche, "On power reduction strategies for the multi-user downlink with decentralized receivers," *Proc. IEEE Vehicular Technology Conf.*, vol. 2, pp. 1007–1011, Apr. 2003.

[66] X. Shao, J. Yuan and P. Rapajic "Precoder design for MIMO broadcast channels," *Proc. Int. Conf. Commun.*, vol. 2, pp. 788–794, May. 2005.

[67] V. Stankovic, M. Haardt and M. Fuchs, "Combination of block diagonalization and THP transmit filtering for downlink beamforming in multi-user MIMO systems," *Eur. Conf. Wireless Technology*, pp. 145–148, 2004.

[68] Y.-C. Liang and F. P. S. Chin, "Downlink channel covariance matrix (DCCM) estimation and its applications in wireless DS-CDMA systems," *IEEE J. Select. Areas Commun.,* vol. 19, no. 2, pp. 222–232, Feb. 2001.

[69] A. Paulraj, R. Nabar, and D. Gore, *Introduction to Space-Time Wireless Communications*, Cambridge Univeristy Press, 2003.

[70] T. Cover and J. Thomas, *Elements of Information Theory,* New York: Wiley, 1991.

[71] B. Hassibi, "A Fast Square-Root Implementation for BLAST," *Asilomar Conf. Signals, Systems, Computers*, pp. 1255–1259, Pacific Grove, Nov. 2000.

[72] Y. Jiang, J. Li and W. W. Hager, "Joint Transceiver Design for MIMO Communications using Geometric Mean Decomposition," *IEEE Trans. Signal Processing*, vol. 53, no. 10, pp. 3791–3803, Oct. 2005.

[73] Y. Jiang, J. Li and W. Hager, "Uniform Channel Decomposition for MIMO Communications," *IEEE Trans. Signal Processing*, vol. 53, no. 11, pp. 4283–4294, Nov. 2005.

[74] P. Viswanath and D. Tse, "Sum Capacity of the Vector Gaussian Broadcast Channel and Uplink-Downlink Duality," *IEEE Trans. Inform. Theory*, vol. 49, no. 8, pp. 1912–1921, Aug. 2003.

[75] S. Vishwanath, N. Jindal and A. Goldsmith, "Duality, Achievable Rates, and Sum-Rate Capacity of Gaussian MIMO Broadcast Channels," *IEEE Trans. Inform. Theory*, vol. 49, no. 10, pp. 2658–2668, Oct. 2003.

[76] W. Yu and J. Cioffi, "Sum Capacity of Gaussian Vector Broadcast Channels," *IEEE Trans. Inform. Theory*, vol. 50, no. 9, pp. 1875–1892, Sep. 2004.

[77] G. Caire and S. Shamai (Shitz), "On the Achievable Throughput of a Multiantenna Gaussian Broadcast Channel," *IEEE Trans. Inform. Theory*, vol. 49, no. 7, pp. 1691–1706, Jul. 2003.

[78] H.Weingarten, Y. Steinberg and S. Shamai, "The capacity region of the Gaussian MIMO broadcast channel," *IEEE Int. Symp. Inform. Theory*, pp. 174, Chicago, Jul. 2004.

[79] N. Jindal, W. Rhee, S. Vishwanath, S. A. Jafar and A. Goldsmith, "Sum Power Iterative Water-Filling for Multi-Antenna Gaussian Broadcast Channels," *IEEE Trans. Inform. Theory*, vol. 51, no. 4, pp. 1570–1580, Apr. 2005.

[80] N. Jindal and A. Goldsmith, "Dirty-paper coding versus TDMA for MIMO Broadcast channels," *IEEE Trans. Inform. Theory*, vol. 51, no. 5, pp. 1783–1794, May 2005.

[81] Z. Pan, K. K. Wong, and T. S. Ng, "Generalized multiuser orthogonal space-division multiplexing," *IEEE Trans. Wireless Commun.*, vol. 3, no. 6, pp. 1969–1973, Nov. 2004.

[82] Q. H. Spencer, A. L. Swindlehurst and M. Haardt, "Zero-forcing methods for downlink spatial multiplexing in multiuser MIMO channels," *IEEE Trans. Signal Processing*, vol. 52, no. 2, pp. 461–471, Feb. 2004.

[83] L. U. Choi and R. D. Murch, "A transmit preprocessing technique for multiuser MIMO systems using a decomposition approach," *IEEE Trans. Wireless Commun.*, vol. 3, no. 1, pp. 20–24, Jan. 2004.

[84] P. Viswanath, D. N. C. Tse, and R. Laroia, "Opportunistic beamforming using dumb antennas," *IEEE Trans. Inform. Theory*, vol. 48, no. 6, pp. 1277–1294, Jun. 2002.

[85] Y.-C. Liang and R. Zhang, "Random beamforming for MIMO systems with multiuser diversity," *Int. Symp. Personal, Indoor and Mobile Radio Commun.*, vol. 1, pp. 290–294, Sep. 2004.

[86] H. Viswanathan, S. Venkatesan and H. Huang, "Downlink capacity evaluation of cellular networks with known-interference cancellation" *IEEE J. Select. Areas Commun.*, vol. 21, pp. 802–811, Jun. 2003.

[87] J. Lee and N. Jindal, "Symmetric Capacity of MIMO Downlink Channels," *IEEE Int. Symp. Inform. Theory*, pp. 1031-1035, Jul. 2006.

[88] M. Mohseni, R. Zhang, and J. M. Cioffi "Optimized Transmission for Fading Multiple-Access and Broadcast Channels With Multiple Antennas," *IEEE J. Select. Areas Commun.*, vol. 24, pp. 1627–1639, Aug. 2006.

[89] C.-H. F. Fung, W. Yu, and T. J. Lim, "Multi-antenna downlink precoding with individual rate constraints: power minimization and user ordering," *Proc. Int. Conf. Commun. Systems*, pp. 45–49, Sep. 2004.

[90] C.-H. F. Fung, W. Yu and T. J. Lim, "Precoding for the Multiantenna Downlink: Multiuser SNR Gap and Optimal User Ordering," *IEEE Trans. Commun.*, vol. 55, no. 1, pp. 188–197, Jan. 2007.

[91] M. Schubert and H. Boche, "Iterative Multiuser Uplink and Downlink Beamforming under SINR Constraints," *IEEE Trans. Signal Processing*, vol. 53, no. 7, pp. 2324–2334, Jul. 2005.

[92] R. Fischer, C. Windpassinger, A. Lampe and J. B. Huber, "Space-Time Transmission using Tomlinson-Harashima Precoding," *Proc. ITG Conf. Source and Channel Coding*, pp. 139–147, Berlin, Jan. 2002.

[93] J. Liu and W. A. Krzymien, "A Novel Nonlinear Precoding Algorithm for the Downlink of Multiple Antenna Multi-user Systems," *Proc. IEEE Vehicular Technology Conf.*, vol. 2, pp. 887–891, May 2005.

[94] V. Stankovic and M. Haardt, "Successive optimization Tomlinson-Harashima precoding (SO THP) for multi-user MIMO systems," *Proc. IEEE Int. Conf. Acoust., Speech, Signal Processing*, vol. 3, pp. 1117–1120, Mar. 2005.

[95] S. Zazo and H. Huang, "Suboptimum Space Multiplexing Structure Combining Dirty Paper Coding and Receive Beamforming," *Proc. IEEE Int. Conf. Acoust., Speech, Signal Processing*, vol. 4, pp. 89–92, May. 2006.

[96] Y. Jiang, J. Li and W. W. Hager, "Transceiver Design using Generalized Triangular Decomposition for MIMO Communications with QoS Constraints," *Asilomar Conf. Signals, Systems, Computers*, pp. 1154–1157, Pacific Grove, Nov. 2004.

[97] Y. Jiang, W. W. Hager, and J. Li, "Tunable Channel Decomposition for MIMO Communications Using Channel State Information," *IEEE Trans. Signal Processing*, vol. 54, no. 11, pp. 4405–4418, Nov. 2006.

[98] P. W. Wolnainsky, G. J. Foschini, G. D. Golden and R. A. Valenzuela, "V-BLAST: An Architecture for Achieving Very High Data Rates over the Rich-Scattering Wireless Channel," *Int. Symp. Signals, Systems, Electronics*, pp. 295–300, Pisa, Oct. 1998.

[99] S. Boyd and L. Vandenberghe, *Convex Optimization.* Cambridge, U.K.: Cambridge Univ. Press, 2004.

[100] Z. Q. Luo and W. Yu, "An Introduction to Convex Optimization for Communications and Signal Processing," *IEEE J. Select. Areas Commun.*, vol. 24, pp. 1426–1438, Aug. 2006.

[101] A. B. Gershman and N. D. Sidiropoulos, *Space-Time Processing for MIMO Communications*, Wiley, 2005.

[102] K. Yu, M. Bengtsson, B. Ottersten, P. Karlsson, D. McNamara, and M. Beach, "Measurement Analysis of NLOS Indoor MIMO Channels," *Proc. IST Mobile Commun. Summit,* pp. 277–282, Sep. 2001.

[103] K. B. Letaief and Y. J. Zhang, "Dynamic multiuser resource allocation and adaptation for wireless systems," *IEEE Wireless Commun.*, vol. 13, no. 4, pp. 38–47, Aug. 2006.

[104] A. J. Goldsmith and S.-G. Chua, "Variable-rate variable-power MQAM for fading channels," *IEEE Trans. Commun.*, vol. 45, no. 10, pp. 1218–1230, Oct. 1997.

[105] Z. Hu, G. Zhu, Y. Xia, and G. Liu, "Multiuser subcarrier and bit allocation for MIMO-OFDM systems with perfect and partial channel information," *Proc. Wireless Commun. and Networking Conf.*, vol. 2, pp. 1188–1193, Mar. 2004.

[106] D. Kivanc, G. Li, and H. Liu, "Computationally Efficient Bandwidth Allocation and Power Control for OFDMA," *IEEE Trans. Wireless Commun.*, vol. 2, no. 6, pp. 1150–1158, Nov. 2003.

[107] K. Seong, M. Mohseni, and J. M. Cioffi, "Optimal Resource Allocation for OFDMA Downlink Systems," *Proc. Int. Symp. Inform. Theory*, pp. 1394–1398, Jul. 2006.

[108] Y. J. Zhang and K. B. Letaief, "An Efficient Resource-Allocation Scheme for Spatial Multiuser Access in MIMO/OFDM Systems," *IEEE Trans. Commun.*, vol. 53, no. 1, pp. 107–116, Jan. 2005.

[109] T. Yoo and A. Goldsmith, "On the Optimality of Multiantenna Broadcast Scheduling Using Zero-Forcing Beamforming," *IEEE J. Select. Areas Commun.*, vol. 24, no. 3, pp. 528–541, Mar. 2006.

[110] W. Yu and R. Lui, "Dual Methods for Nonconvex Spectrum Optimization of Multicarrier Systems," *IEEE Trans. Commun.*, vol. 54, no. 7, pp. 1310–1322, Jul. 2006

[111] R. Freund, "15.084J / 6.252J Nonlinear Programming, Spring 2004," *MIT OpenCourseWare.*

[112] M. Stanford, Wirevolution, "How does 802.11n get to 600Mbps?," 7 Sep. 2007, <http://www.wirevolution.com/2007/09/07/how-does-80211n-get-to-600mbps/>, accessed on 16 Jul. 2008.

[113] T. Paul and T. Ogunfunmi, "Wireless LAN Comes of Age: Understanding the IEEE 802.11n Amendment," *IEEE Circuits Syst. Mag.*, vol. 8, no. 1, pp. 28–54, First Quarter 2008.

[114] Broadcom Corporation, "Where to buy 802.11n products?," n.d., <http://80211n.com/where-to-buy.html>, accessed on 16 Jul. 2008.

[115] J. G. Andrews, A. Ghosh, R. Muhamed, *Fundamentals of WiMAX: Understanding Broadband Wireless Networking,* Prentice Hall, 27 Feb. 2007.

[116] P. Piggin, "Emerging Mobile WiMax antenna technologies," *IET Commun. Engineer*, vol. 4, no. 5, pp. 29–33, Oct./Nov. 2006.

[117] The 3rd Generation Partnership Project (3GPP), "UTRA-UTRAN Long Term Evolution (LTE) and 3GPP System Architecture Evolution (SAE)," 6 May 2008, <http://www.3gpp.org/Highlights/LTE/lte.htm>, accessed on 16 Jul. 2008.

[118] C. Spiegel, J. Berkmann, Z. Bai, T. Scholand, C. Drewes, G. H. Bruck, B. Gunzelmann, and P. Jung, "On MIMO for UTRA LTE," *Proc. ISCCSP*, pp. 1004–1008, Mar. 2008.

[119] J. Mitola III and G. Q. Maguire Jr., "Cognitive Radio: Making Software Radios More Personal," *IEEE Wireless Commun.*, vol. 6, no. 4, pp. 13–18, Aug. 1999.

[120] K. Challapali, C. Cordeiro, and D. Birru, "Evolution of Spectrum-Agile Cognitive Radios: First Wireless Internet Standard and Beyond," *Proc. of ACM WICON*, vol. 220, no. 27, Aug. 2006.

[121] S. Shamai (Shitz) and R. Laroia, "The intersymbol interference channel: lower bounds on capacity and channel precoding loss," *IEEE Trans. Inform. Theory*, vol. 42, no. 5, pp. 1388–1404, Sep. 1996.

[122] W. Yu, D. P. Varodayan, and J. M. Cioffi, "Trellis and Convolutional Precoding for Transmitter-Based Interference Presubtraction," *IEEE Trans. Commun.*, vol. 53, no. 7, pp. 1220–1230, Jul. 2005.

[123] R. D. Wesel, and J. M. Cioffi, "Achievable rates for Tomlinson-Harashima precoding," *IEEE Trans. Inform. Theory,* vol. 44, no. 2, pp. 824–831, Mar. 1998.

[124] R. Habendorf and G. Fettweis, "On Ordering Optimization for MIMO Systems with Decentralized Receivers," *Proc. IEEE Vehicular Technology Conf.*, vol. 4, pp. 1844–1848, May. 2006.

[125] G. D. Forney Jr., "Trellis Shaping," *IEEE Trans. Inform. Theory*, vol. 38, no. 2, pp. 281–300, Mar. 1992.

[126] W. Yu and J. M. Cioffi, "Trellis Precoding for the Broadcast Channel," *Proc. Global Commun. Conf.*, vol. 2, pp. 1344–1348, Nov. 2001.

[127] C. B. Peel, B. M. Hochwald, and A. L. Swindlehurst, "A Vector-Perturbation Technique for Near-Capacity Multiantenna Multiuser Communication - Part I: Channel Inversion and Regularization," *IEEE Trans. Commun.*, vol. 53, no. 1, pp. 195–202, Jan. 2005.

[128] B. M. Hochwald, C. B. Peel, and A. L. Swindlehurst, "A Vector-Perturbation Technique for Near-Capacity Multiantenna Multiuser Communication - Part II: Perturbation," *IEEE Trans. Commun.*, vol. 53, no. 3, pp. 537–544, Mar. 2005.

[129] C. Windpassinger, R. F. H. Fischer, and J. B. Huber, "Lattice-Reduction-Aided Broadcast Precoding," *IEEE Trans. Commun.*, vol. 52, no. 12, pp. 2057–2060, Dec. 2004.

[130] P. Ding, D. J. Love, and M. D. Zoltowski, "Multiple Antenna Broadcast Channels With Limited Feedback," *Proc. IEEE Int. Conf. Acoust., Speech, Signal Processing*, vol. 4, May 2006.

[131] P. Piantanida and P. Duhamel, "Dirty-Paper Coding without Channel Information at the Transmitter and Imperfect Estimation at the Receiver," *Proc. Int. Conf. Commun.*, pp. 5406–5411, Jun. 2007.

[132] A. P. Liavas, "Tomlinson-Harashima Precoding With Partial Channel Knowledge," *IEEE Trans. Commun.*, vol. 53, no. 1, pp. 5–9, Jan. 2005.

[133] F. A. Dietrich, P. Breun, and W. Utschick, "Tomlinson-Harashima Precoding: A Continuous Transition From Complete to Statistical Channel Knowledge," *Proc. Global Commun. Conf.*, vol. 4, pp. 2379–2384, Nov. 2005.

[134] C. E. Shannon, "Two-Way Communication Channels," *Proc. 4th Berkeley Symp. Math. Stat. and Prob.*, vol. 1, pp. 611–644, 1961.

[135] E. C. Van Der Meulen, "Three-Terminal Communication Channels," *Adv. Appl. Prob.*, vol. 3, pp. 120–154, 1971.

[136] T. M. Cover and A. A. El Gamal, "Capacity Theorems for the Relay Channel," *IEEE Trans. Inform. Theory*, vol. 25, no. 5, pp. 572-584, Sep. 1979.

[137] R. Ahlswede, N. Cai, S.-Y. R. Li, and R. W. Yeung, "Network Information Flow," *IEEE Trans. Inform. Theory*, vol. 46, no. 4, pp. 1204–1216, Jul. 2000.

[138] G. Kramer, M. Gastpar, and P. Gupta, "Cooperative Strategies and Capacity Theorems for Relay Networks," *IEEE Trans. Inform. Theory*, vol. 51, no. 9, pp. 3037–3063, Sep. 2005.

[139] T. Q. S. Quek, M. Z. Win, H. Shin, and M. Chiani, "Optimal Power Allocation for Amplify-And-Forward Relay Networks via Conic Programming," *Proc. Int. Conf. Commun.*, pp. 5058–5063, Jun. 2007.

[140] N. Varanese, O. Simeone, Y. Bar-Ness, and U. Spagnolini, "Achievable Rates of Multi-Hop and Cooperative MIMO Amplify-and-Forward Relay Systems with Full CSI," *Proc. IEEE SPAWC*, pp. 1–5, Jul. 2006.

[141] O. Munoz-Medina, J. Vidal, and A. Agustin, "Linear Transceiver Design in Nonregenerative Relays With Channel State Information," *IEEE Trans. Signal Processing*, vol. 55, no. 6, pp. 2593–2604, Jun. 2007.

[142] Z. Fang, Y. Hua, and J. C. Koshy, "Joint Source and Relay Optimization for a Non-Regenerative MIMO Relay," *Proc. IEEE SAM*, pp. 239–243, 2006.

[143] X. Tang and Y. Hua, "Optimal Design of Non-Regenerative MIMO Wireless Relays," *IEEE Trans. Wireless Commun.*, vol. 6, no. 4, pp. 1398–1407, Apr. 2007.

[144] I. Hammerstrom and A. Wittneben, "Power Allocation Schemes for Amplify-and-Forward MIMO-OFDM Relay Links," *IEEE Trans. Wireless Commun.*, vol. 6, no. 8, pp. 2798–2802, Aug. 2007.

[145] B. Rankov and A. Wittneben, "Achievable Rate Regions for the Two-way Relay Channel," *Proc. Int. Symp. Inform. Theory*, pp. 1668–1672, Jul. 2006.

[146] S. Zhang, S.-C. Liew, P. P. Lam "Physical-Layer Network Coding," *Proc. of MobiCom,* pp. 358–365, 2006.

[147] S. Katti, I. Maric, A. Goldsmith, D. Katabi, and M. Medard, "Joint Relaying and Network Coding in Wireless Networks," *Proc. Int. Symp. Inform. Theory*, 2007.

[148] S. Katti, S. Gollakota, and D. Katabi, "Embracing Wireless Interference: Analog Network Coding," *Proc. of ACM SIGCOMM*, pp. 397–408, 2007.

[149] P. Popovski and H. Yomo, "Physical Network Coding in Two-Way Wireless Relay Channels," *Proc. Int. Conf. Commun.*, pp. 707–712, Jun. 2007.

[150] Y.-C. Liang and R. Zhang, "Optimal Analogue Relaying with Multi-Antennas for Physical Layer Network Coding," *Proc. Int. Conf. Commun.*, pp. 3893–3897, May. 2008.

[151] N. Lee, H. Park, and J. Chun, "Linear Precoder and Decoder Design for Two-Way AF MIMO Relaying System," *Proc. IEEE Vehicular Technology Conf.*, pp. 1221–1225, May. 2008.

[152] T. Unger and A. Klein, "Applying Relay Stations with Multiple Antennas in the One- and Two-Way Relay Channel," *Int. Symp. Personal, Indoor and Mobile Radio Commun.*, pp. 1–5, Sep. 2007.

[153] T. Unger and A. Klein, "Duplex Schemes in Multiple Antenna Two-Hop Relaying," *EURASIP J. on Advances in Signal Processing*, Article ID 128592, 2008.

[154] T. J. Oechtering, C. Schnurr, I. Bjelakovic, and H. Boche, "Broadcast Capacity Region of Two-Phase Bidirectional Relaying," *IEEE Trans. Inform. Theory*, vol. 54, no. 1, pp. 454–458, Jan. 2008.

[155] B. Rankov and A. Wittneben, "Spectral Efficient Protocols for Half-Duplex Fading Relay Channels," *IEEE J. Select. Areas Commun.*, vol. 25, no. 2, pp. 379–389, Feb. 2007.

[156] E. Visotsky and U. Madhow, "Space-time transmit precoding with imperfect feedback," *IEEE Trans. Inform. Theory,* vol. 47, no. 6, pp. 2632–2639, Sep. 2001.

[157] S. A. Jafar, S. Vishwanath, A. Goldsmith, "Channel capacity and beamforming for multiple transmit and receive antennas with covariance feedback," *Proc. Int. Conf. Commun.,* vol. 7, pp. 2266–2270, Jun. 2001.

[158] S. A. Jafar and A. Goldsmith, "On Optimality of Beamforming for Multiple Antenna Systems with Imperfect Feedback ," *Proc. Int. Symp. Inform. Theory*, pp. 321, Jun. 2001.

[159] S. H. Simon and A. L. Moustakas, "Optimizing MIMO Antenna Systems With Channel Covariance Feedback," *IEEE J. Select. Areas Commun.*, vol. 21, no. 3, pp. 406–417, Apr. 2003.

[160] E. A. Jorswieck and H. Boche, "Optimal Transmission with Imperfect Channel State Information at the Transmit Antenna Array," *Wireless Personal Commun.*, vol. 27, no. 1, pp. 33–56, Oct. 2003.

[161] S. A. Jafar and A. Goldsmith, "Transmitter Optimization and Optimality of Beamforming for Multiple Antenna Systems," *IEEE Trans. Wireless Commun.*, vol. 3, no. 4, pp. 1165–1175, Jul. 2004.

[162] E. A. Jorswieck and H. Boche, "Channel Capacity and Capacity-Range of Beamforming in MIMO Wireless Systems Under Correlated Fading With Covariance Feedback," *IEEE Trans. Wireless Commun.*, vol. 3, no. 5, pp. 1543–1553, Sep. 2004.

[163] E. A. Jorswieck and H. Boche, "Optimal Transmission Strategies and Impact of Correlation in Multiantenna Systems with Different Types of Channel State Information," *IEEE Trans. Signal Processing*, vol. 52, no. 12, pp. 3440–3453, Dec. 2004.

[164] M. Vu and A. Paulraj, "Capacity optimization for Rician correlated MIMO wireless channels," *Proc. Asilomar Conf. Signals, Systems, Computers*, pp. 133–138, Oct. 2005.

[165] A. M. Tulino, A. Lozano, and S. Verdu, "Capacity-Achieving Input Covariance for Single-User Multi-Antenna Channels," *IEEE Trans. Wireless Commun.*, vol. 5, no. 3, pp. 662–671, Mar. 2006.

[166] A. Soysal and S. Ulukus, "Optimum Power Allocation for Single-User MIMO and Multi-User MIMO-MAC with Partial CSI," *IEEE J. Select. Areas Commun.*, vol. 25, no. 7, pp. 1402–1412, Sep. 2007.

[167] M. Vu and A. Paulraj, "On the Capacity of MIMO Wireless Channels with Dynamic CSIT," *IEEE J. Select. Areas Commun.*, vol. 25, no. 7, pp. 1269–1283, Sep. 2007.

[168] Y.-C. Liang, R. Zhang, and J. M. Cioffi, "Subchannel Grouping and Statistical Waterfilling for Vector Block-Fading Channels," *IEEE Trans. Commun.*, vol. 54, no. 6, pp. 1131–1142, Jun. 2006.

[169] Z. Yi and I.-M. Kim, "Joint Optimization of Relay-Precoders and Decoders with Partial Channel Side Information in Cooperative Networks," *IEEE J. Select. Areas Commun.*, vol. 25, no. 2, pp. 447–458, Feb. 2007.

[170] J. Wagner, B. Rankov, and A. Wittneben, "Large n Analysis of Amplify-and-Forward MIMO Relay Channels with Correlated Rayleigh Fading," *IEEE Trans. Inform. Theory*, submitted —

[171] C. S. Patel, G. L. Stuber, and T. G. Pratt, "Statistical Properties of Amplify and Forward Relay Fading Channels," *IEEE Trans. Vehicular Technology*, vol. 55, no. 1, pp. 1–9, Jan. 2006.

[172] M. Herdin, "MIMO Amplify-and-Forward Relaying in Correlated MIMO Channels," *Proc. IEEE ICICS*, pp. 796–800, Dec. 2005.

[173] W. W. L. Ho and Y.-C. Liang, "Precoder Design for MIMO Systems with Transmit Antenna Correlations," *Proc. IEEE Vehicular Technology Conf.*, pp. 1382–1386, May 2006.

[174] S. Lin, W. W. L. Ho, and Y.-C. Liang, "Block-diagonal Geometric Mean Decomposition (BD-GMD) for Multiuser MIMO Broadcast Channels," *Int. Symp. Personal, Indoor and Mobile Radio Commun.*, pp. 1–5, Helsinki, 11–14 Sep. 2006.

[175] S. Lin, W. W. L. Ho, and Y.-C. Liang, "MIMO Broadcast Communications using Block-Diagonal Uniform Channel Decomposition (BD-UCD)," *Int. Symp. Personal, Indoor and Mobile Radio Commun.*, pp. 1–5, Helsinki, 11–14 Sep. 2006.

[176] W. W. L. Ho and Y.-C. Liang, "Efficient Power Minimization for MIMO Broadcast Channels with BD-GMD," *Proc. Int. Conf. Commun.*, pp. 2791–2796, Glasgow, Jun. 2007.

[177] S. Lin, W. W. L. Ho, and Y.-C. Liang, "Block Diagonal Geometric Mean Decomposition (BD-GMD) for MIMO Broadcast Channels," *IEEE Trans. Wireless Commun.*, vol. 7, no. 7, pp. 2778–2789, Jul. 2008.

[178] W. W. L. Ho and Y.-C. Liang, "Optimal Resource Allocation for Multiuser MIMO-OFDM Systems with User Rate Constraints," *IEEE Trans. Vehicular Technology*, accepted for publication.

[179] W. W. L. Ho and Y.-C. Liang, "User Ordering and Subchannel Selection for Power Minimization in MIMO Broadcast Channels using BD-GMD," *Proc. IEEE Vehicular Technology Conf.*, accepted for publication, Sep. 2008.

[180] W. W. L. Ho and Y.-C. Liang, "Efficient Resource Allocation for Power Minimization in MIMO-OFDM Downlink," *Proc. IEEE Vehicular Technology Conf.*, accepted for publication, Sep. 2008.

[181] W. W. L. Ho and Y.-C. Liang, "Two-Way Relaying with Multiple Antennas using Covariance Feedback," *Proc. IEEE Vehicular Technology Conf.*, accepted for publication, Sep. 2008.

Appendix A

Proof of Theorem 1

Proof. Write $\mathbf{F} = \alpha\widetilde{\mathbf{F}}$. The condition $\mathrm{Tr}(\mathbf{F}^H\mathbf{F}) \leq E_s$ can now be expressed as

$$\alpha^2 \leq \frac{E_s}{\mathrm{Tr}(\widetilde{\mathbf{F}}^H\widetilde{\mathbf{F}})} , \tag{A.1}$$

so maximizing α is the same as minimizing $\mathrm{Tr}(\widetilde{\mathbf{F}}^H\widetilde{\mathbf{F}})$. Thus, (3.13) is equivalent to the problem

$$\begin{aligned} \text{minimize} \quad & \mathrm{Tr}(\widetilde{\mathbf{F}}^H\widetilde{\mathbf{F}}) \\ \text{subject to} \quad & \mathbf{J} \in \mathbb{L} \ , \ \mathbf{A} \in \mathbb{B} \ , \\ & \mathbf{AH}\widetilde{\mathbf{F}} = \mathbf{J} \ , \\ & \|\mathbf{A}(i,:)\|_2 = 1 \qquad \text{for } 1 \leq i \leq N_R \ . \end{aligned} \tag{A.2}$$

The Lagrangian $\mathscr{L}(\widetilde{\mathbf{F}}, \mathbf{A}, \mathbf{\Theta}, \mathbf{\Gamma})$ of this problem is

$$\mathrm{Tr}(\widetilde{\mathbf{F}}^H\widetilde{\mathbf{F}} - \mathrm{Re}(2\mathbf{\Theta}^H(\mathbf{AH}\widetilde{\mathbf{F}} - \mathbf{I})) + \mathbf{\Gamma}(\mathbf{AA}^H - \mathbf{I})) \ , \tag{A.3}$$

where $\mathbf{\Theta}$, $\mathbf{\Gamma}$ are Lagrange multipliers. $\mathbf{\Theta}$ is a complex upper triangular matrix, $\mathbf{\Gamma}$ is a real-valued diagonal matrix and $\mathrm{Re}(\mathbf{X})$ is the real-part of a complex matrix

$\mathbf{X}$. If $\widetilde{\mathbf{F}}$ and $\mathbf{A}$ are optimal, then they satisfy

$$\nabla_{\widetilde{\mathbf{F}}}\mathscr{L} = 0 \implies \widetilde{\mathbf{F}} = (\mathbf{AH})^H\boldsymbol{\Theta} \tag{A.4}$$

$$\nabla_{\mathbf{A}_k}\mathscr{L} = 0 \implies [\boldsymbol{\Theta}(\mathbf{H}\widetilde{\mathbf{F}})^H]_k = \boldsymbol{\Gamma}_k\mathbf{A}_k \quad \text{for } 1 \le k \le K\ , \tag{A.5}$$

where $\mathbf{A}_k$, $\boldsymbol{\Gamma}_k$, and $[\boldsymbol{\Theta}(\mathbf{H}\widetilde{\mathbf{F}})^H]_k$ are the k-th diagonal block of each matrix respectively. We begin by noting the following two important relations

$$\begin{aligned}\mathbf{J}^H\boldsymbol{\Theta} &= (\widetilde{\mathbf{F}}^H\mathbf{H}^H\mathbf{A}^H)\boldsymbol{\Theta} \\ &= \widetilde{\mathbf{F}}^H(\mathbf{H}^H\mathbf{A}^H\boldsymbol{\Theta}) \\ &= \widetilde{\mathbf{F}}^H\widetilde{\mathbf{F}}\end{aligned} \tag{A.6}$$

$$\begin{aligned}\boldsymbol{\Gamma}_k\mathbf{A}_k\mathbf{A}_k^H &= [\boldsymbol{\Theta}\widetilde{\mathbf{F}}^H\mathbf{H}^H]_k\mathbf{A}_k^H \\ &= [\boldsymbol{\Theta}\widetilde{\mathbf{F}}^H\mathbf{H}^H\mathbf{A}^H]_k \\ &= [\boldsymbol{\Theta}\mathbf{J}^H]_k \\ &= \boldsymbol{\Theta}_k\mathbf{J}_k^H\end{aligned} \tag{A.7}$$

Lemma 5. *There exists an optimal solution to (A.2) where* $\mathbf{A}$ *is unitary.*

Proof. Pick any optimal solution to (A.2), and consider its matrix $\mathbf{A}$. From the third line in (A.2), $\det(\mathbf{J}) \neq 0$ implies that $\mathbf{A}$, $\mathbf{H}$ and $\widetilde{\mathbf{F}}$ have full rank. Similarly, by (A.4), $\det(\boldsymbol{\Theta}) \neq 0$. Then, by (A.7), $\det(\boldsymbol{\Gamma}_k) \neq 0$. Therefore, the diagonal elements of $\boldsymbol{\Gamma}_k$ are non-zero.

From (A.7), $\mathbf{A}_k\mathbf{A}_k^H = \boldsymbol{\Gamma}_k^{-1}\boldsymbol{\Theta}_k\mathbf{J}_k^H$ is upper triangular. On the other hand, $\mathbf{A}_k\mathbf{A}_k^H = [\mathbf{A}_k\mathbf{A}_k^H]^H$ is lower triangular. Thus, $\mathbf{A}_k\mathbf{A}_k^H$ must be diagonal. Since the rows of $\mathbf{A}_k$ are of unit norm, we have $\mathbf{A}_k\mathbf{A}_k^H = \mathbf{I}$ so $\mathbf{A}_k$ is unitary. Since $\mathbf{A}_k$ is

unitary for all k, the lemma follows. □

Lemma 6. *There exists an optimal solution to (A.2) where* $\mathbf{A}$ *is unitary and* $\widetilde{\mathbf{F}} = \widetilde{\mathbf{Q}}\widetilde{\mathbf{\Omega}}$ *where* $\widetilde{\mathbf{Q}}$ *has orthonormal columns and* $\widetilde{\mathbf{\Omega}}$ *is diagonal with non-negative real elements.*

Proof. Using Lemma 5, pick any optimal solution to (A.2) in which $\mathbf{A}$ is unitary. From (A.6), we have $\widetilde{\mathbf{F}}^H\widetilde{\mathbf{F}} = \mathbf{J}^H\mathbf{\Theta}$ which is upper triangular. On the other hand, $\widetilde{\mathbf{F}}^H\widetilde{\mathbf{F}} = [\widetilde{\mathbf{F}}^H\widetilde{\mathbf{F}}]^H$ is lower triangular, so $\widetilde{\mathbf{F}}^H\widetilde{\mathbf{F}}$ must be diagonal. Furthermore, we can write $\widetilde{\mathbf{F}}^H\widetilde{\mathbf{F}} = \widetilde{\mathbf{\Omega}}^2$ where $\widetilde{\mathbf{\Omega}}$ is the diagonal matrix of the column norms of $\widetilde{\mathbf{F}}$, so $\widetilde{\mathbf{\Omega}}$ has non-negative real elements. Let $\widetilde{\mathbf{Q}}$ be the matrix of the unit column vectors of $\mathbf{F}$. Hence, $\widetilde{\mathbf{F}} = \widetilde{\mathbf{Q}}\widetilde{\mathbf{\Omega}}$. It is easy to check that $\widetilde{\mathbf{Q}}^H\widetilde{\mathbf{Q}} = \mathbf{I}$ from $\widetilde{\mathbf{F}}^H\widetilde{\mathbf{F}} = \widetilde{\mathbf{\Omega}}^2$, so $\widetilde{\mathbf{Q}}$ has orthonormal columns and this completes the lemma. □

As a result of these two lemmas, and the third line in (A.2),

$$\mathbf{A}\mathbf{H}\widetilde{\mathbf{F}}\widetilde{\mathbf{\Omega}}^{-1} = \mathbf{A}\mathbf{H}\widetilde{\mathbf{Q}} = \mathbf{J}\widetilde{\mathbf{\Omega}}^{-1} \text{ , and}$$
$$\mathbf{H} = \mathbf{A}^H(\mathbf{J}\widetilde{\mathbf{\Omega}}^{-1})\widetilde{\mathbf{Q}}^H \text{ .} \tag{A.8}$$

Define $\widetilde{\mathbf{L}} = \mathbf{J}\widetilde{\mathbf{\Omega}}^{-1}$. Denote each diagonal block of $\widetilde{\mathbf{L}}$ corresponding to user k as $[\widetilde{\mathbf{L}}]_k$. It follows that $\det([\widetilde{\mathbf{L}}]_k) = \det([\widetilde{\mathbf{\Omega}}^{-1}]_k)$. Define $\widehat{\mathbf{H}}_k = [\mathbf{H}_1^T, \ldots, \mathbf{H}_k^T]^T$. Since $\mathbf{A}$ is block diagonal unitary and $\widetilde{\mathbf{Q}}$ has orthonormal columns, it can be seen that $\det([\widetilde{\mathbf{L}}]_k) = \sqrt{\frac{\det(\widehat{\mathbf{H}}_k\widehat{\mathbf{H}}_k^H)}{\det(\widehat{\mathbf{H}}_{k-1}\widehat{\mathbf{H}}_{k-1}^H)}}$. Thus, $\det([\widetilde{\mathbf{\Omega}}]_k)$ is a constant determined by the $\mathbf{H}$. As $\mathrm{Tr}(\widetilde{\mathbf{F}}^H\widetilde{\mathbf{F}}) = \mathrm{Tr}(\widetilde{\mathbf{\Omega}}^2)$, $\mathrm{Tr}(\widetilde{\mathbf{F}}^H\widetilde{\mathbf{F}})$ will be minimized when the diagonal elements of $[\widetilde{\mathbf{\Omega}}]_k$ are equal. Since $\widetilde{\mathbf{L}} = \mathbf{J}\widetilde{\mathbf{\Omega}}^{-1}$, the diagonal elements of $[\widetilde{\mathbf{L}}]_k$ are equal. Therefore, referring to (A.8), the BD-GMD ($\mathbf{H} = \mathbf{P}\mathbf{L}\mathbf{Q}^H$) provides the solution

to the optimization (A.2), where

$$\widetilde{\mathbf{L}} = \mathbf{J}\widetilde{\mathbf{\Omega}}^{-1} = \mathbf{L} \ , \quad \widetilde{\mathbf{Q}} = \mathbf{Q} \ , \quad \text{and} \quad \mathbf{A} = \mathbf{P}^H \ . \tag{A.9}$$

Consequently, $\widetilde{\mathbf{\Omega}}^{-1} = \text{diag}(\mathbf{L}) = \mathbf{\Lambda}$, and $\mathbf{J} = \mathbf{L}\mathbf{\Lambda}^{-1}$.

$$\mathbf{F} = \alpha\widetilde{\mathbf{F}} = \alpha\mathbf{Q}\mathbf{\Lambda}^{-1} \quad \text{and} \quad \alpha^2 = \frac{E_s}{\text{Tr}(\widetilde{\mathbf{F}}\widetilde{\mathbf{F}}^H)} = \frac{E_s}{\text{Tr}(\mathbf{\Lambda}^{-2})} \ . \tag{A.10}$$

This completes the proof for theorem 1. □

Appendix B

Proof of Theorem 2

Proof. The Lagrangian $\mathscr{L}(\mathbf{F}, \mathbf{A}, \boldsymbol{\alpha}, \widetilde{\boldsymbol{\rho}}, \boldsymbol{\mu})$ for problem (4.4) is

$$\mathrm{Tr}(\mathbf{F}^H\mathbf{F} + \mathrm{Re}(\widetilde{\boldsymbol{\rho}}^H(\mathbf{AHF} - \sqrt{N_0}\boldsymbol{\Gamma}^{1/2})) + \boldsymbol{\mu}(\mathbf{A}\mathbf{A}^H - \mathbf{I})) \ , \tag{B.1}$$

where $\widetilde{\boldsymbol{\rho}}$, $\boldsymbol{\mu}$ are Lagrange multipliers, $\widetilde{\boldsymbol{\rho}}$ an upper triangular complex matrix, $\boldsymbol{\mu}$ a real-valued diagonal matrix, and $\mathrm{Re}(\mathbf{X})$ the real-part of a complex matrix $\mathbf{X}$. If $\mathbf{F}$ and $\mathbf{A}$ are optimal, then they satisfy

$$\nabla_{\mathbf{F}}\mathscr{L} = 2\mathbf{F} + (\mathbf{AH})^H\widetilde{\boldsymbol{\rho}} = \mathbf{0} \tag{B.2}$$

$$\nabla_{\mathbf{A}_k}\mathscr{L} = [\widetilde{\boldsymbol{\rho}}(\mathbf{HF})^H]_k + 2\boldsymbol{\mu}_k\mathbf{A}_k = \mathbf{0} \quad \text{for } 1 \leq k \leq K \tag{B.3}$$

where $\mathbf{A}_k$, $\boldsymbol{\mu}_k$ and $[(\widetilde{\boldsymbol{\rho}}\mathbf{HF})^H]_k$ are the k-th diagonal block of each matrix respectively. Begin by letting $\boldsymbol{\rho} = -\frac{1}{2}\widetilde{\boldsymbol{\rho}}$, also upper triangular. From (B.2),

$$\mathbf{F} = \mathbf{H}^H\mathbf{A}^H\boldsymbol{\rho} \ . \tag{B.4}$$

Define $\bar{\mathbf{J}} = \sqrt{N_0}\mathbf{\Gamma}^{1/2}\mathbf{B}$, a lower triangular matrix. From (B.3),

$$\begin{aligned}\boldsymbol{\mu}_k \mathbf{A}_k \mathbf{A}_k^H &= \left[-\frac{1}{2}\widetilde{\boldsymbol{\rho}}\mathbf{F}^H\mathbf{H}^H\right]_k \mathbf{A}_k^H \\ &= [\boldsymbol{\rho}\mathbf{F}^H\mathbf{H}^H]_k \mathbf{A}_k^H \\ &= [\boldsymbol{\rho}\mathbf{F}^H\mathbf{H}^H\mathbf{A}^H]_k \\ &= [\boldsymbol{\rho}\bar{\mathbf{J}}^H]_k \ . \end{aligned} \tag{B.5}$$

Since $\boldsymbol{\mu}_k$ is diagonal, $\mathbf{A}_k\mathbf{A}_k^H$ is upper triangular. As $\mathbf{A}_k\mathbf{A}_k^H$ is also hermitian, it has to be diagonal. Together with the constraint of unit row norm of $\mathbf{A}$, it follows that $\mathbf{A}$ is unitary. Likewise,

$$\begin{aligned}(\bar{\mathbf{J}}^H)\boldsymbol{\rho} &= (\mathbf{F}^H\mathbf{H}^H\mathbf{A}^H)\boldsymbol{\rho} \\ &= \mathbf{F}^H\mathbf{F} \ . \end{aligned} \tag{B.6}$$

Since $\mathbf{F}^H\mathbf{F}$ is upper triangular and hermitian, it is diagonal.

$$\mathbf{F}^H\mathbf{F} = \mathrm{diag}(\boldsymbol{\rho})\sqrt{N_0}\mathbf{\Gamma}^{1/2} \ . \tag{B.7}$$

As the diagonal elements of $\mathbf{F}^H\mathbf{F}$ are positive real, the diagonal elements of $\boldsymbol{\rho}$ are also positive real. Define

$$\bar{\mathbf{\Lambda}} = (\mathbf{F}^H\mathbf{F})^{-1/2} \ , \tag{B.8}$$

where $\bar{\mathbf{\Lambda}}$ is a diagonal matrix of positive real entries. Therefore

$$(\mathbf{F}\bar{\mathbf{\Lambda}})^H(\mathbf{F}\bar{\mathbf{\Lambda}}) = \mathbf{I} \ , \tag{B.9}$$

Let the unitary matrix $\mathbf{F}\bar{\mathbf{\Lambda}}$ be denoted by $\bar{\mathbf{Q}}$. Then by (4.4),

$$\mathbf{AHF}\bar{\mathbf{\Lambda}} = \mathbf{AH}\bar{\mathbf{Q}} = \bar{\mathbf{J}}\bar{\mathbf{\Lambda}} \tag{B.10}$$

$$\mathbf{H} = \mathbf{A}^H(\bar{\mathbf{J}}\bar{\mathbf{\Lambda}})\bar{\mathbf{Q}}^H \ , \tag{B.11}$$

where $\bar{\mathbf{J}}\bar{\mathbf{\Lambda}}$ is lower triangular. Let $\bar{\mathbf{L}} = \bar{\mathbf{J}}\bar{\mathbf{\Lambda}}$. So $\mathrm{diag}(\bar{\mathbf{L}}) = \sqrt{N_0}\mathbf{\Gamma}^{1/2}\bar{\mathbf{\Lambda}}$. Denote each diagonal block of $\bar{\mathbf{L}}$ corresponding to user k as $[\bar{\mathbf{L}}]_k$. It follows that

$$\begin{aligned}\det([\bar{\mathbf{L}}]_k) &= \det([\bar{\mathbf{J}}]_k)\det([\bar{\mathbf{\Lambda}}]_k) \\ &= (\sqrt{N_0\gamma_k})^{n_k}\det([\bar{\mathbf{\Lambda}}]_k) \ .\end{aligned} \tag{B.12}$$

Define $\widehat{\mathbf{H}}_k = [\mathbf{H}_1^T, \ldots, \mathbf{H}_k^T]^T$. Since $\mathbf{A}$ is block diagonal unitary and $\bar{\mathbf{Q}}$ is unitary, it can be seen that

$$\det([\bar{\mathbf{L}}]_k) = \sqrt{\frac{\det(\widehat{\mathbf{H}}_k\widehat{\mathbf{H}}_k^H)}{\det(\widehat{\mathbf{H}}_{k-1}\widehat{\mathbf{H}}_{k-1}^H)}} \ . \tag{B.13}$$

Thus $\det([\bar{\mathbf{\Lambda}}]_k)$ is a constant determined by the $\mathbf{H}$, γ_k and n_k. Recall from (4.6) and (B.9) that the power needed is

$$E_s = \mathrm{Tr}(\mathbf{F}^H\mathbf{F}) = \mathrm{Tr}(\bar{\mathbf{\Lambda}}^{-2}) \ . \tag{B.14}$$

Therefore, E_s will be minimized when the diagonal elements of $[\bar{\mathbf{\Lambda}}]_k$ are equal. Since the diagonal elements of $[\bar{\mathbf{J}}]_k$ are equal, the same is true for the diagonal values of $[\bar{\mathbf{L}}]_k$. Therefore, from (B.11), and the BD-GMD decomposition, $\mathbf{H} = \mathbf{PLQ}^H$,

$$\bar{\mathbf{L}} = \bar{\mathbf{J}}\bar{\mathbf{\Lambda}} = \mathbf{L} \ , \quad \bar{\mathbf{Q}} = \mathbf{Q} \ , \quad \mathbf{A} = \mathbf{P}^H \ , \tag{B.15}$$

where

$$\bar{\mathbf{\Lambda}} = \text{diag}(\bar{\mathbf{J}})^{-1}\text{diag}(\mathbf{L}) = (\sqrt{N_0}\mathbf{\Gamma}^{1/2})^{-1}\mathbf{\Lambda} \ . \tag{B.16}$$

Define

$$\mathbf{\Omega} = \bar{\mathbf{\Lambda}}^{-1} = \sqrt{N_0}\mathbf{\Gamma}^{1/2}\mathbf{\Lambda}^{-1} \ . \tag{B.17}$$

Finally,

$$\begin{aligned} \mathbf{F} &= \mathbf{Q}\mathbf{\Omega} \ , \\ \mathbf{B} &= (\sqrt{N_0}\mathbf{\Gamma}^{1/2})^{-1}\mathbf{L}\bar{\mathbf{\Lambda}}^{-1} = \mathbf{\Omega}^{-1}\mathbf{\Lambda}^{-1}\mathbf{L}\mathbf{\Omega} \end{aligned} \tag{B.18}$$

completes the solution to (4.4). □